High-Contrast Instruments (Theory)

N. Jeremy Kasdin
Princeton University

Imaging a Star–A Simple Ray Optics Description

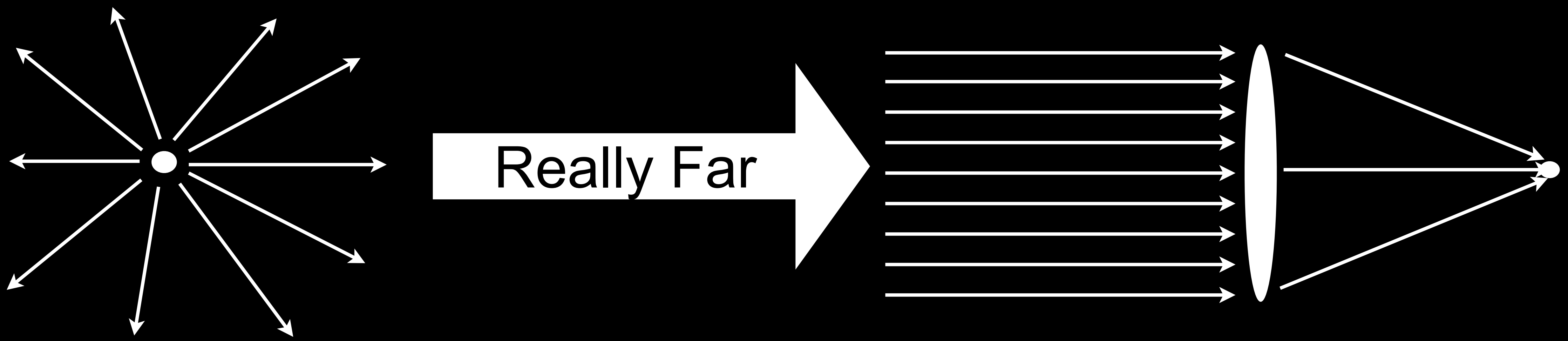

Imaging a Star–A Simple Ray Optics Description

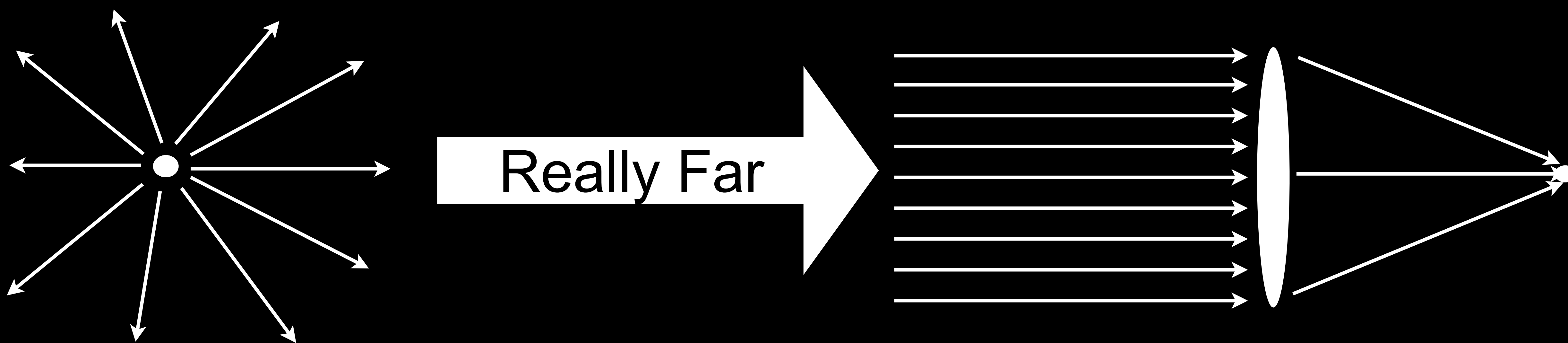

Star and Planet

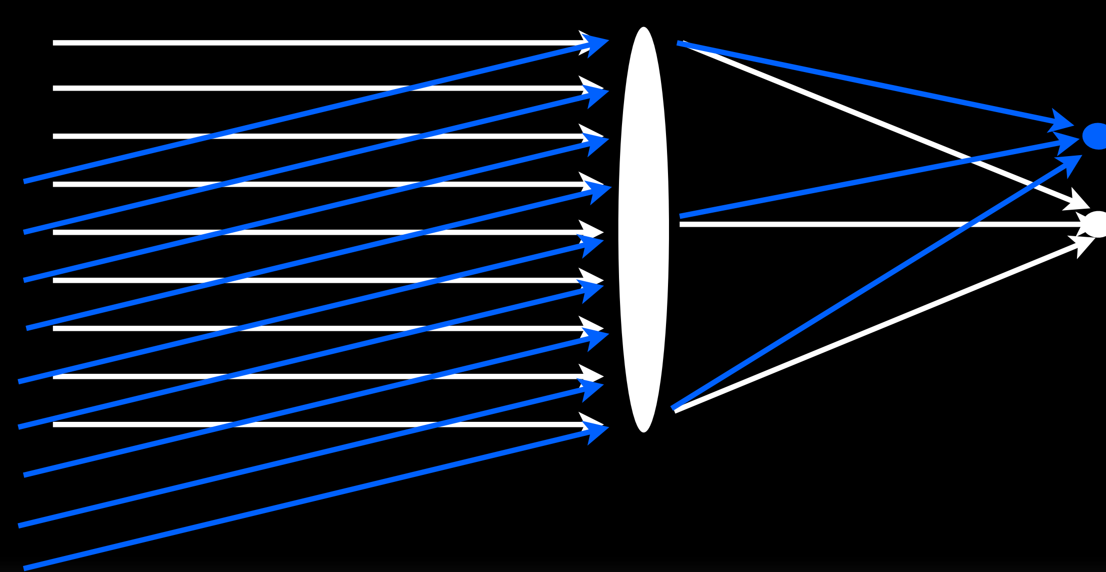

However, we need to include diffraction

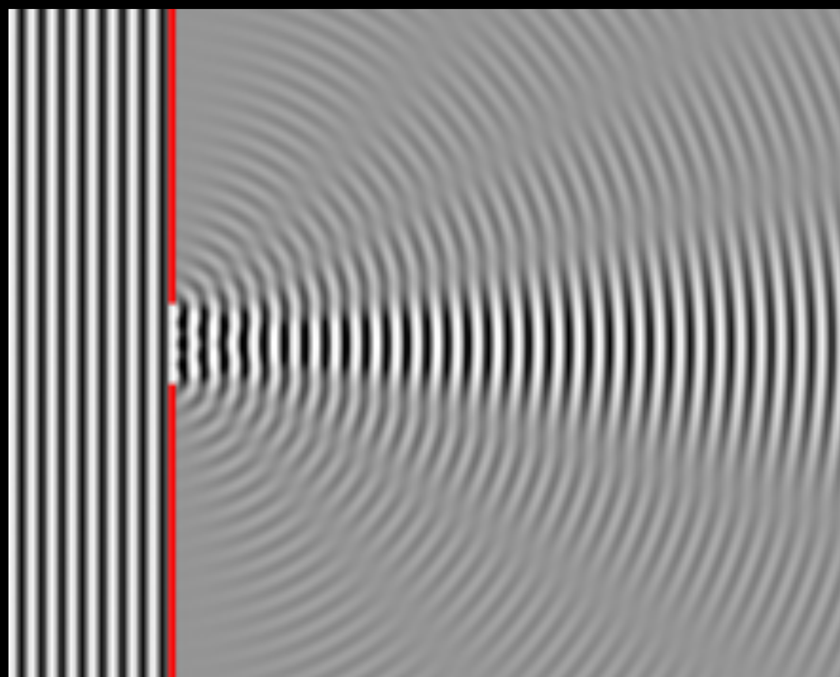

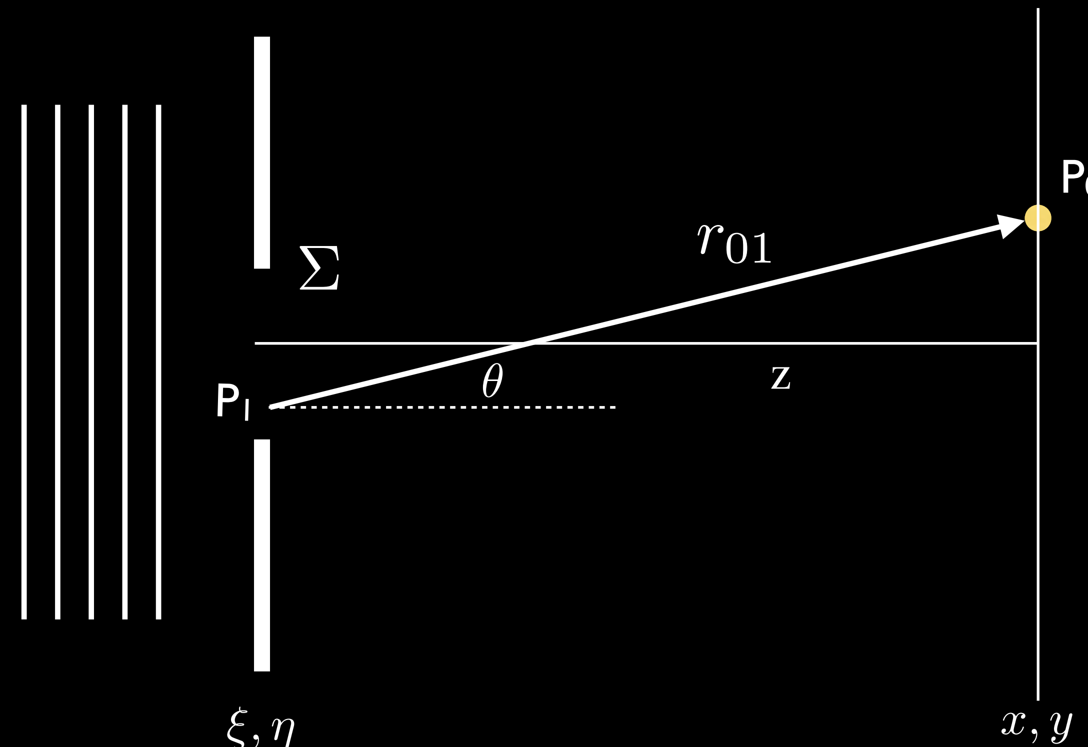

$$E_0(x,y) = \frac{1}{j\lambda}\int\int_{\Sigma} E_1(\xi,\eta)\frac{\exp(jkr_{01})}{r_{01}}\cos\theta d\xi d\eta$$

$$r_{01} = \sqrt{z^2 + (x-\xi)^2 + (y-\eta)^2}$$

The Huygens-Fresnel Principle

See Goodman, *Introduction to Fourier Optics*

However, we need to include diffraction

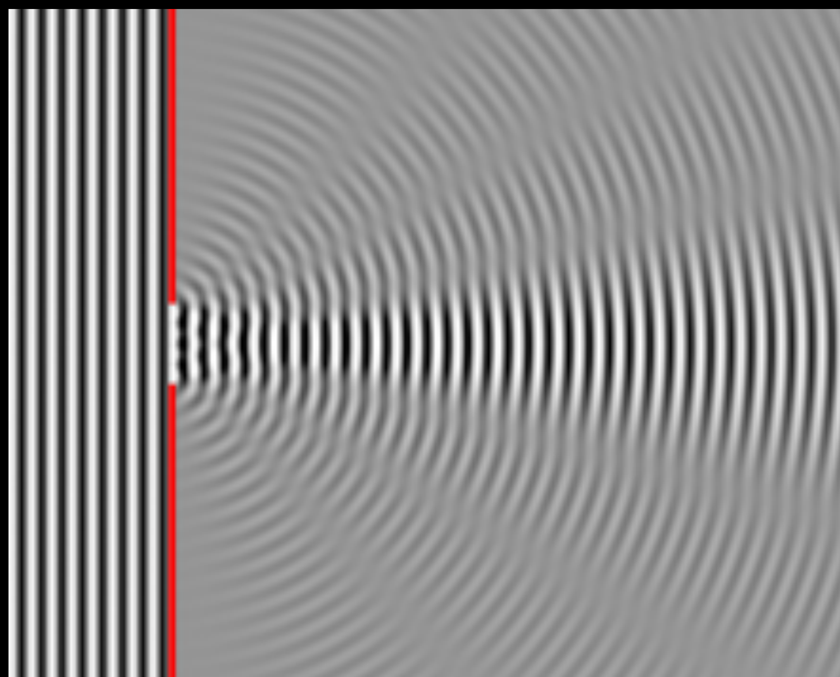

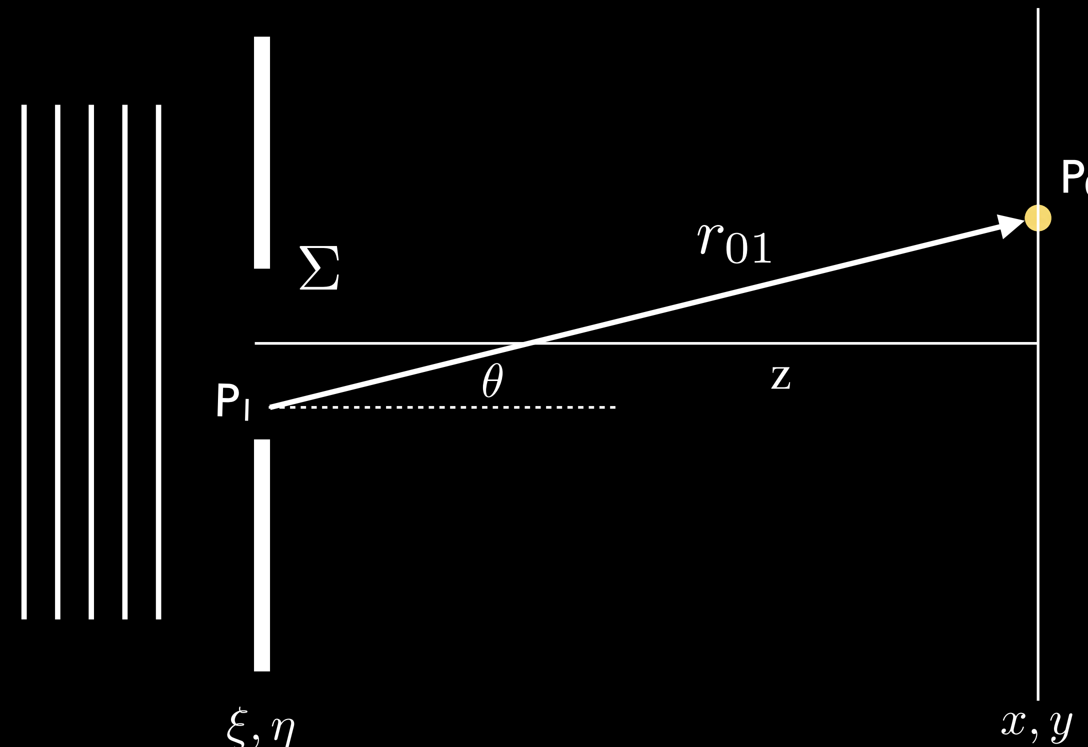

$$E_0(x,y) = \frac{1}{j\lambda} \int \int_{\Sigma} E_1(\xi,\eta) \frac{\exp(jkr_{01})}{r_{01}} \cos\theta d\xi d\eta$$

$$r_{01} = \sqrt{z^2 + (x-\xi)^2 + (y-\eta)^2}$$

The Huygens-Fresnel Principle

This is too complicated so we approximate in different regimes.

See Goodman, *Introduction to Fourier Optics*

Important approximations . . .

S-Huygens (very near field)

$$E(x,y) = \frac{e^{jkS}}{j\lambda z} \int\int_{-\infty}^{\infty} E(\xi,\eta) e^{j\frac{k}{2S}\left[(x-\xi)^2+(y-\eta)^2\right]} d\xi d\eta$$

$$S = \sqrt{z^2+x^2+y^2}$$

Fresnel Number

$$\frac{R^2}{\lambda S} \sim \mathcal{O}(1)$$

Fresnel (near field)

$$E(x,y) = \frac{e^{jkz}}{j\lambda z} \int\int_{-\infty}^{\infty} E(\xi,\eta) e^{j\frac{k}{2z}\left[(x-\xi)^2+(y-\eta)^2\right]} d\xi d\eta$$

$$\frac{R^2}{\lambda z} \sim \mathcal{O}(1) \quad x, y \ll z$$

Fraunhoffer (far field)

$$E(x,y) = \frac{e^{jkz} e^{j\frac{k}{2z}(x^2+y^2)}}{j\lambda z} \int\int_{-\infty}^{\infty} E(\xi,\eta) e^{-j\frac{2\pi}{\lambda z}(x\xi+y\eta)} d\xi d\eta$$

$$\frac{R^2}{\lambda z} \ll 1$$

Fourier Transform

Or a focusing lens

Important approximations . . .

S-Huygens (very near field)

$$E(x,y) = \frac{e^{jkS}}{j\lambda z} \int\int_{-\infty}^{\infty} E(\xi,\eta) e^{j\frac{k}{2S}\left[(x-\xi)^2+(y-\eta)^2\right]} d\xi d\eta$$

$$S = \sqrt{z^2 + x^2 + y^2}$$

Fresnel Number

$$\frac{R^2}{\lambda S} \sim \mathcal{O}(1)$$

Fresnel (near field)

$$E(x,y) = \frac{e^{jkz}}{j\lambda z} \int\int_{-\infty}^{\infty} E(\xi,\eta) e^{j\frac{k}{2z}\left[(x-\xi)^2+(y-\eta)^2\right]} d\xi d\eta$$

$$\frac{R^2}{\lambda z} \sim \mathcal{O}(1) \quad x, y \ll z$$

Fraunhoffer (far field)

$$E(x,y) = \frac{e^{jkz} e^{j\frac{k}{2z}(x^2+y^2)}}{j\lambda z} \int\int_{-\infty}^{\infty} E(\xi,\eta) e^{-j\frac{2\pi}{\lambda z}(x\xi+y\eta)} d\xi d\eta$$

$$\frac{R^2}{\lambda z} \ll 1$$

Fourier Transform

Or a focusing lens

Star & Planet with Diffraction

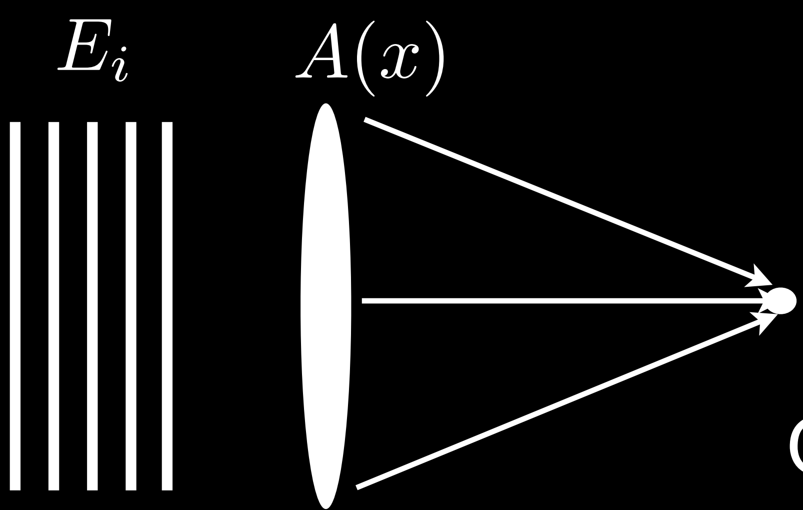

$$P_c(\omega) = |\mathcal{F}\{E_i A(x)\}|^2$$

On-Axis Point Spread Function

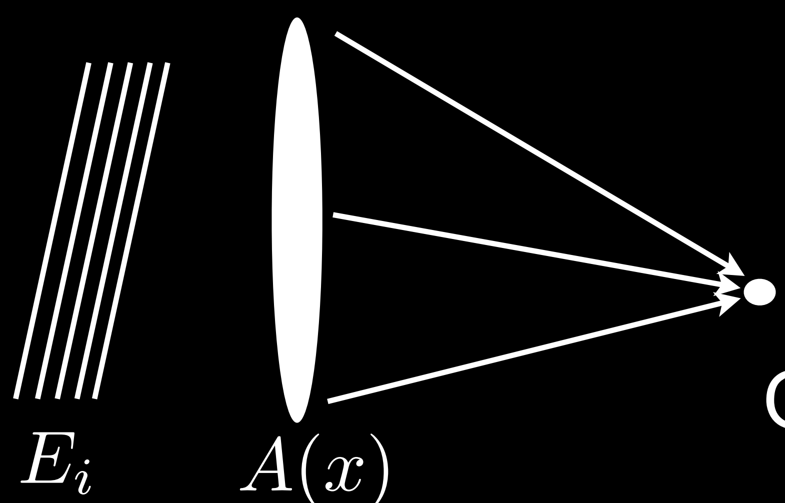

$$P_c(\omega) = |\mathcal{F}\{E_i e^{-x\theta/\lambda} A(x)\}|^2$$

Off-Axis Point Spread Function

Star & Planet with Diffraction

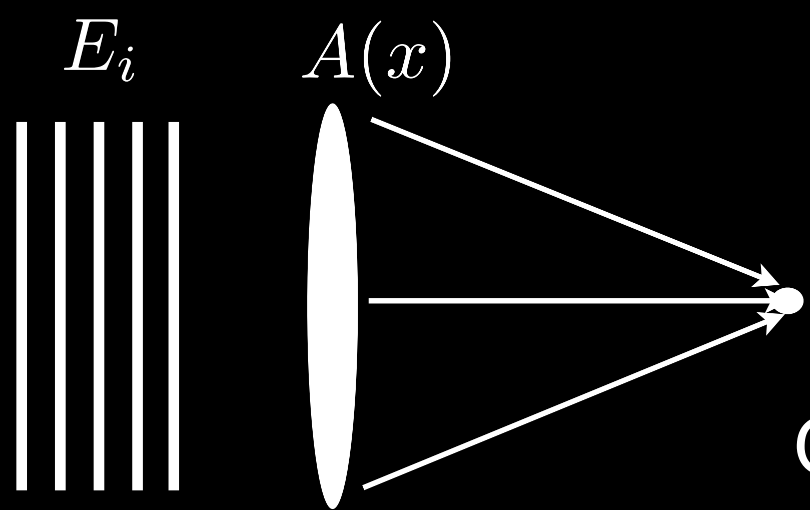

$$P_c(\omega) = |\mathcal{F}\{E_i A(x)\}|^2$$

On-Axis Point Spread Function

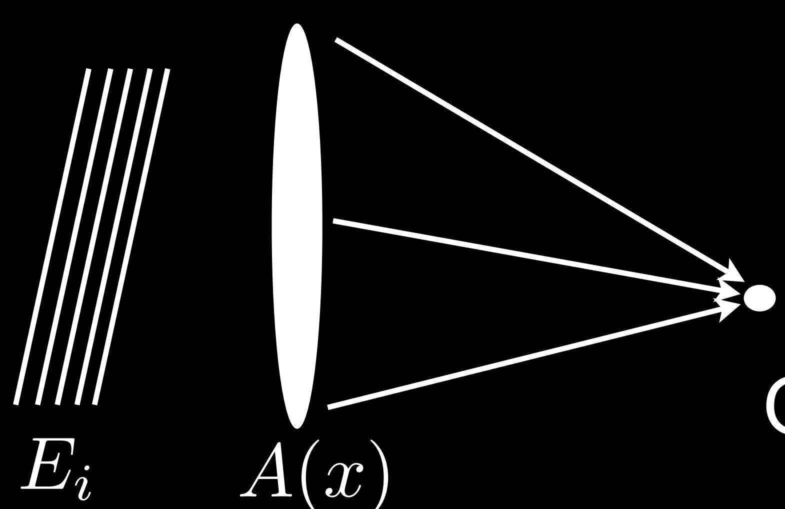

$$P_c(\omega) = |\mathcal{F}\{E_i e^{-x\theta/\lambda} A(x)\}|^2$$

Off-Axis Point Spread Function

Star & Planet with Diffraction

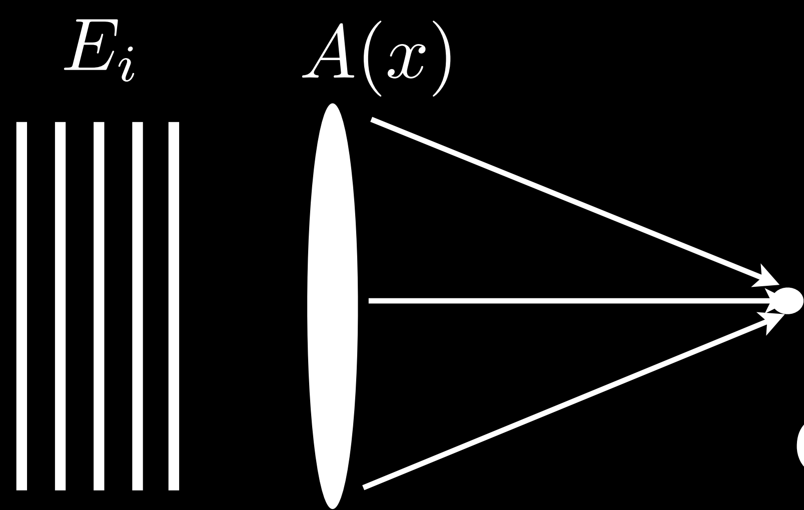

$$P_c(\omega) = |\mathcal{F}\{E_i A(x)\}|^2$$

On-Axis Point Spread Function

Circular Aperture

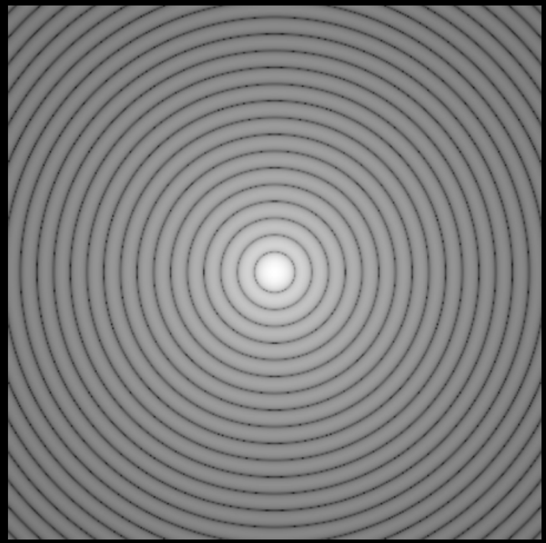

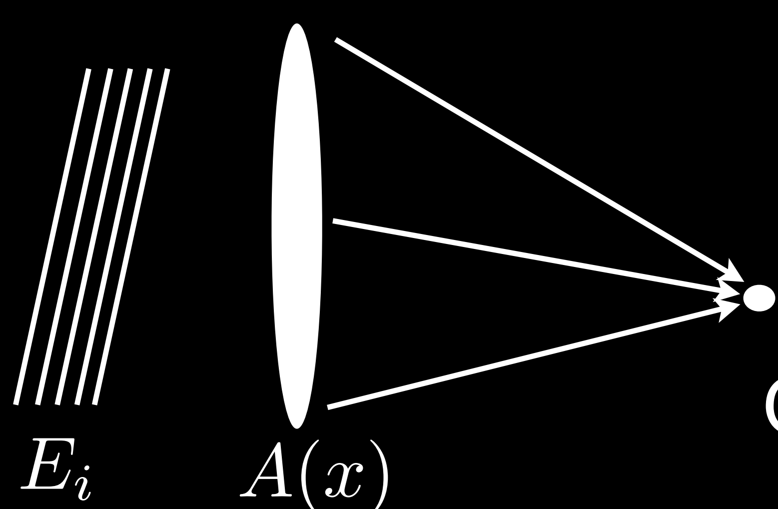

$$P_c(\omega) = |\mathcal{F}\{E_i e^{-x\theta/\lambda} A(x)\}|^2$$

Off-Axis Point Spread Function

Resolution

Two Meter Telescope　　　Ten Meter Telescope

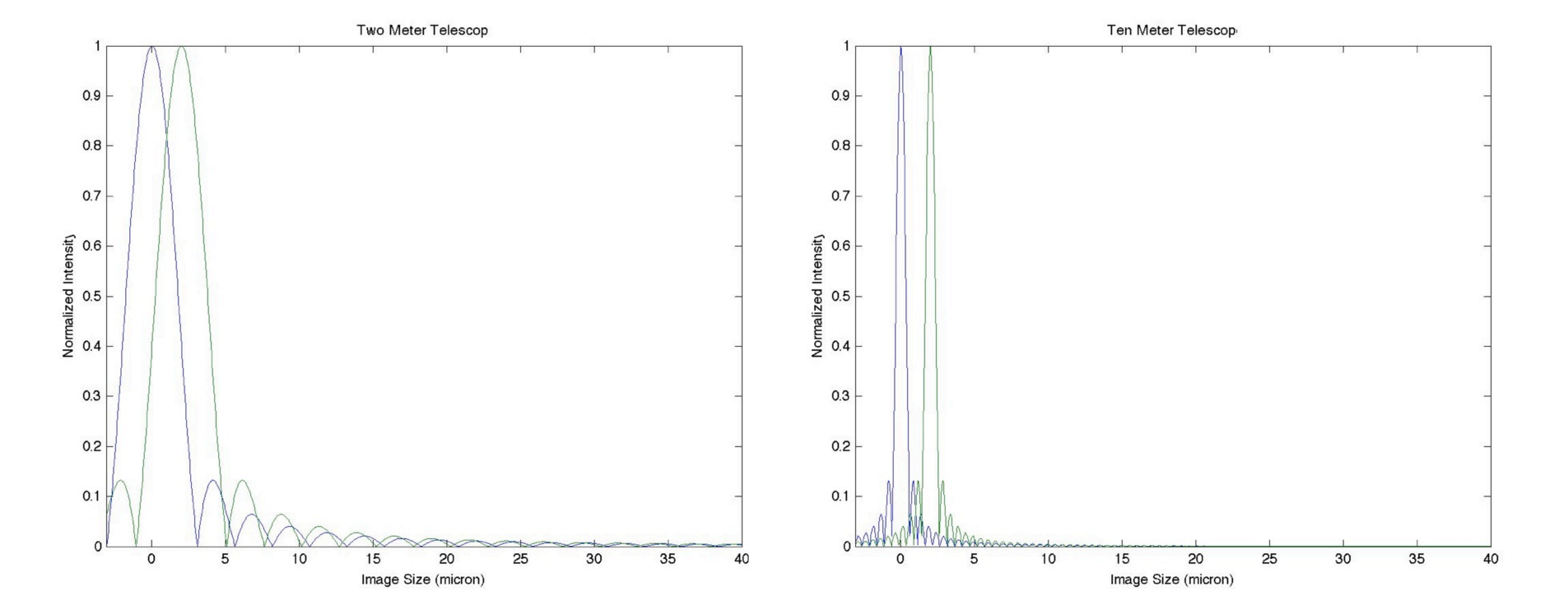

Even a two-meter telescope can resolve a planet at 1 AU about closest stars.

The Problem is Contrast

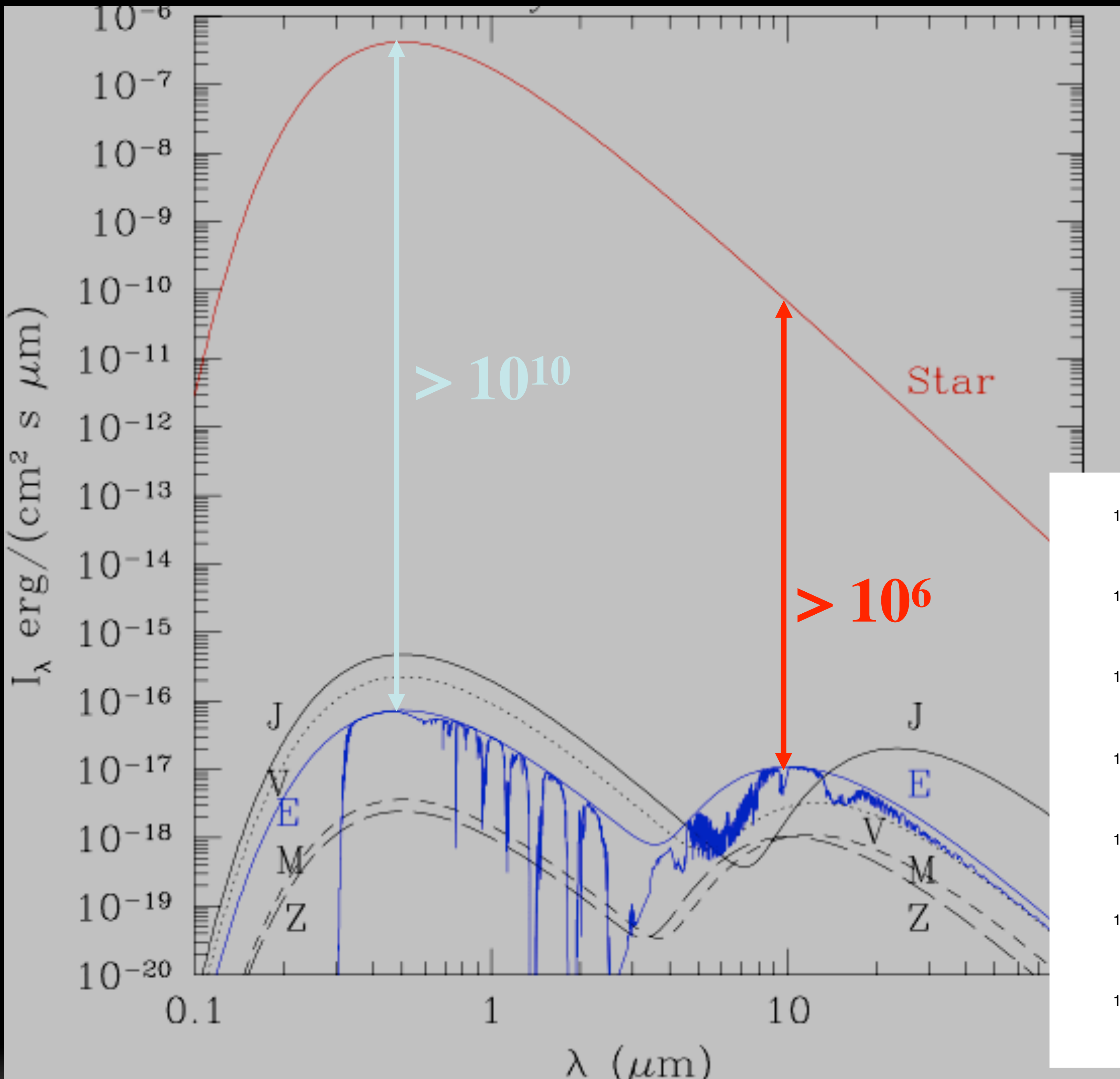

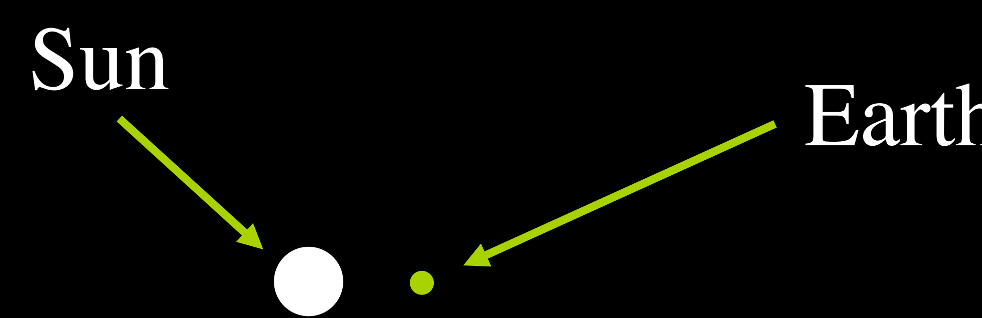

At 10 pc, angular separation is 100 marcsec

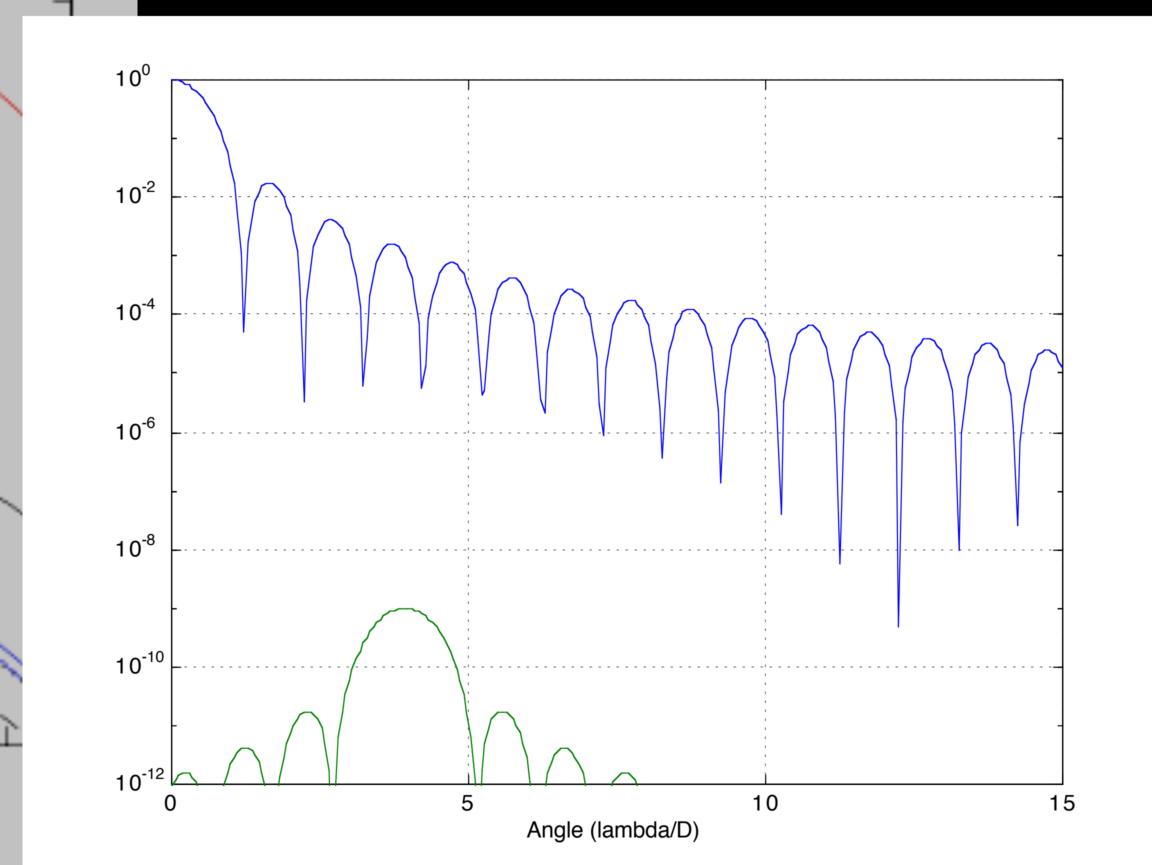

Traub & Jucks

High-Contrast Imaging

To image the planet with a ground or space telescope there are five important metrics:

- **Contrast:** The ratio of the peak of the stellar point spread function to the halo at the planet location.
- **Inner Working Angle:** The smallest angle on the sky at which the needed contrast is achieved and the planet is reduced by no more than 50% relative to other angles.
- **Throughput:** The ratio of the open telescope area remaining after high-contrast is achieved.
- **Bandwidth:** The wavelengths at which high contrast is achieved.
- **Sensitivity:** The degree to which contrast is degraded in the presence of aberations.

High-Contrast Imaging

To image the planet with a ground or space telescope there are five important metrics:

- **Contrast:** The ratio of the peak of the stellar point spread function to the halo at the planet location.
- **Inner Working Angle:** The smallest angle on the sky at which the needed contrast is achieved and the planet is reduced by no more than 50% relative to other angles.
- **Throughput:** The ratio of the fraction of light in the central core of the PSF to the same fraction in an Airy function.
- **Bandwidth:** The wavelengths at which high contrast is achieved.
- **Sensitivity:** The degree to which contrast is degraded in the presence of aberations.

In the remainder of this talk I will describe how we achieve high-contrast using a coronagraph.

Later, Aki Roberge will describe how it is done using a Starshade.

Tomorrow, Laurent Pueyo will describe how the planet is extracted from the image.

Coronagraphy

Modify the optical path of the telescope to reduce the stellar halo in the planet "discovery zone" (increase contrast) while allowing sufficient planet light to transmit through.

The "Lyot Coronagraph"

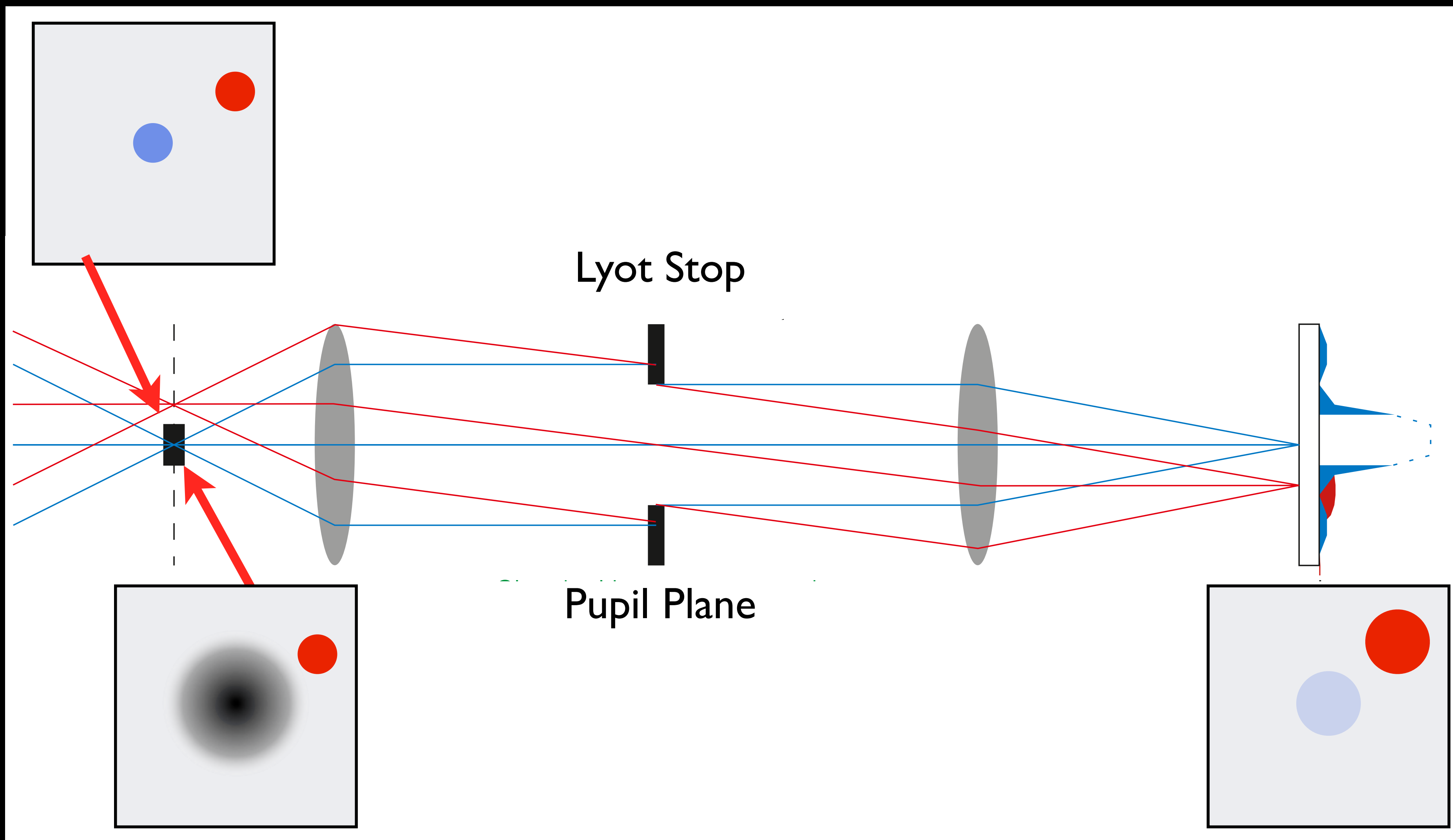

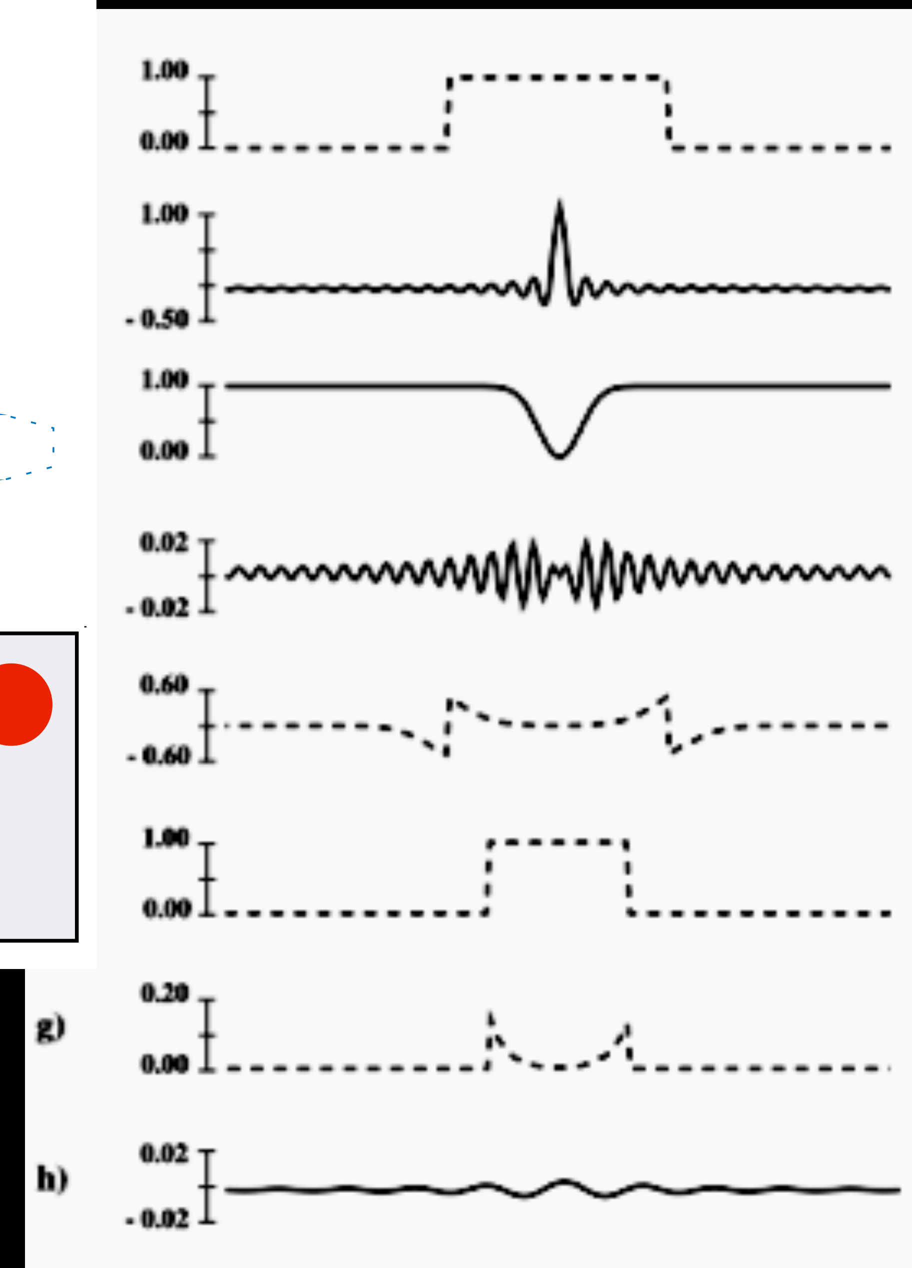

from Matt Kenworthy, University of Leiden

The “Lyot Coronagraph”

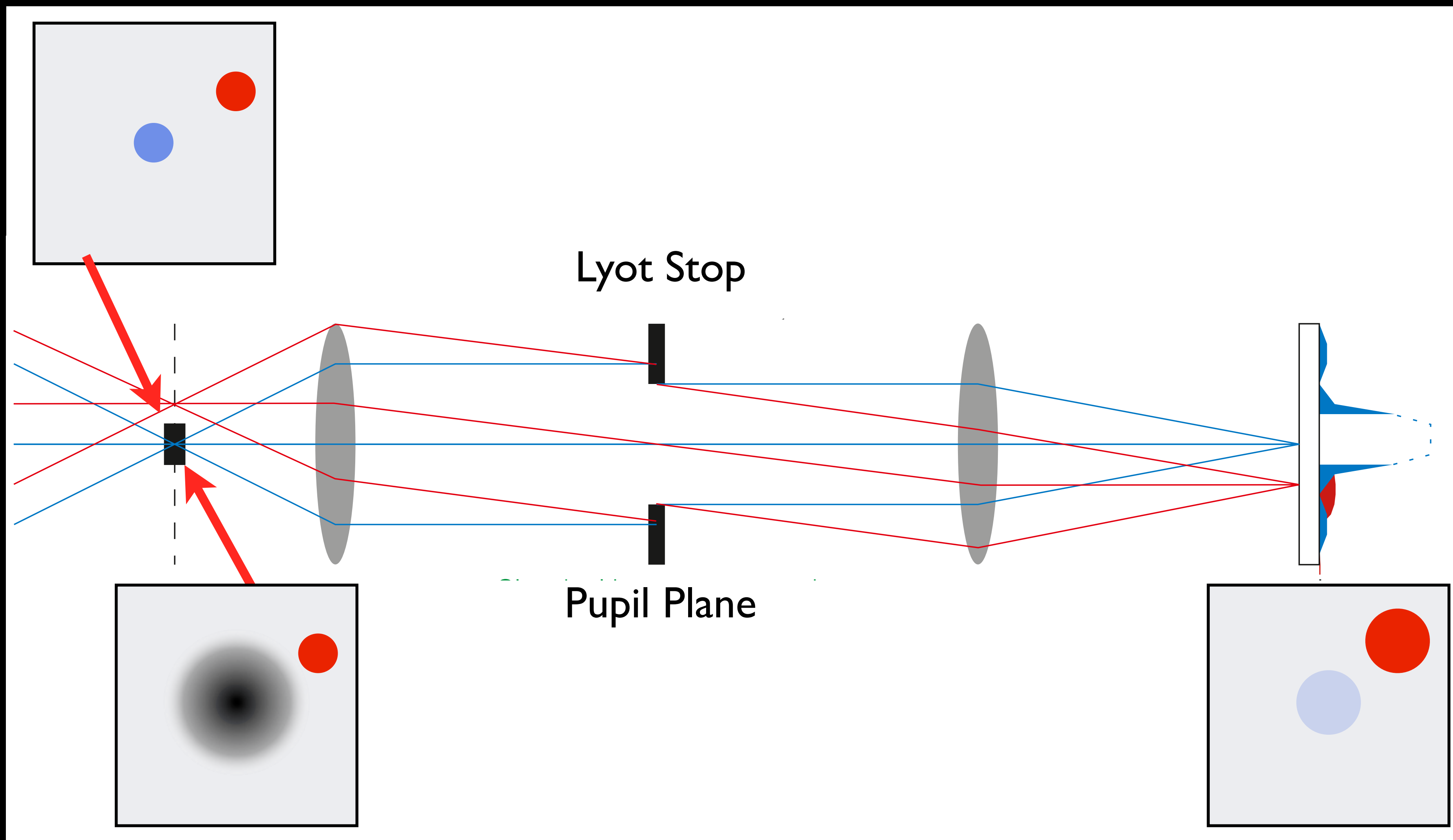

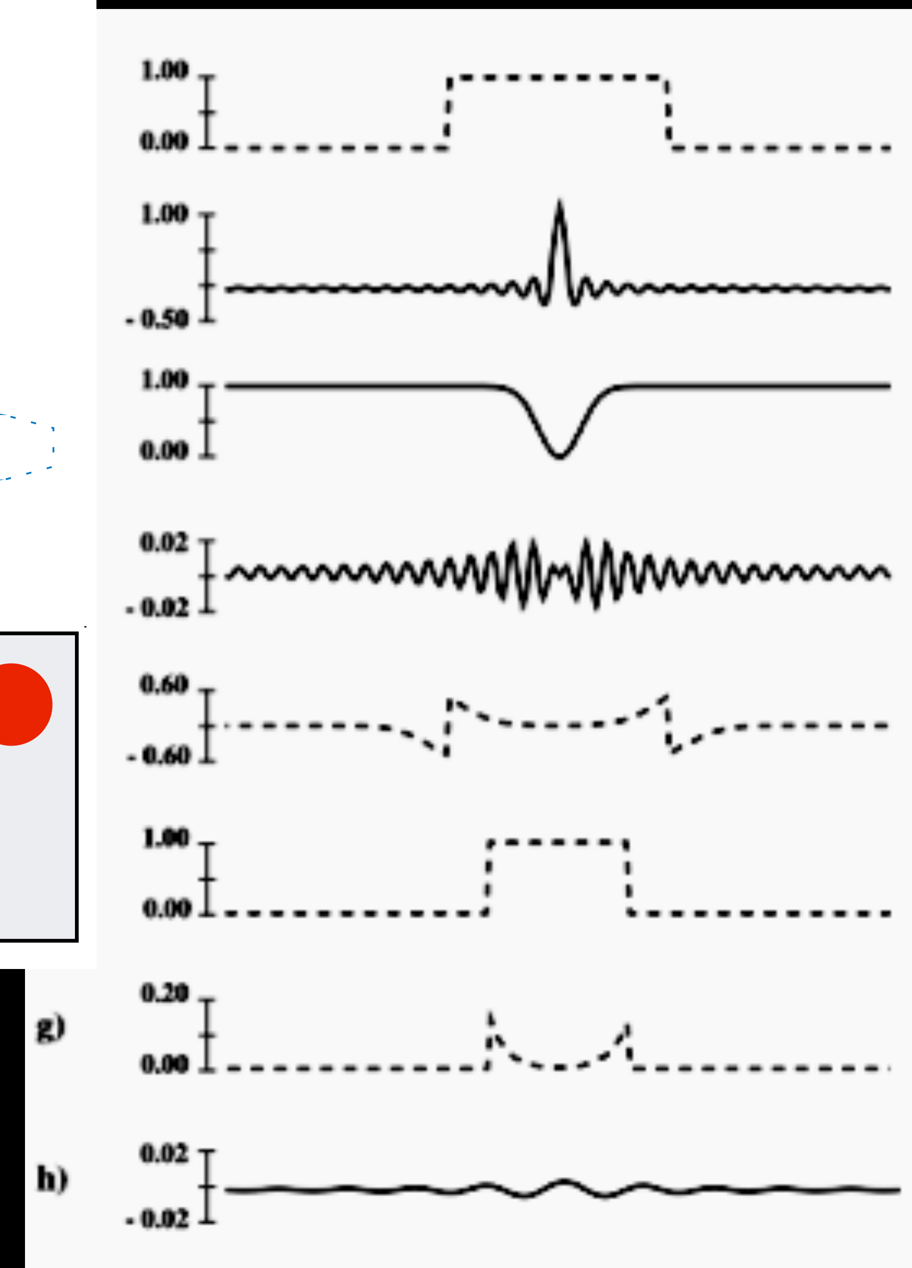

from Matt Kenworthy, University of Leiden

What is the bandwidth?

Bandlimited Lyot

Classical Lyot (Gaussian)

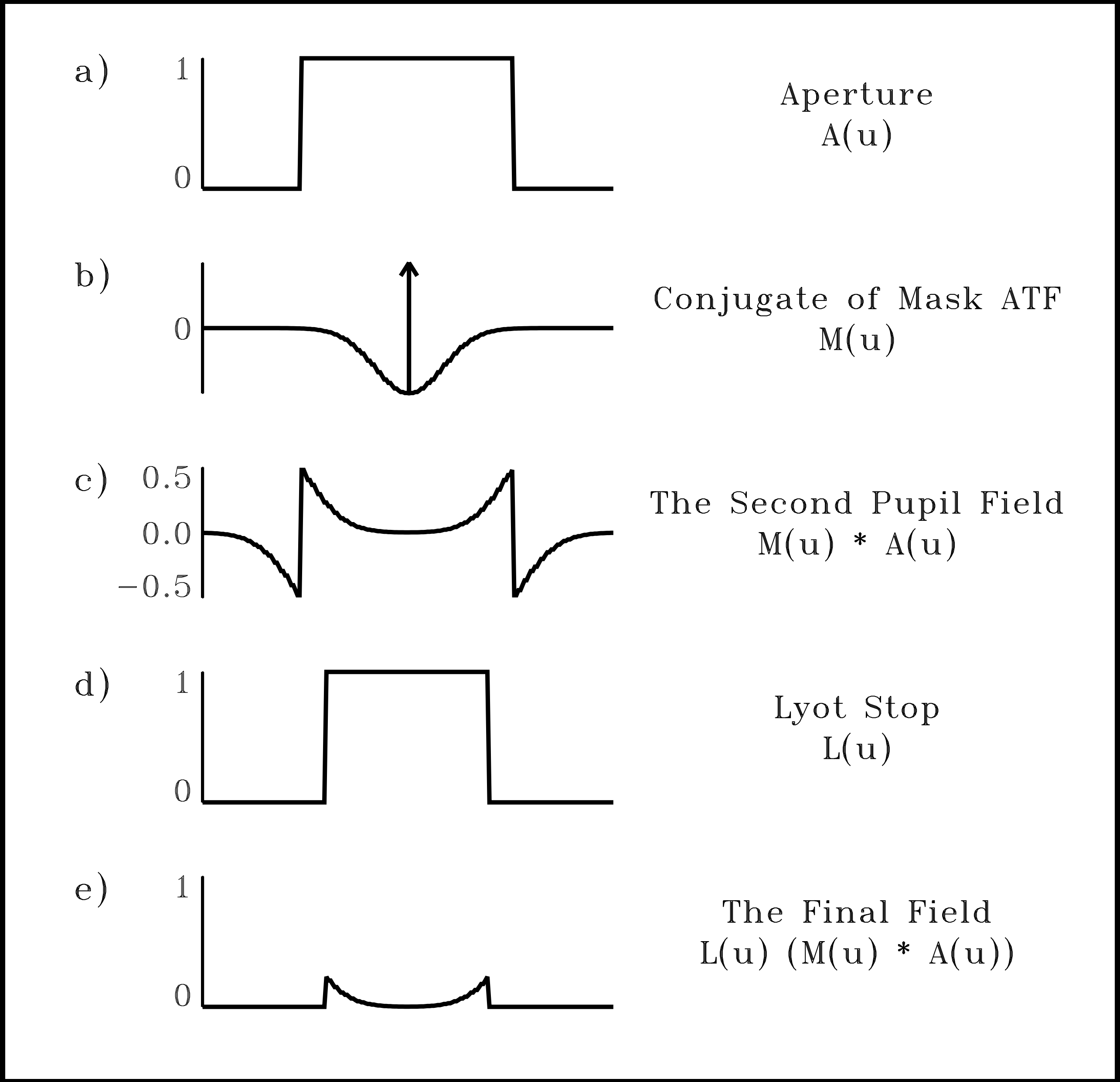

Kuchner & Traub (2002)

Bandlimited Lyot

Bandlimited Lyot

Classical Lyot (Gaussian)

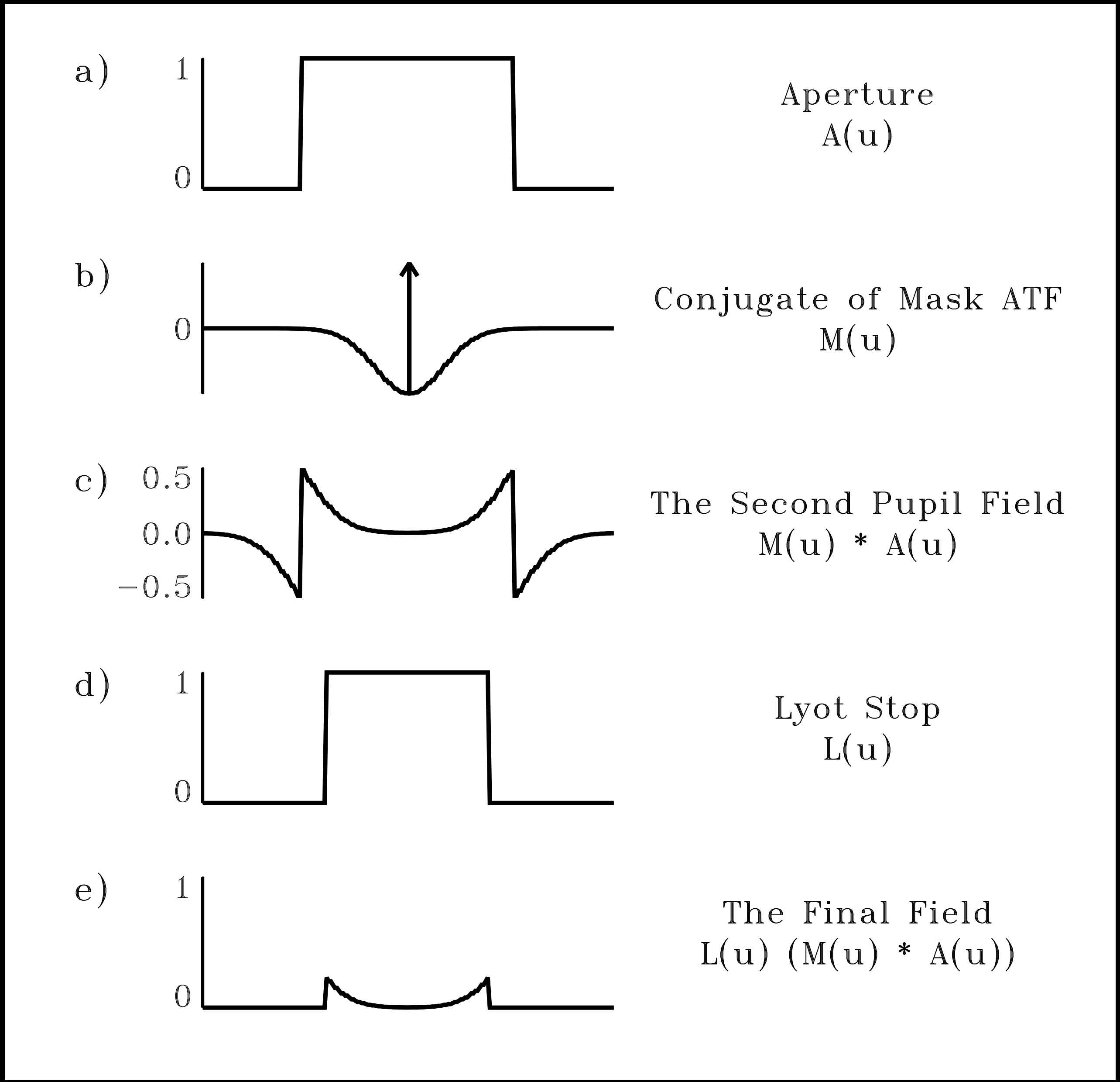

Bandlimited Lyot

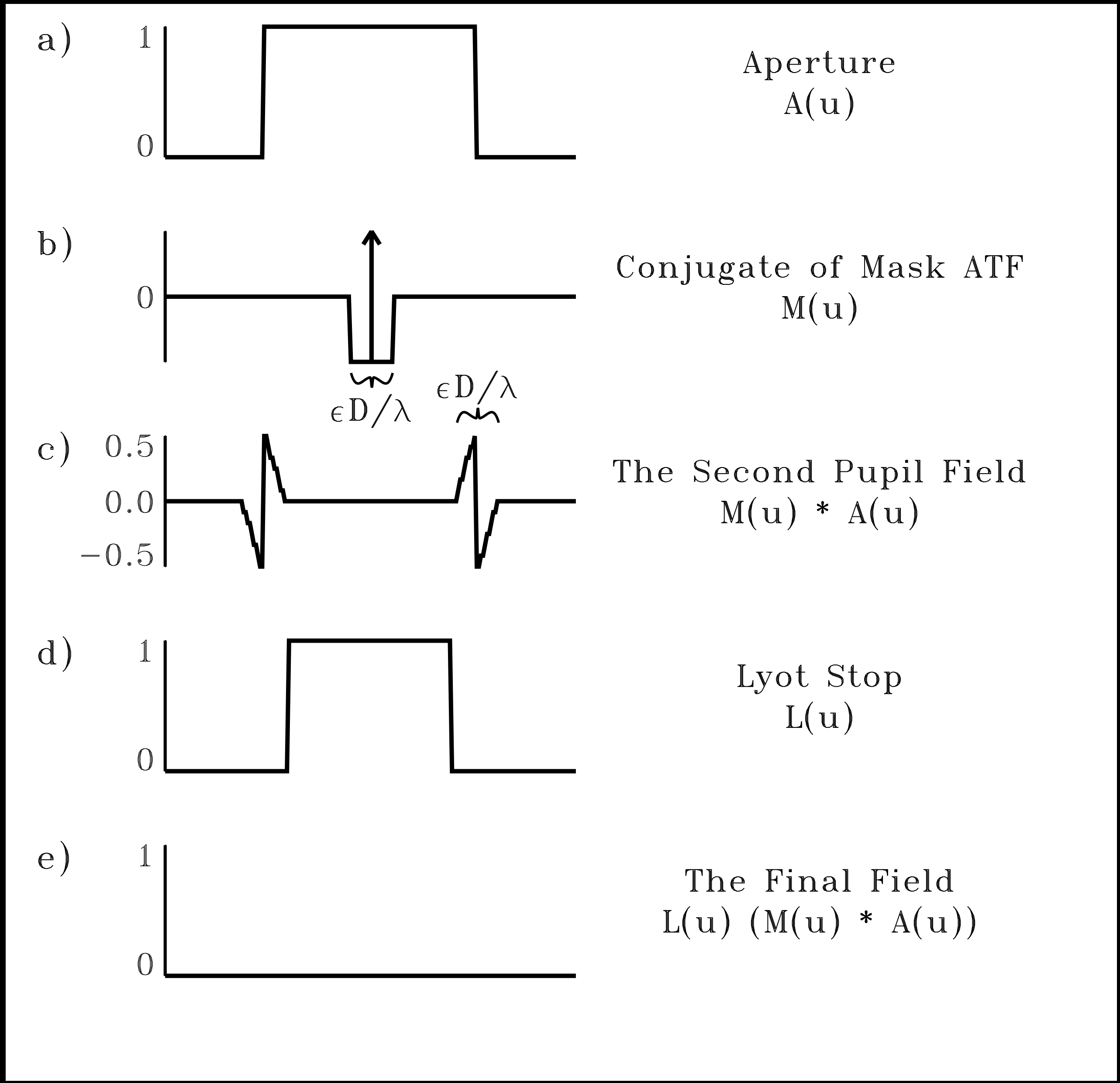

Kuchner & Traub (2002)

A sin^4 mask.

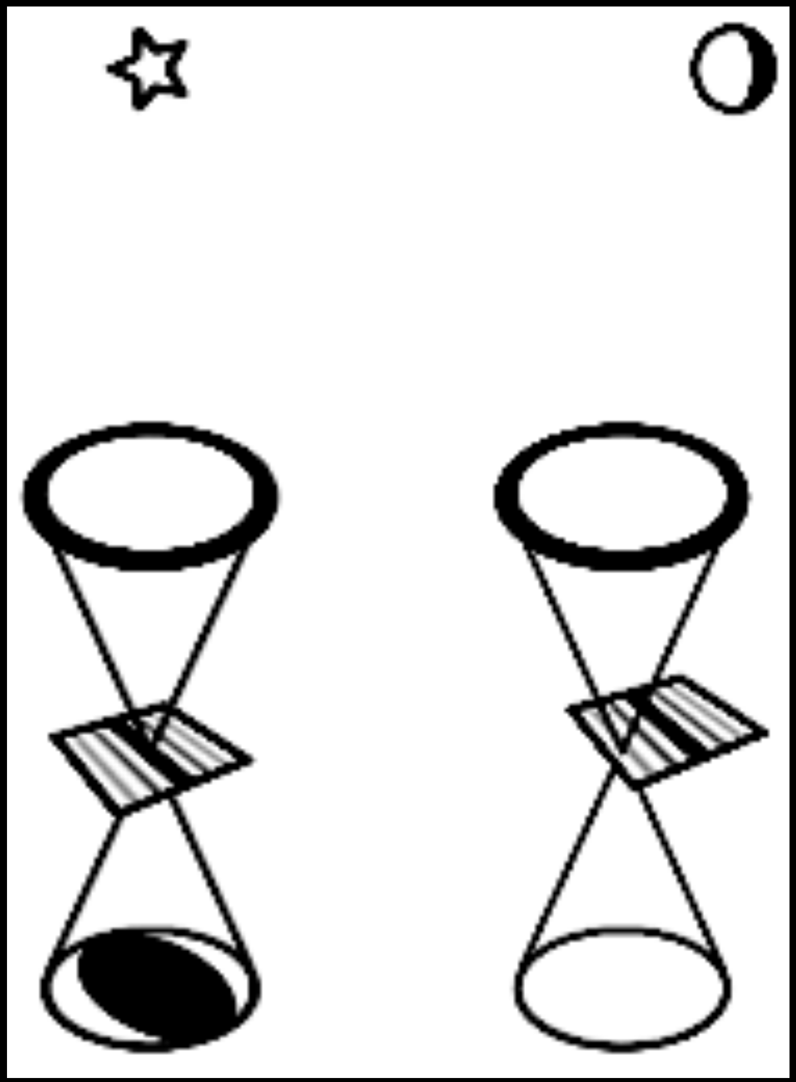

Throughput reduced by image plane mask & Lyot stop.

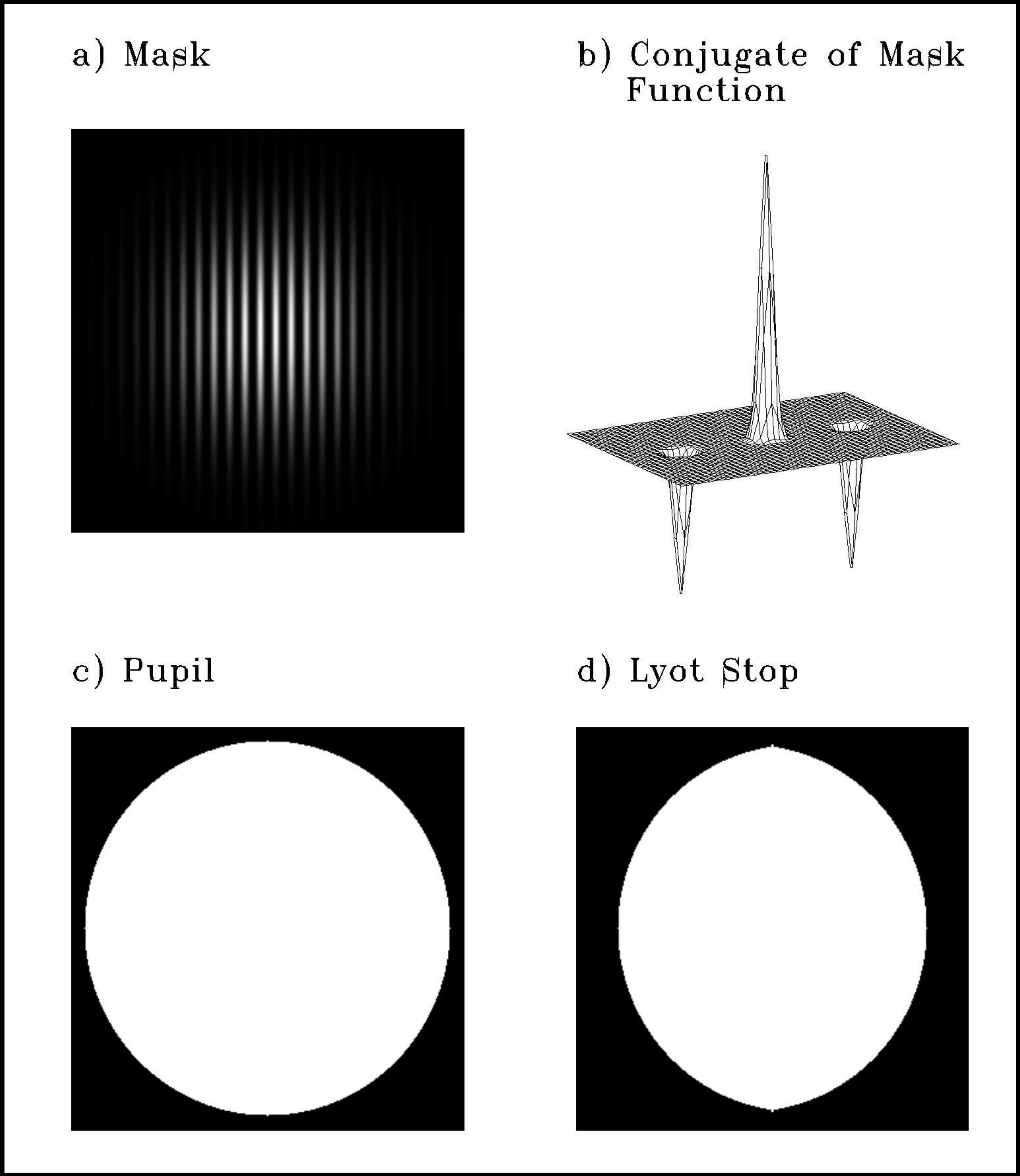

A General Picture

Coronagraph is a linear operator

E_i $\mathcal{A}(x)$ $\mathcal{C}\{E_i\}$ $\mathcal{A}_c(x) = A_c(x)e^{i\psi(x)}$

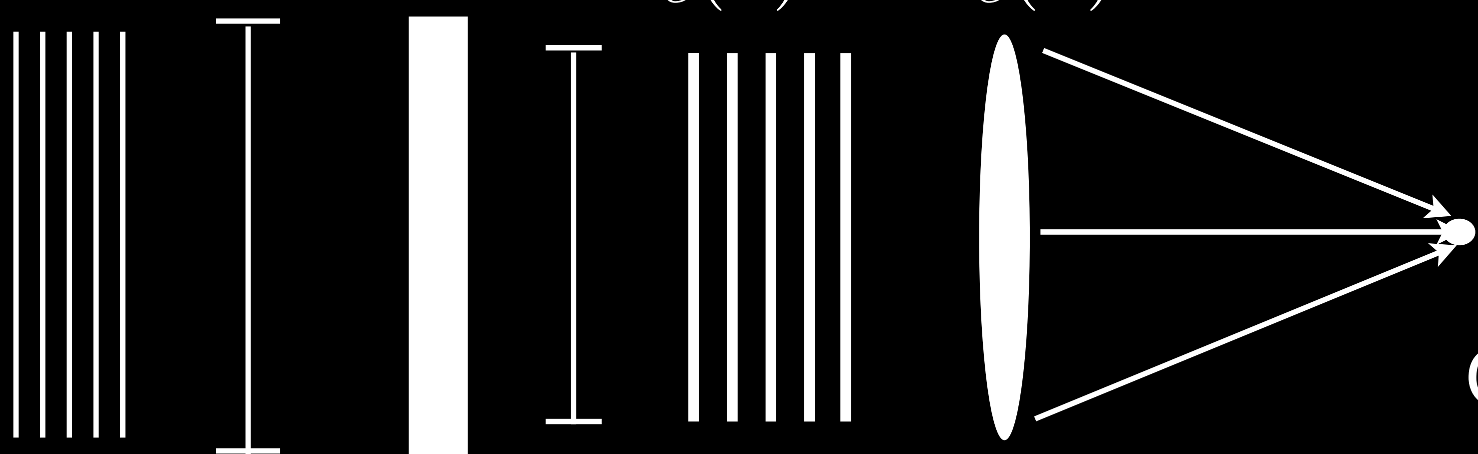

$$P_c(\omega) = \left|\mathcal{F}\left\{A_c(x)e^{i\psi(x)}\right\}\right|^2$$

On-Axis Point Spread Function

metric: contrast, bandwidth

A General Picture

Coronagraph is a linear operator

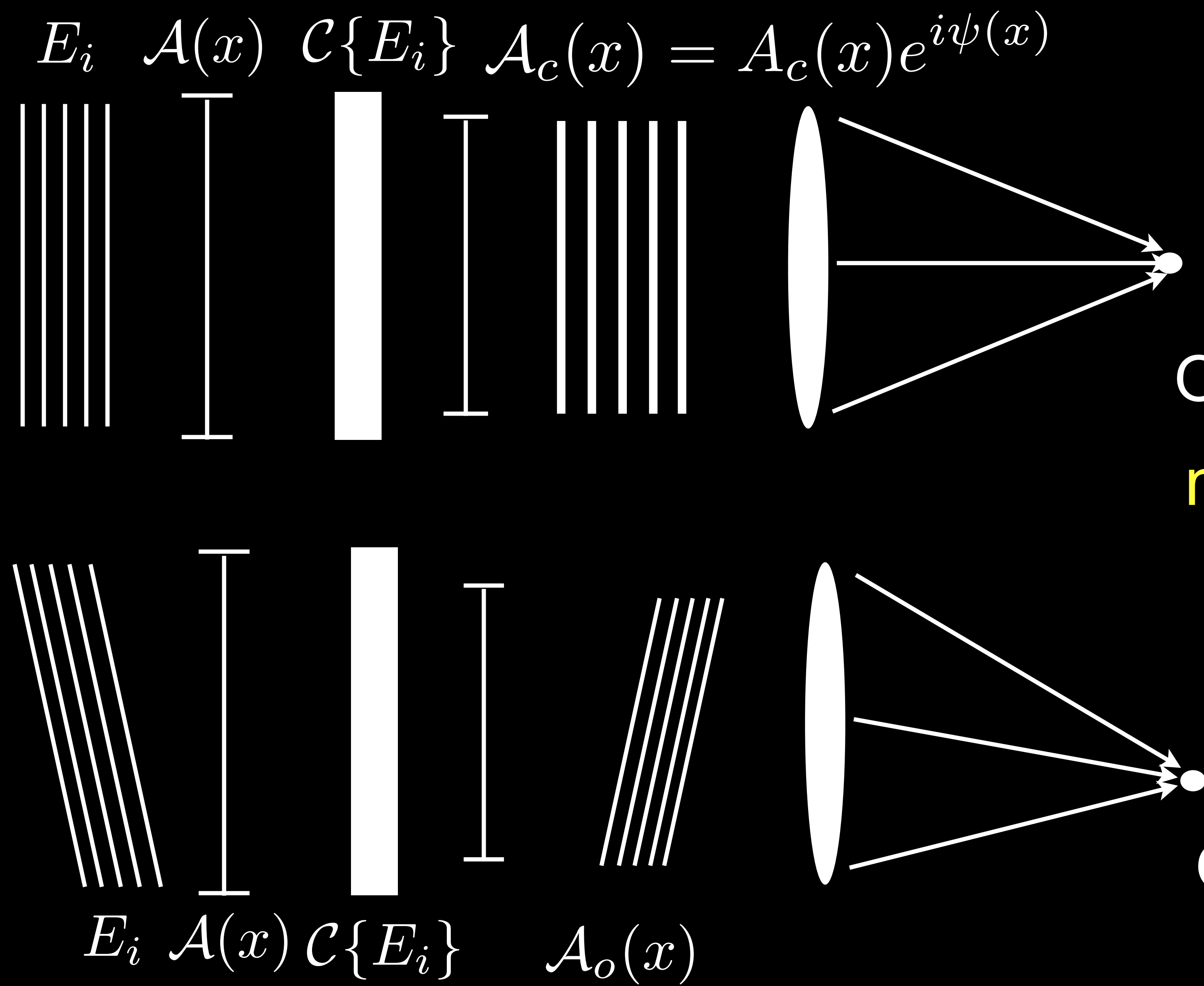

$$P_c(\omega) = \left|\mathcal{F}\left\{A_c(x)e^{i\psi(x)}\right\}\right|^2$$

On-Axis Point Spread Function

metric: contrast, bandwidth

$$P_o(\omega) = \left|\mathcal{F}\left\{\mathcal{A}_o\right\}\right|^2$$

Off-Axis Point Spread Function

metrics: iwa, throughput, sharpness

A General Picture

Coronagraph is a linear operator

E_i $\mathcal{A}(x)$ $\mathcal{C}\{E_i\}$ $\mathcal{A}_c(x) = A_c(x)e^{i\psi(x)}$

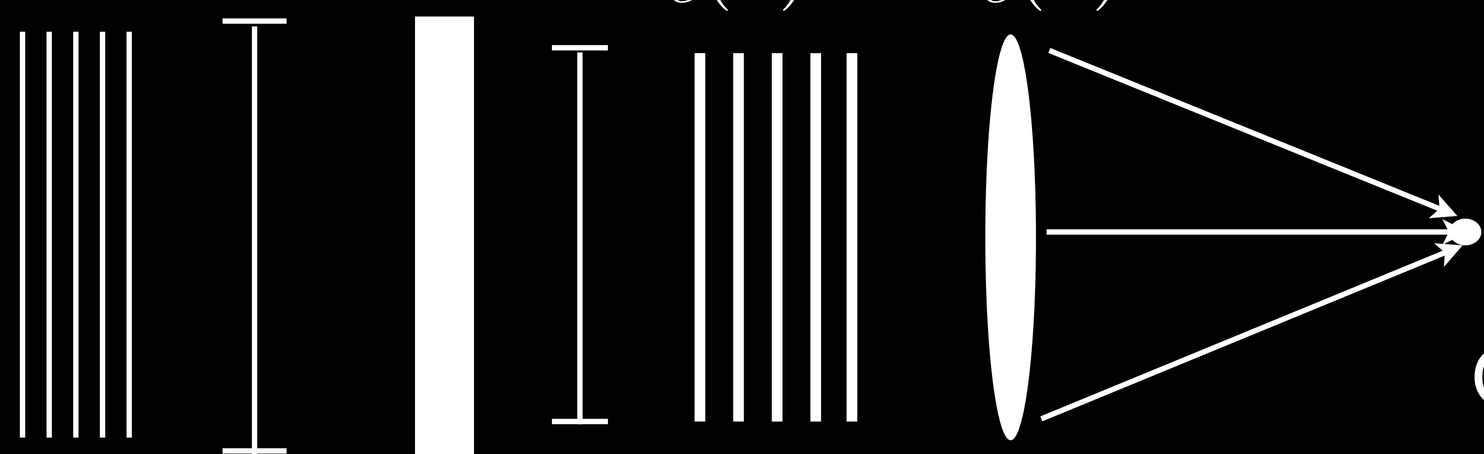

$$P_c(\omega) = \left|\mathcal{F}\left\{A_c(x)e^{i\psi(x)}\right\}\right|^2$$

On-Axis Point Spread Function

metric: contrast, bandwidth

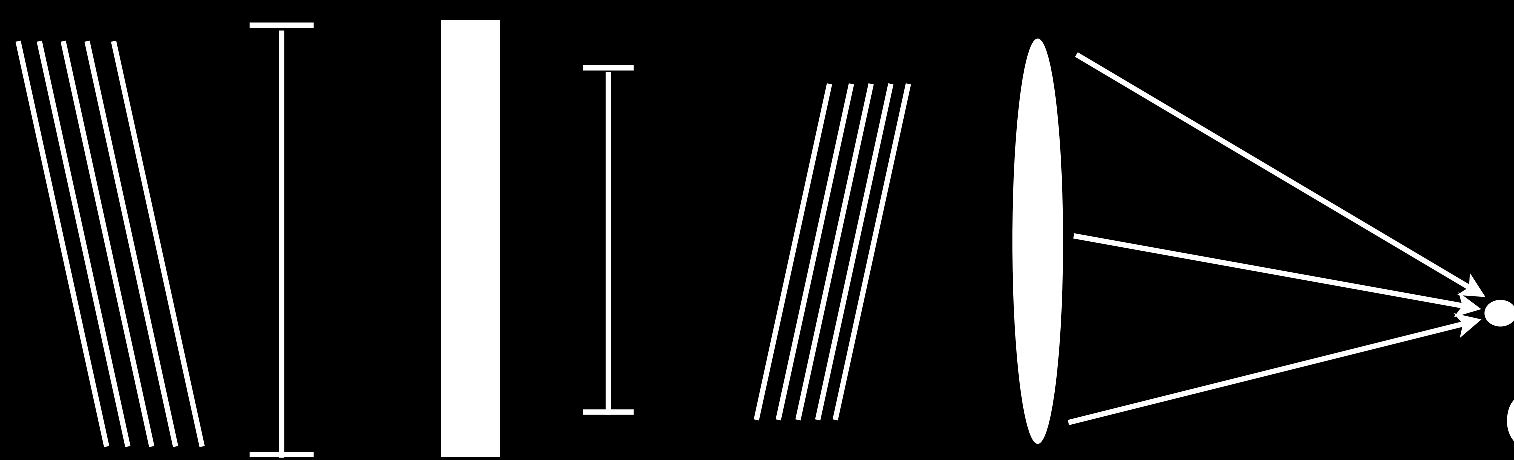

E_i $\mathcal{A}(x)$ $\mathcal{C}\{E_i\}$ $\mathcal{A}_o(x)$

$$P_o(\omega) = \left|\mathcal{F}\left\{\mathcal{A}_o\right\}\right|^2$$

Off-Axis Point Spread Function

metrics: iwa, throughput, sharpness

Instrument Contrast (on-axis behavior)

E_i $\quad \mathcal{A}(x)$ $\quad \mathcal{C}\{E_i\}$ $\quad \mathcal{A}_c(x) = A_c(x)e^{i\psi(x)}$

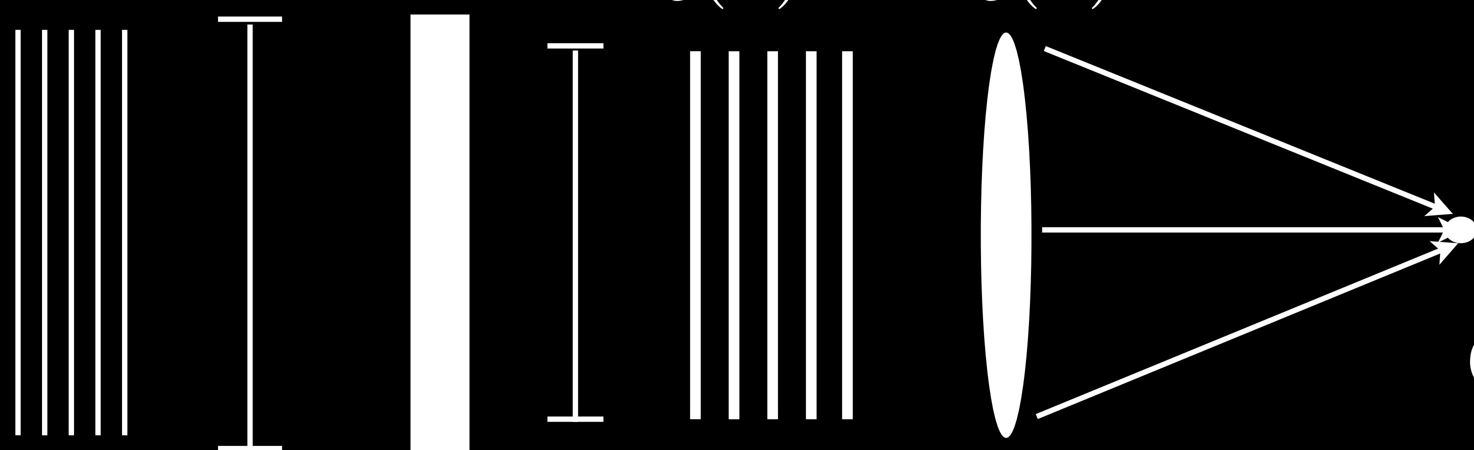

$$P_c(\omega) = \left|\mathcal{F}\left\{A_c(x)e^{i\psi(x)}\right\}\right|^2$$

On-Axis Point Spread Function

The Instrument Contrast Ratio (at a specific wavelength)

$$C_i = \frac{\int_{\Delta\Omega} P_c(\omega)d\omega}{\Delta\Omega P_o(0)} = \frac{\int_S |\mathcal{A}_c(x)|^2 dx}{\Delta\Omega A_o^2}\left[1 - \frac{\int_{\Delta C} P_c(\omega)d\omega}{\int_{-\infty}^{\infty} P_c(\omega)d\omega}\right]$$

Instrument Contrast (on-axis behavior)

$$E_i \quad \mathcal{A}(x) \quad \mathcal{C}\{E_i\} \quad \mathcal{A}_c(x) = A_c(x)e^{i\psi(x)}$$

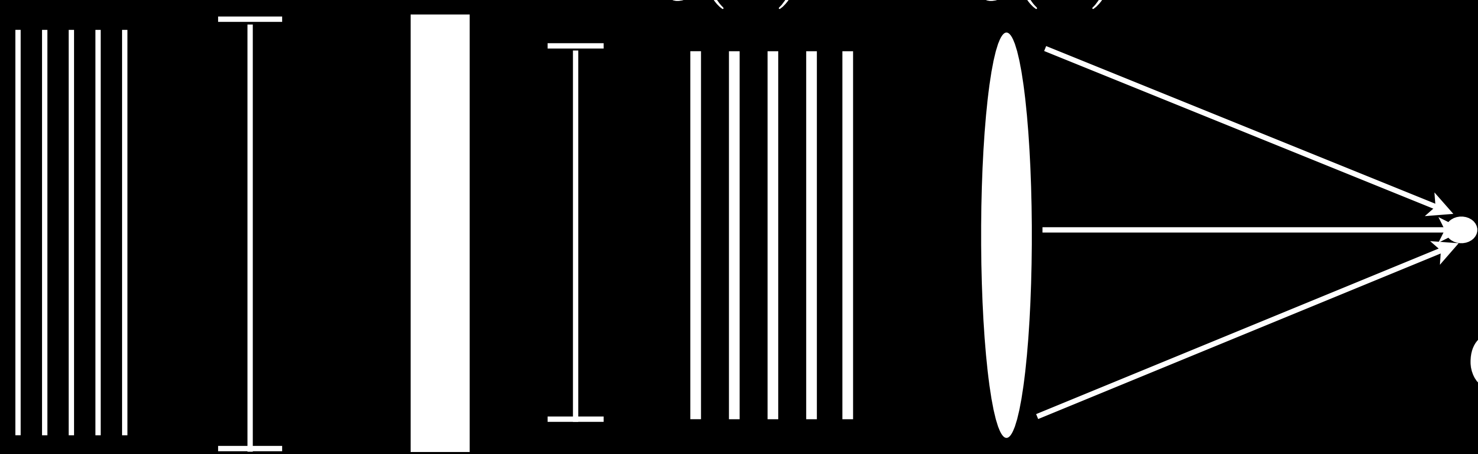

$$P_c(\omega) = \left|\mathcal{F}\left\{A_c(x)e^{i\psi(x)}\right\}\right|^2$$

On-Axis Point Spread Function

The Instrument Contrast Ratio (at a specific wavelength)

$$C_i = \frac{\int_{\Delta\Omega} P_c(\omega)d\omega}{\Delta\Omega P_o(0)} = \frac{\int_S |\mathcal{A}_c(x)|^2 dx}{\Delta\Omega A_o^2}\left[1 - \frac{\int_{\Delta C} P_c(\omega)d\omega}{\int_{-\infty}^{\infty} P_c(\omega)d\omega}\right]$$

Reduce the exit amplitude

Instrument Contrast (on-axis behavior)

$E_i \quad \mathcal{A}(x) \quad \mathcal{C}\{E_i\} \quad \mathcal{A}_c(x) = A_c(x)e^{i\psi(x)}$

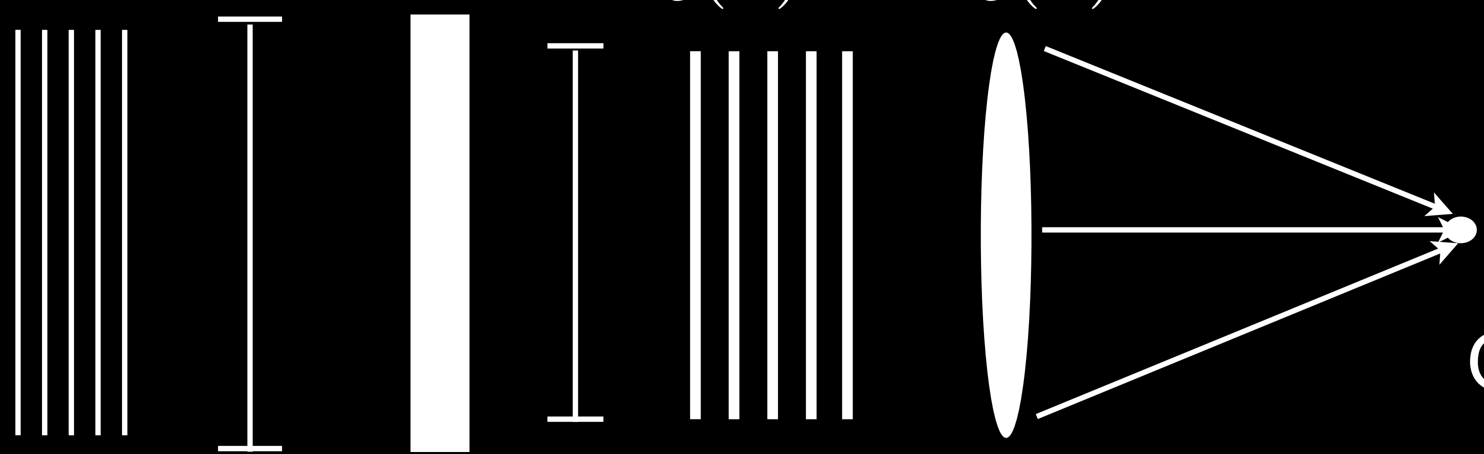

$$P_c(\omega) = \left| \mathcal{F}\left\{ A_c(x)e^{i\psi(x)} \right\} \right|^2$$

On-Axis Point Spread Function

The Instrument Contrast Ratio (at a specific wavelength)

$$C_i = \frac{\int_{\Delta\Omega} P_c(\omega)d\omega}{\Delta\Omega P_o(0)} = \frac{\int_S |\mathcal{A}_c(x)|^2 dx}{\Delta\Omega A_o^2} \left[1 - \frac{\int_{\Delta C} P_c(\omega)d\omega}{\int_{-\infty}^{\infty} P_c(\omega)d\omega} \right]$$

Reduce the exit amplitude

Shift the energy
(uncertainty principal)

Coronagraph Families

- Lyot & Bandlimited Lyot (Gemini, Keck, Hubble, Subaru, Palomar, VLT, JWST NICI, AFTA)
- 4 Quadrant Phase Mask (JWST MIRI, VLT, LBT)
- Optical Vortex (Palomar, VLT, LBT)
- AIC, VNC and other nullers

- Apodized pupils (VLT)
- Shaped pupils (SPICA, Subaru, AFTA)
- Pupil remappers (PIAA) (Subaru)
- Apodized phase plate (MMT, Magellan, VLT)

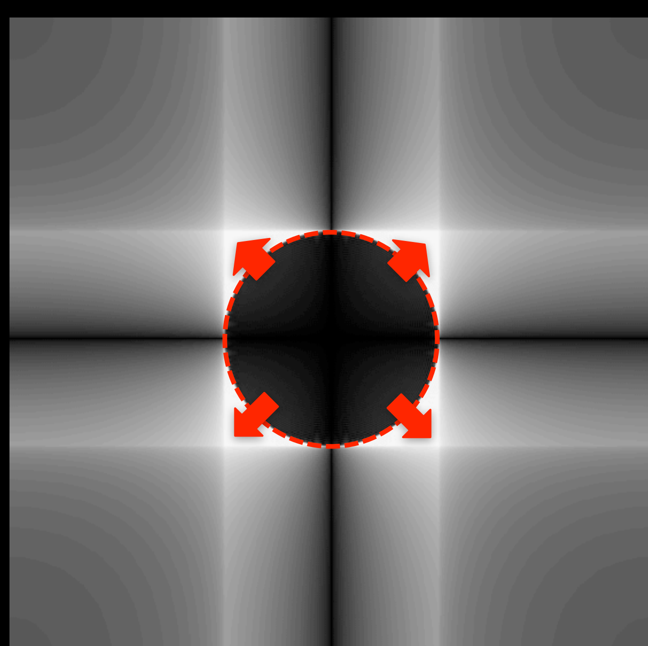

APLC
(GPI, VLT/SPHERE, Palomar)

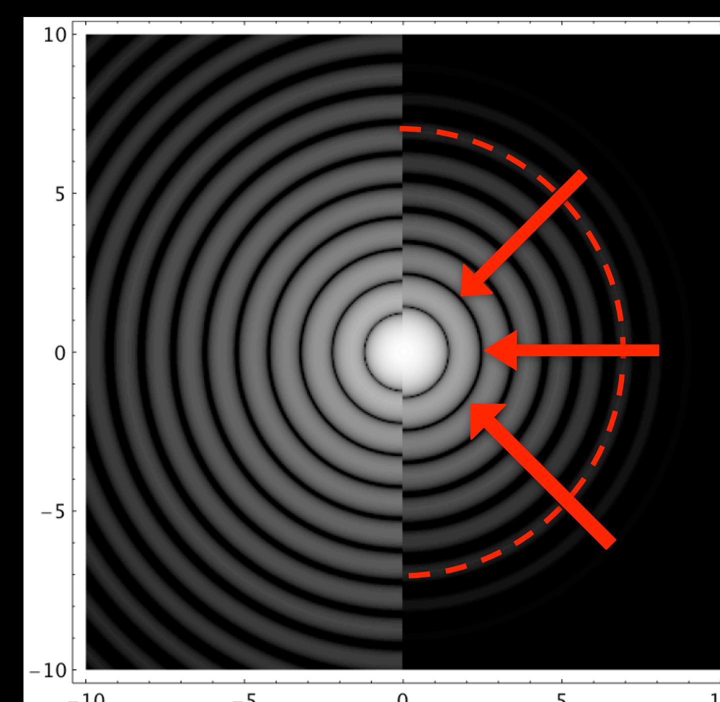

Coronagraphs That Change Amplitude

Focal Plane Amplitude Mask: Lyot & Bandlimited Lyot, AIC

Focal Plane Phase Mask: 4QPM, Vector Vortex

Four-Quadrant Phase Mask coronagraph (Rouan) (4QPM)

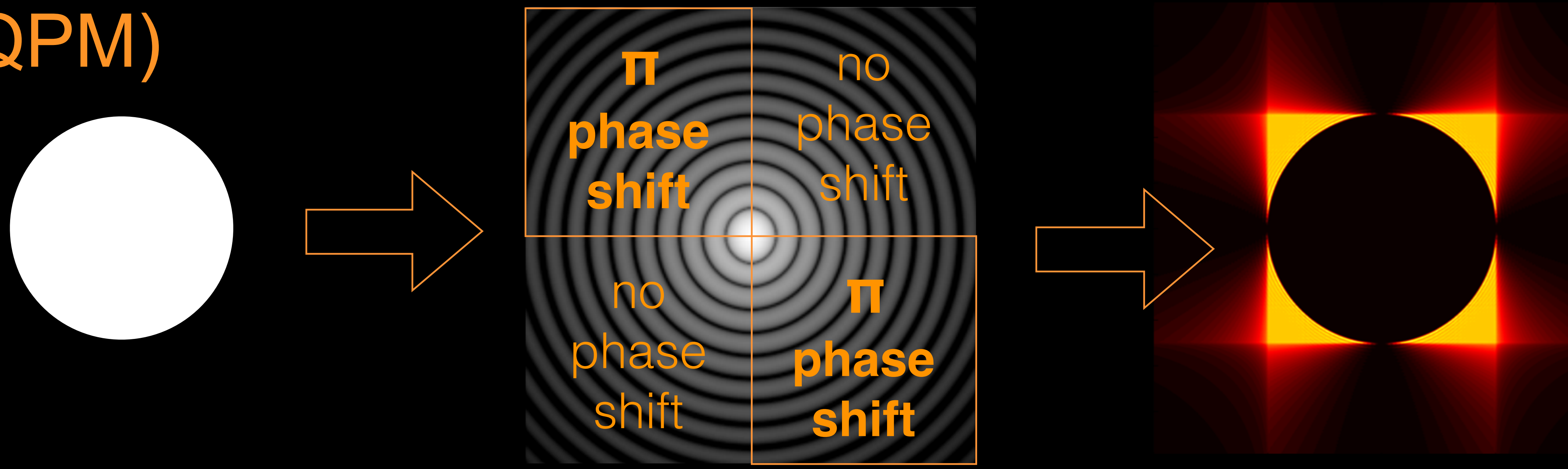

Pupil plane Image plane w/ mask Pupil plane

Vector vortex coronagraph (Mawet)

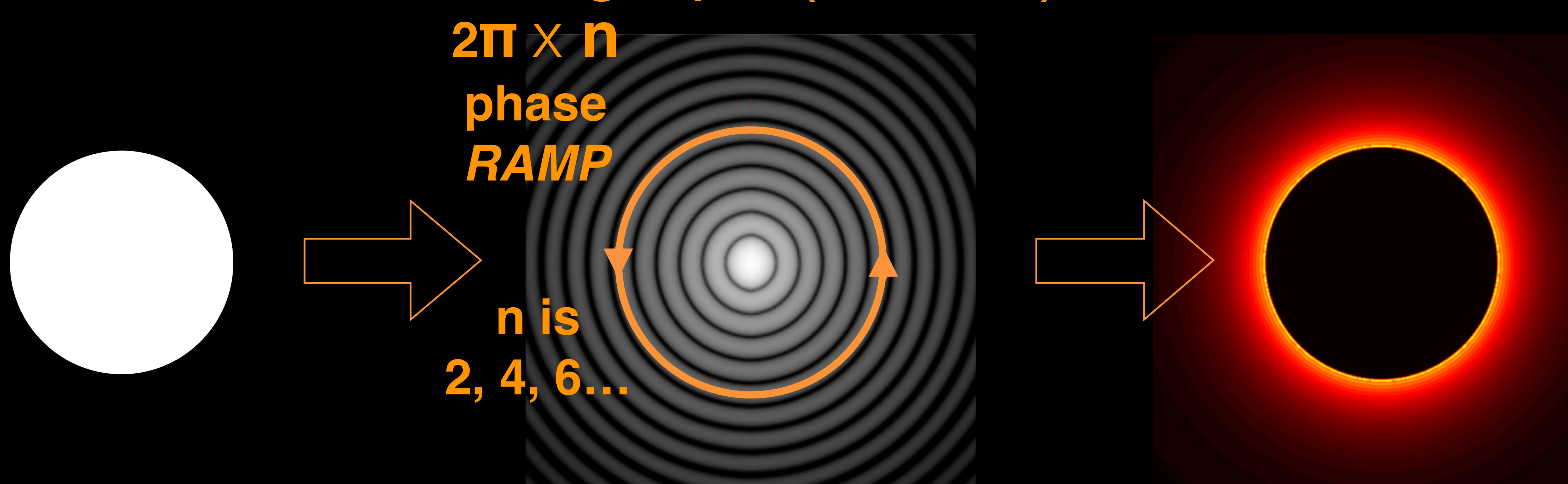

Coronagraphs That Reshape PSF

Pupil Plane Amplitude Mask: Shaped Pupils, PIAA

Pupil Plane Phase Mask: APP

Pupil Apodization to Reshape PSF

Slepian, D., "Analytic Solution of Two Apodization Problems", September, 1965

Pupil Apodization

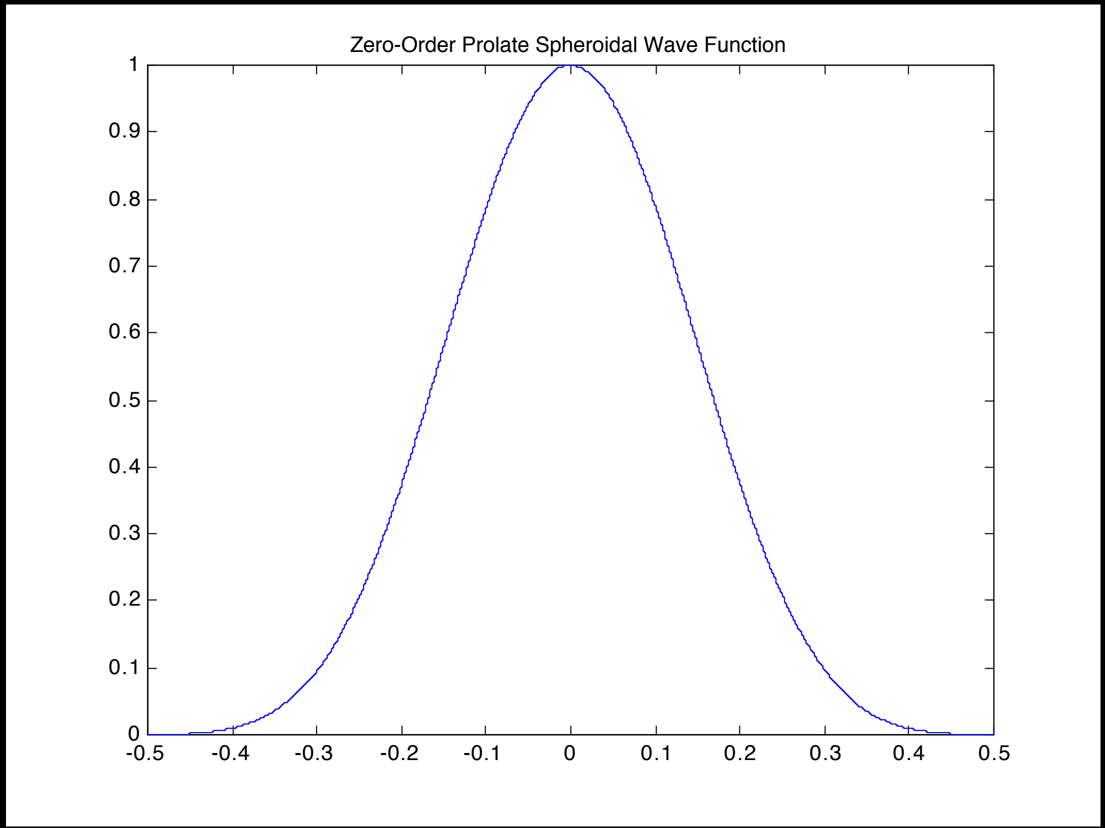

Point Spread Function

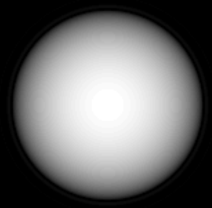

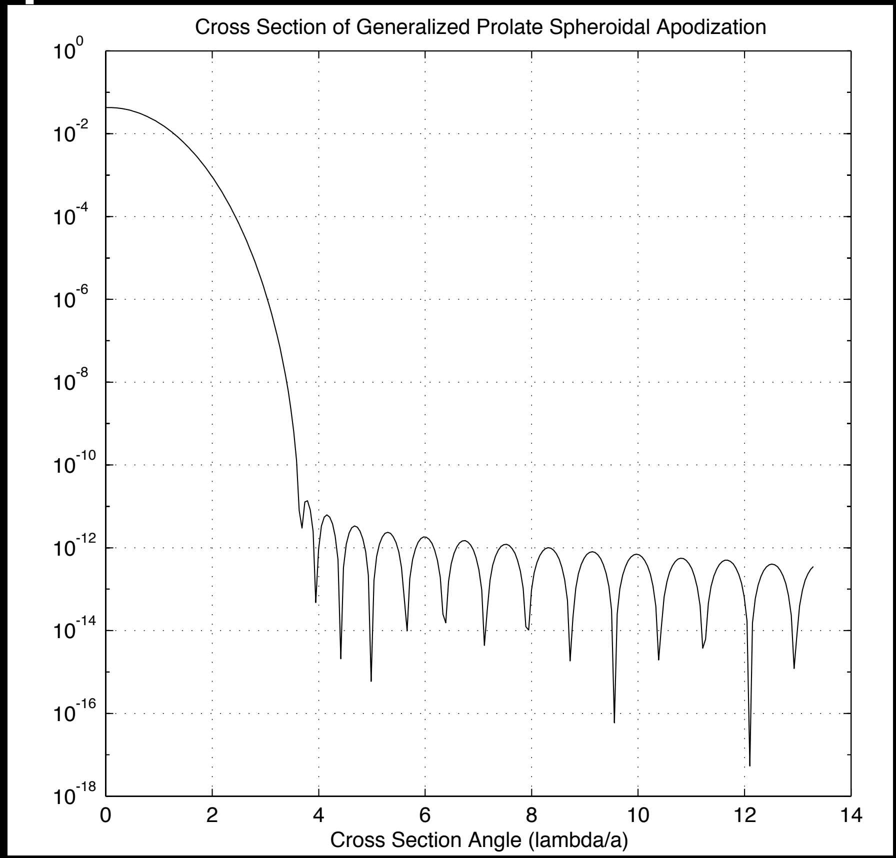

The "optimal" apodization that maximally concentrates light is the Prolate Spheroidal Wavefunction, based on finite uncertainty principle.

Pupil Apodization to Reshape PSF

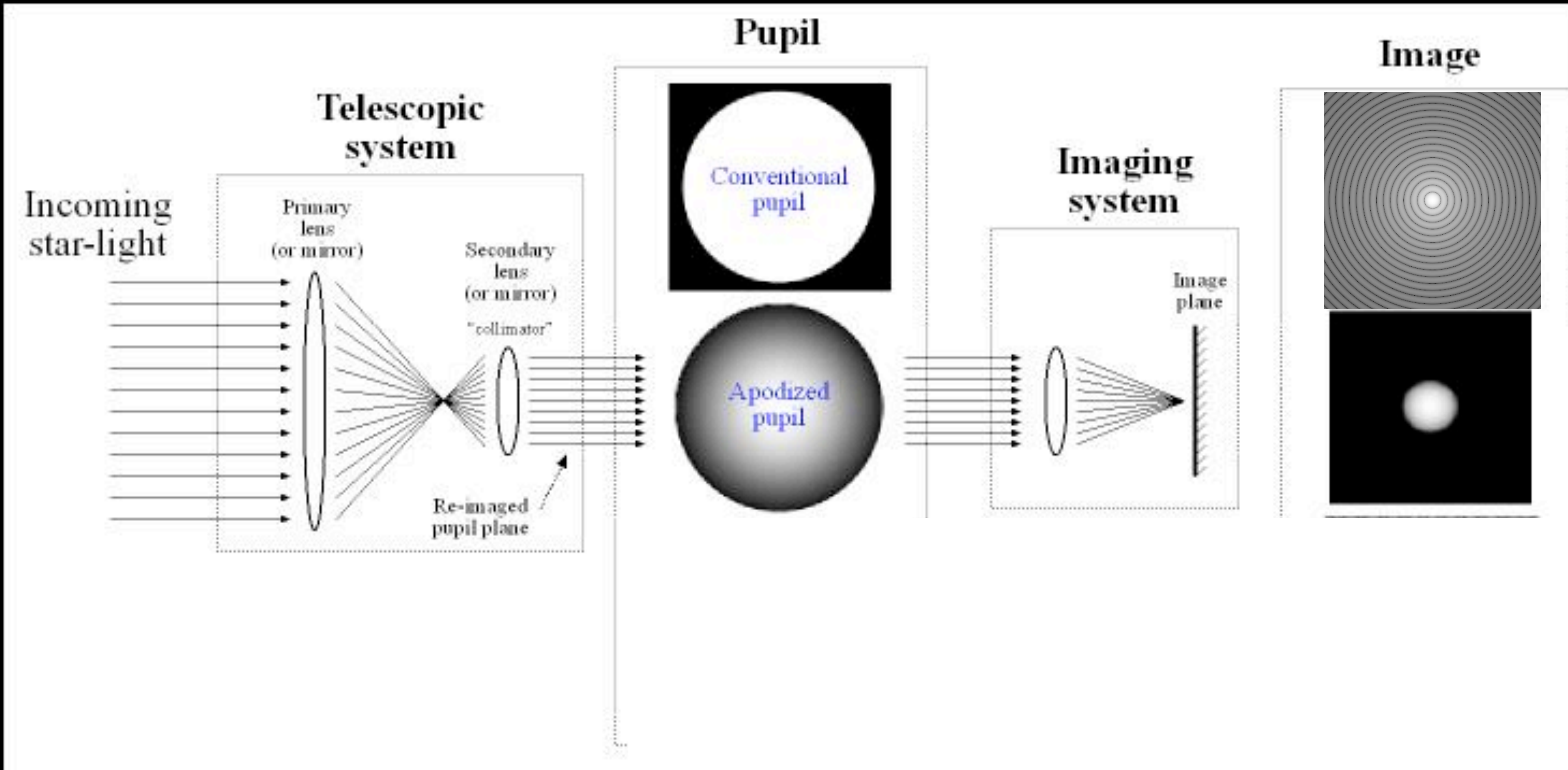

Shaped pupil contrast independent of wavelength.

Pupil Apodization to Reshape PSF

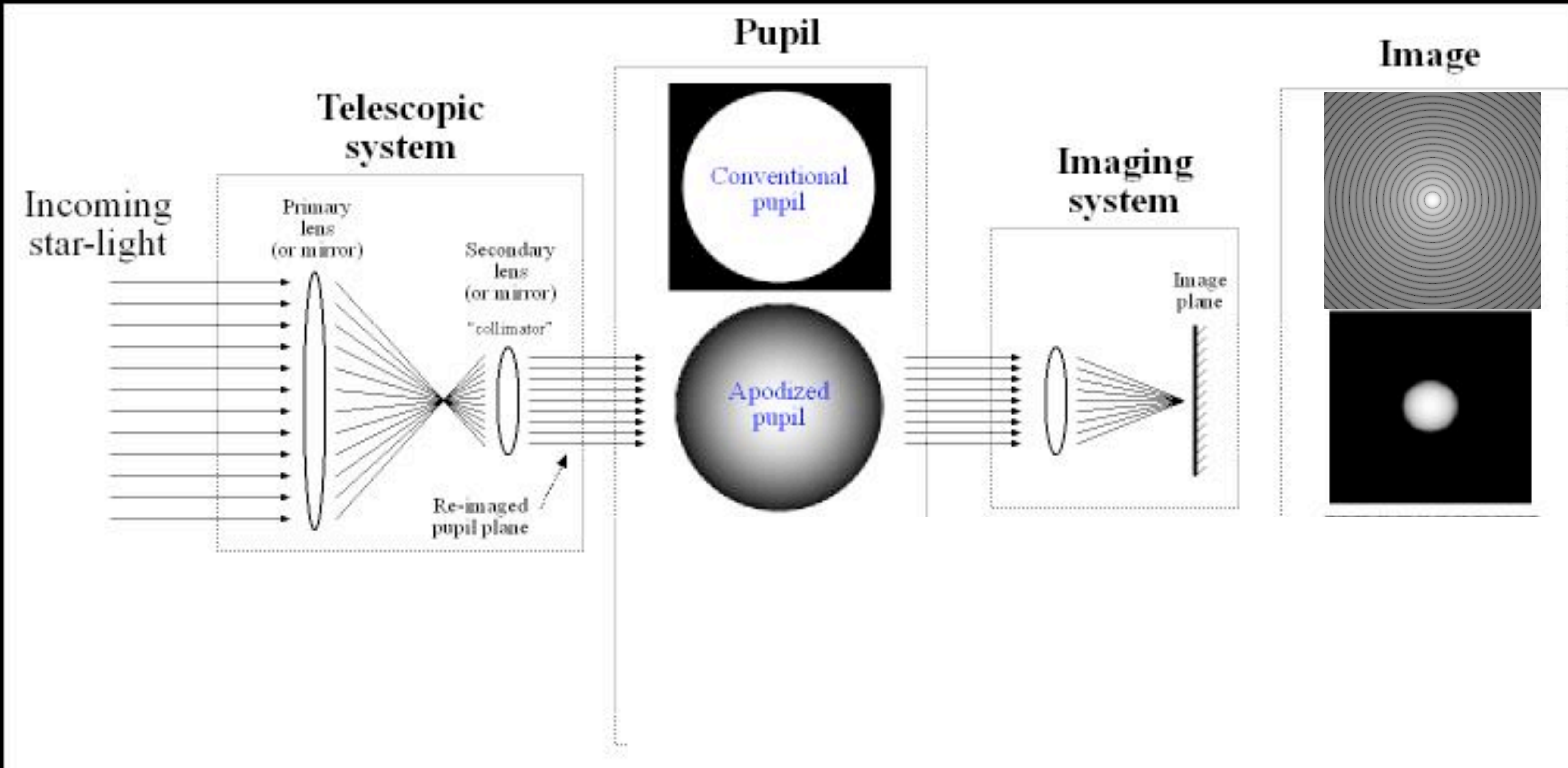

Shaped pupil contrast independent of wavelength.

Pupil Apodization to Reshape PSF

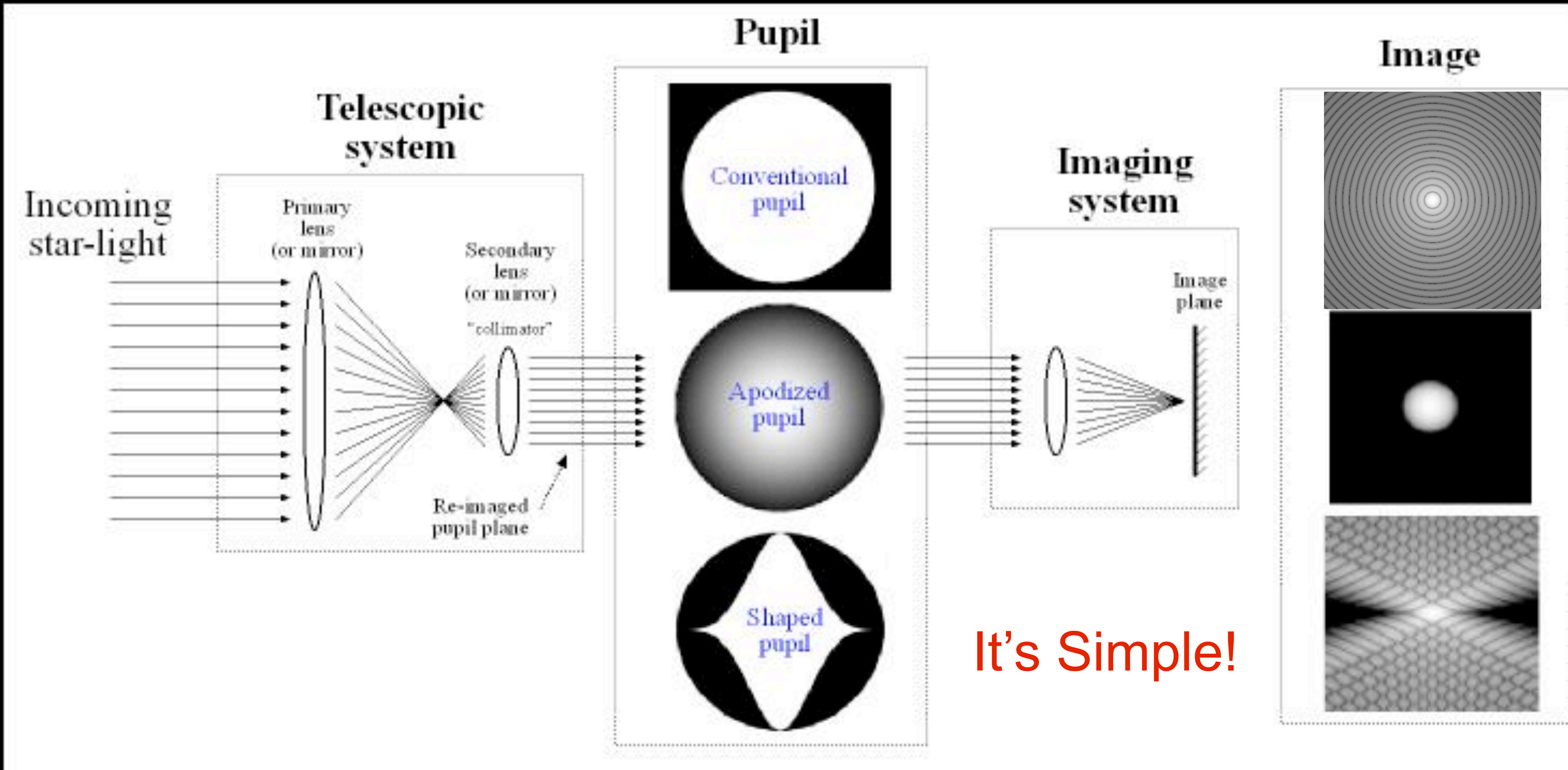

Shaped pupil contrast independent of wavelength.

Shaped Pupil Zoo (1D)

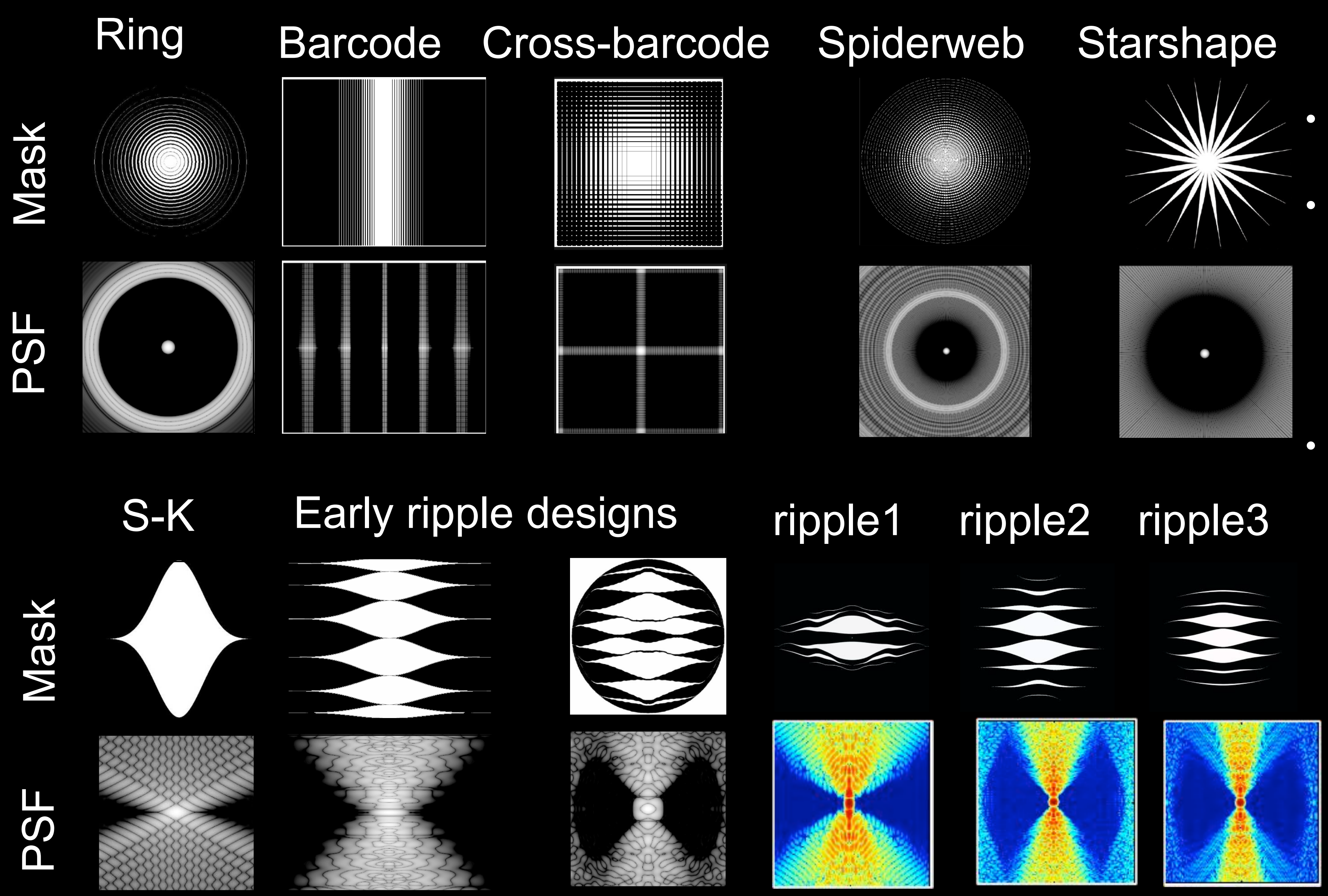

- Shaped pupils: A(x,y) is zero-one valued (holes in masks)
- Advantages:
  - simple to manufacture
  - inherently broadband
  - minimally sensitive to aberrations
  - no off-axis degradation of PSF
- Disadvantages:
  - throughput (though roughly the same as 8^{th} order Lyot coronagraph)
  - IWA (better IWA can be achieved through less discovery space or greater simplicity)

Pupils designed via optimization under certain constraints

Direct 2 D Optimization of SPs

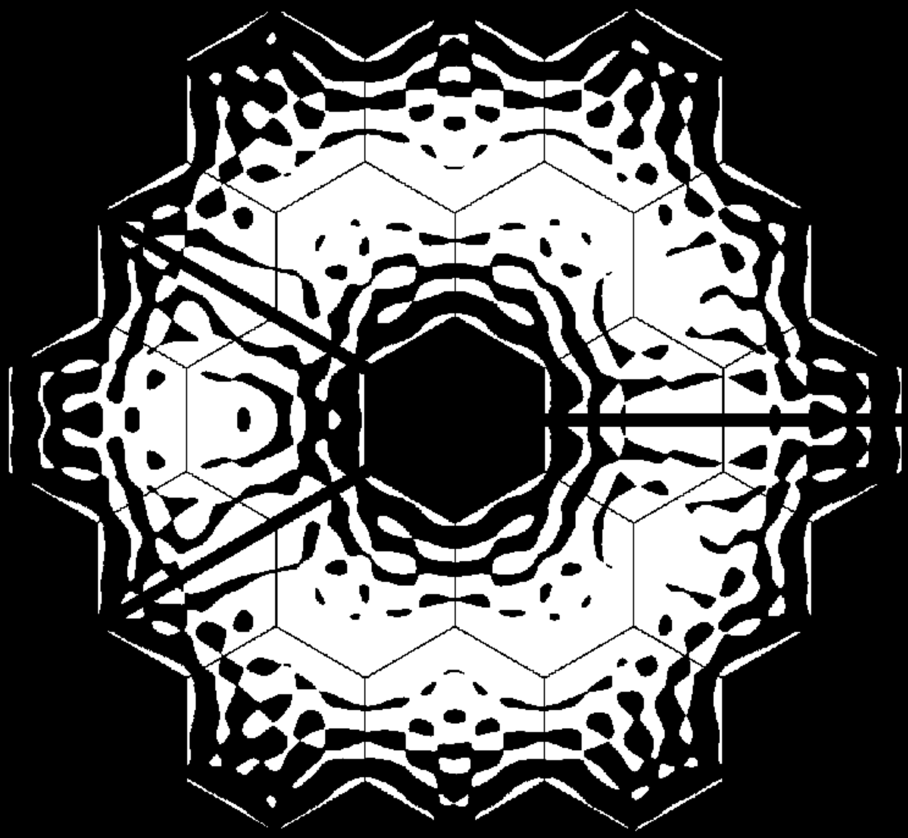

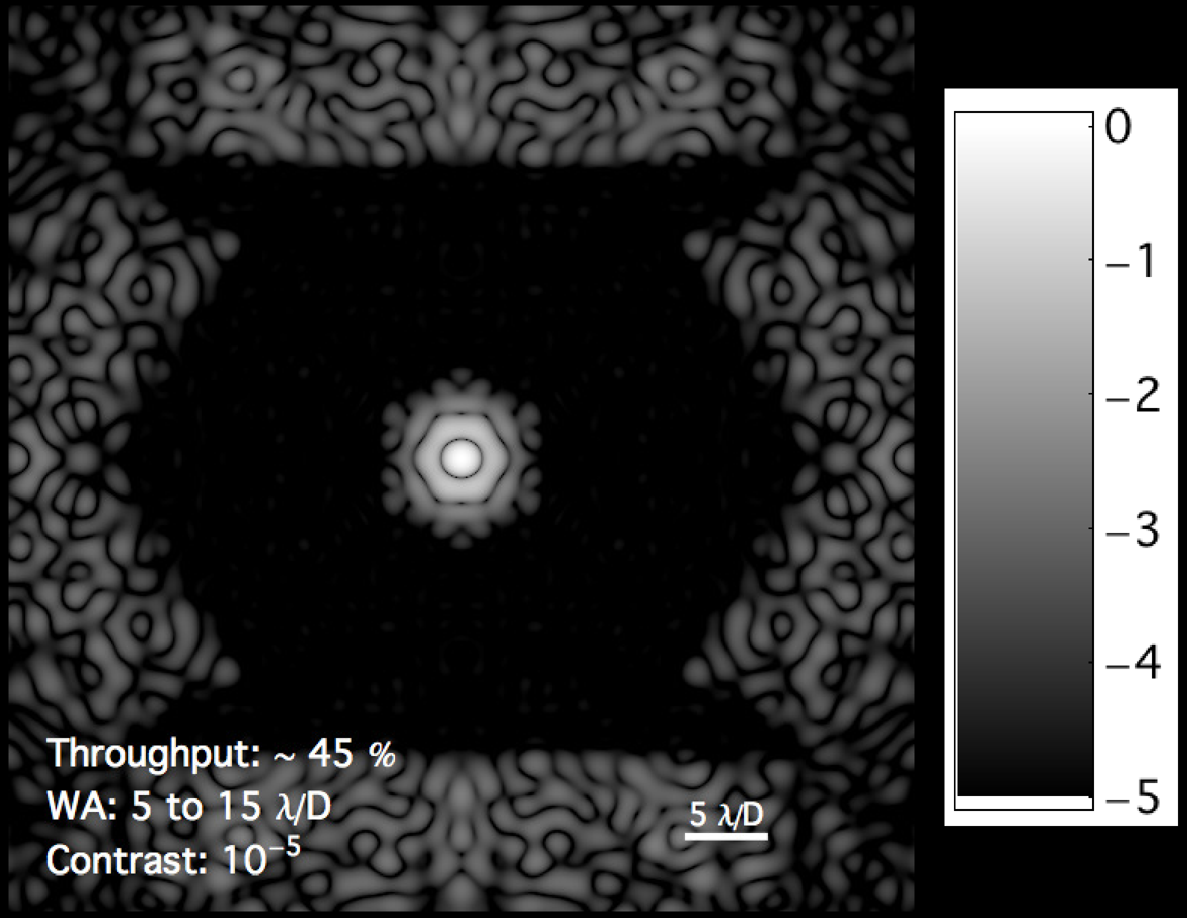

JWST

45% Throughput

5 to 15 lambda/D

10^{-5} Contrast

First Lab Test of 2D SP at Princeton

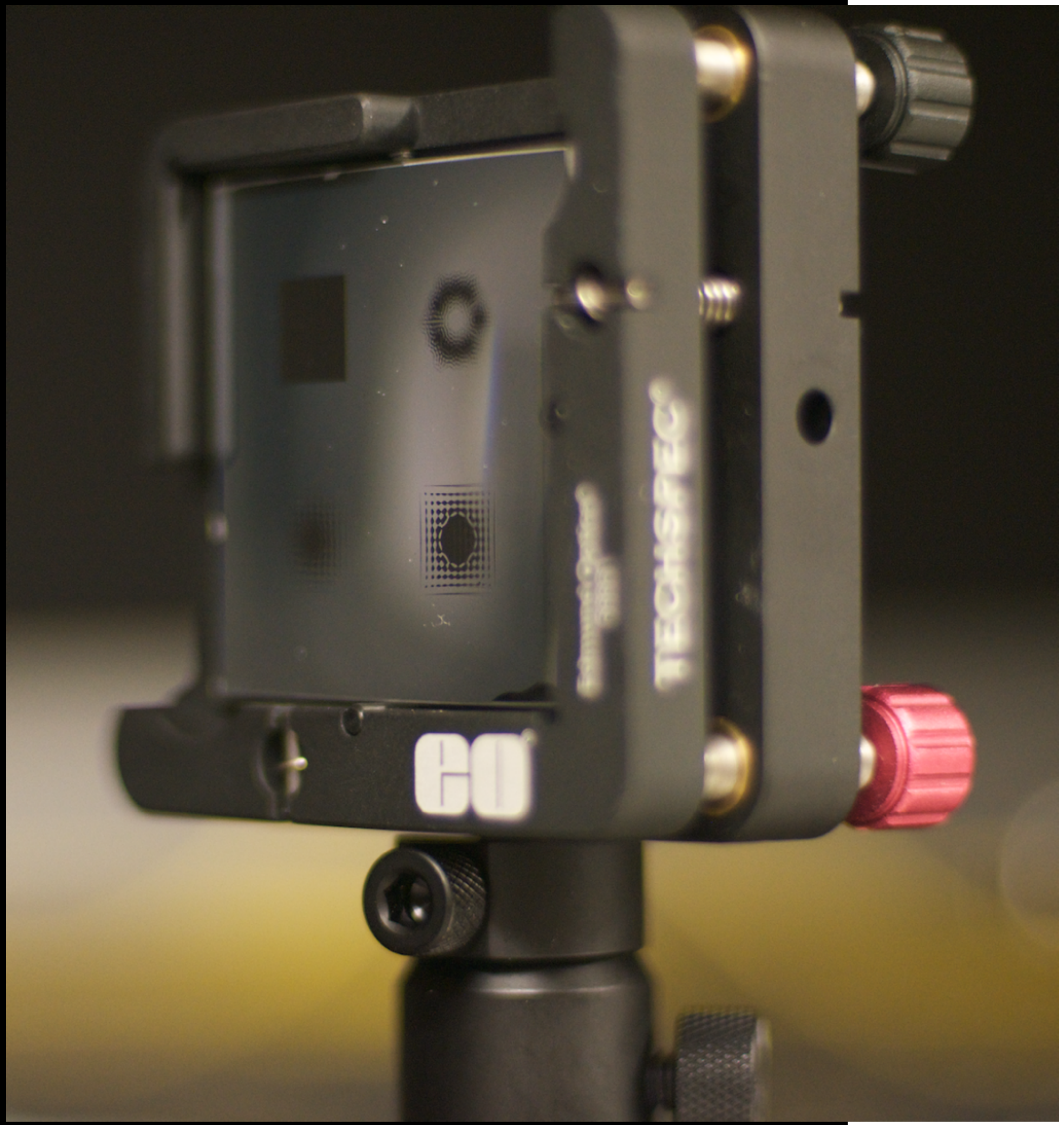

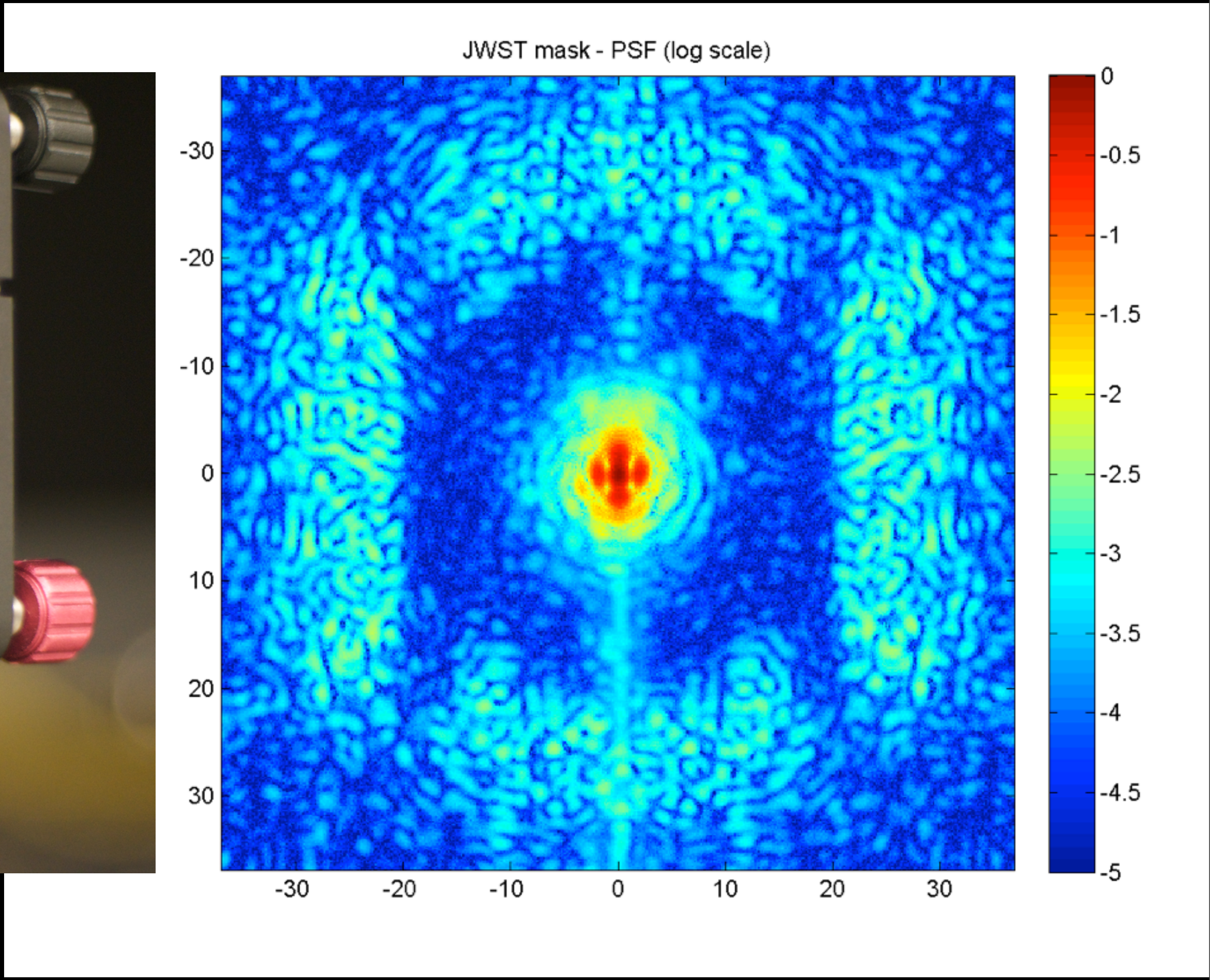

A. Carlotti, E. Young, G. Che

Manufacturing 2D-Optimized Shaped Pupils

- Recent breakthrough: Reflective SPs (RSPs)
  - Silicon wafers with absorptive (**black silicon**) and reflective regions

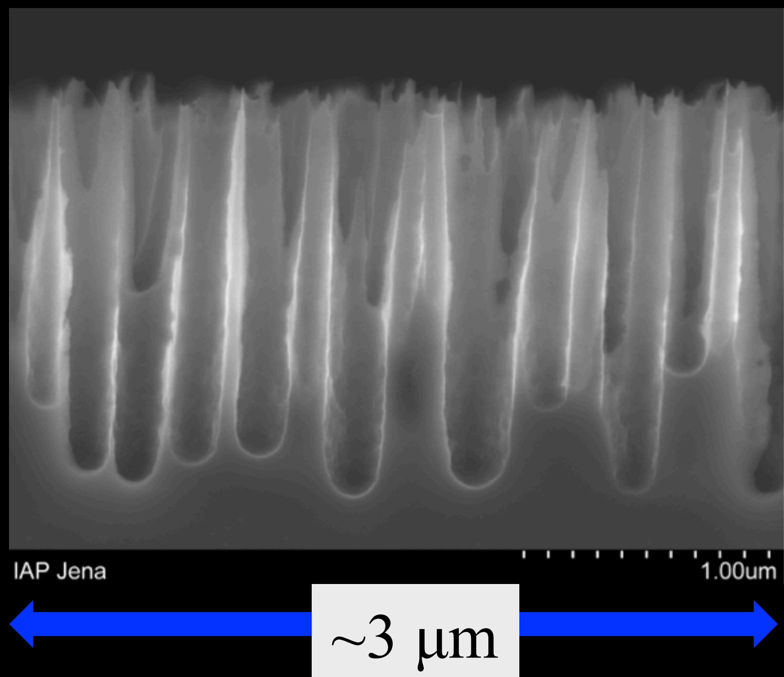

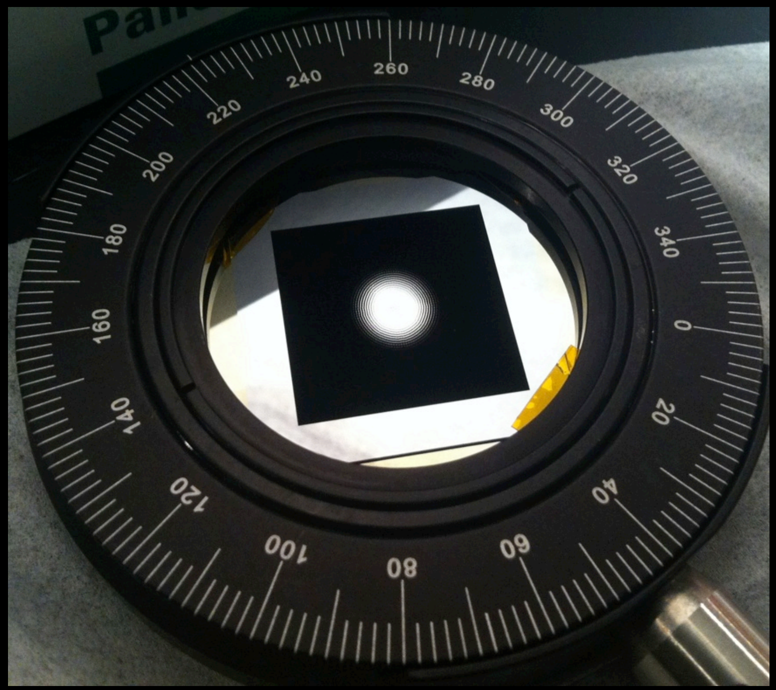

  - Testing 1st black Si masks now in HCIL.

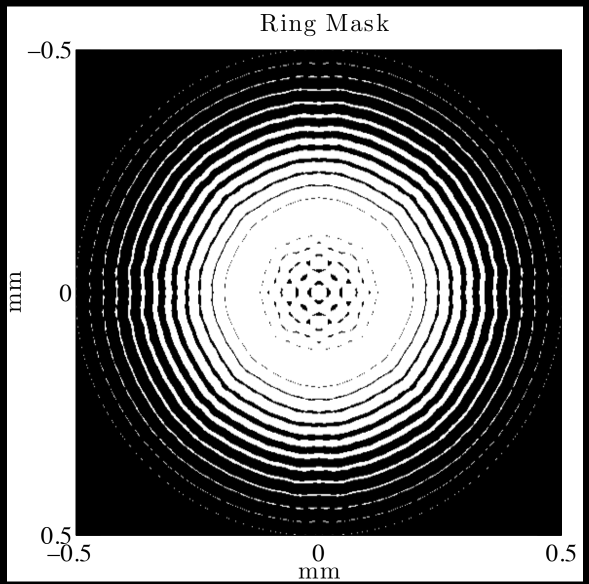

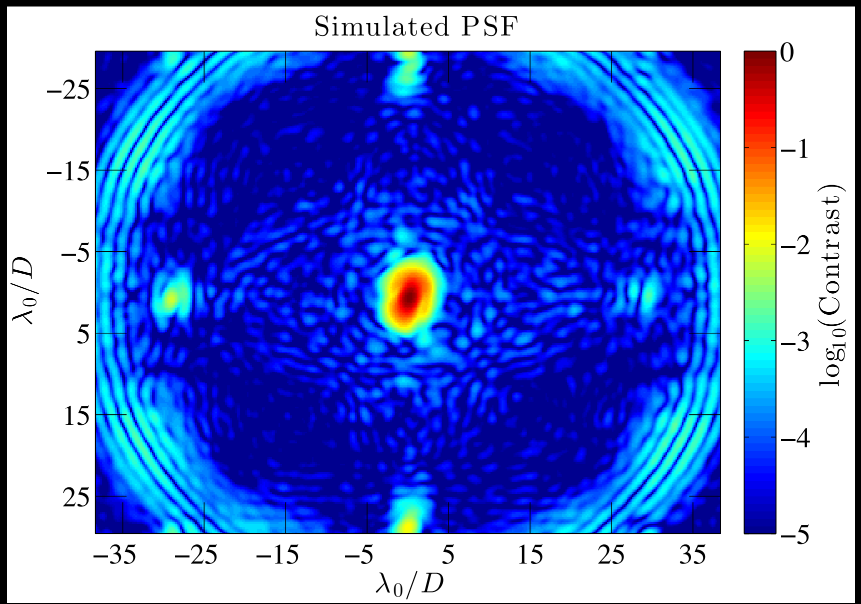

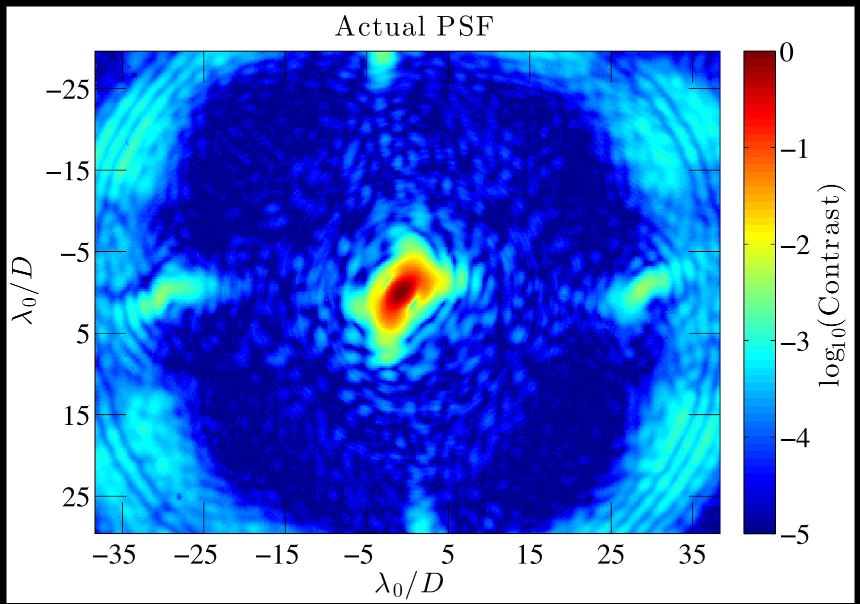

Friday, July 25, 14

Shaped Pupil Coronagraph for WFIRST-AFTA

Riggs et al. (2014)

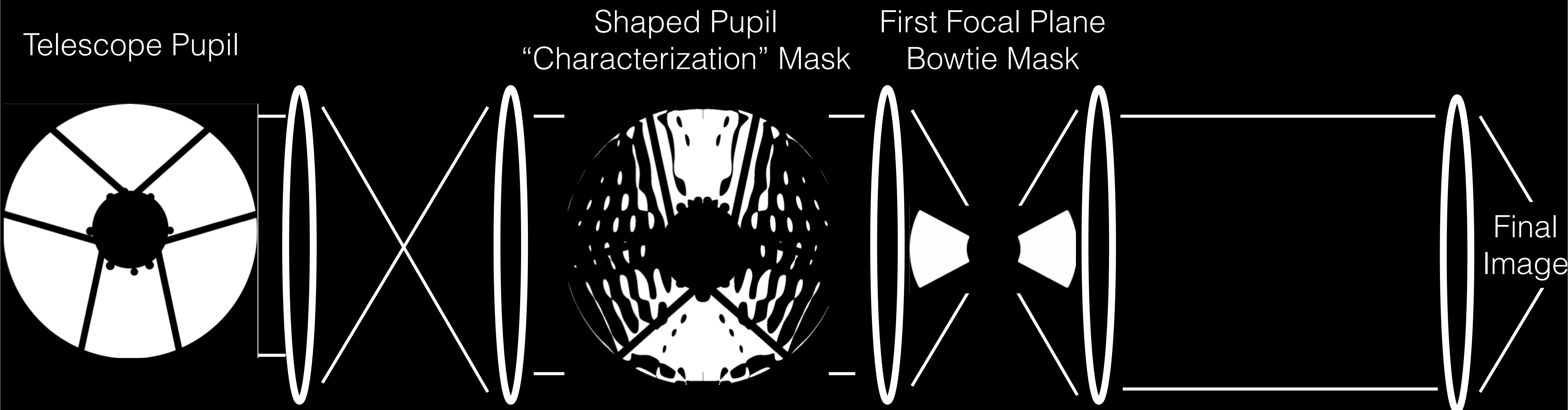

Intensity in First Focal Plane

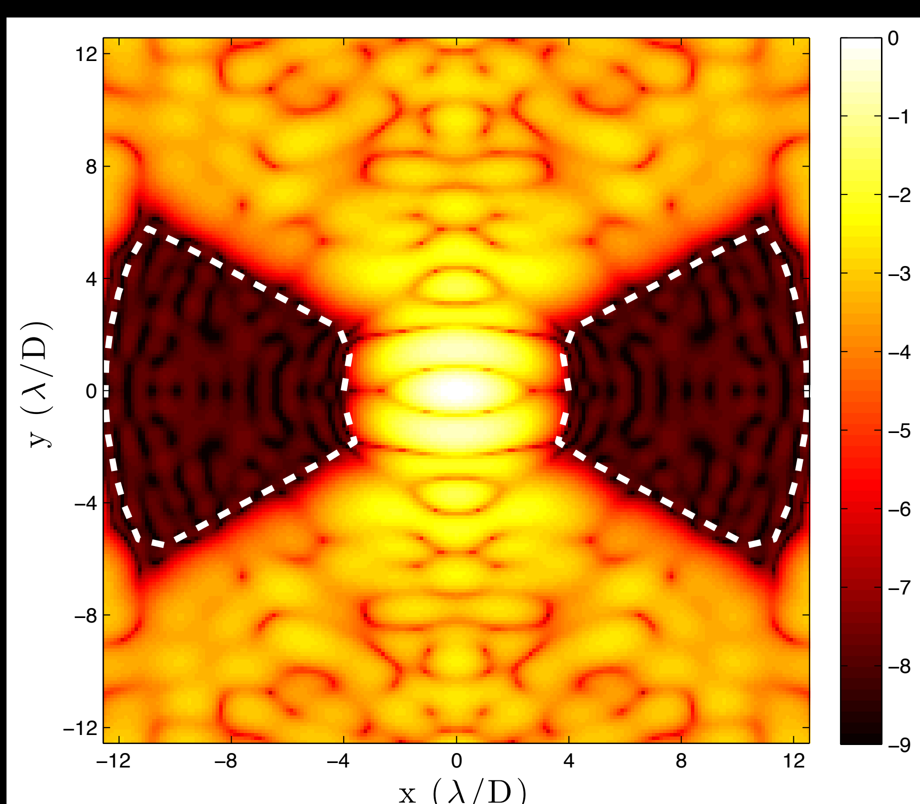

Contrast in Final Image (10^{-8})

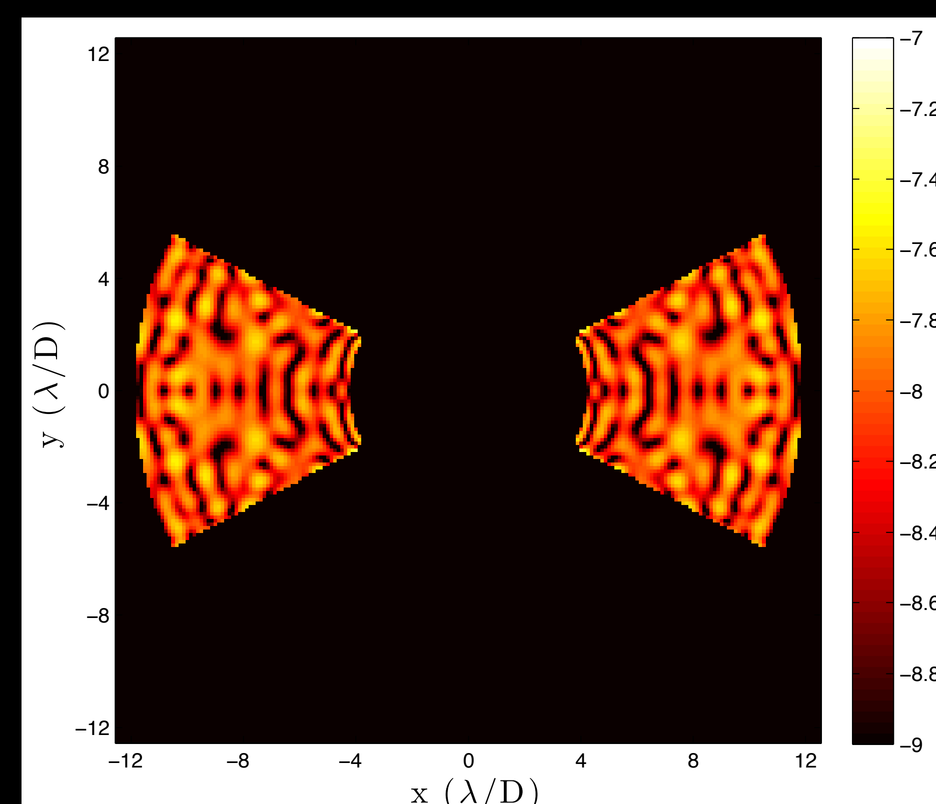

Pupil Mapping (PIAA)

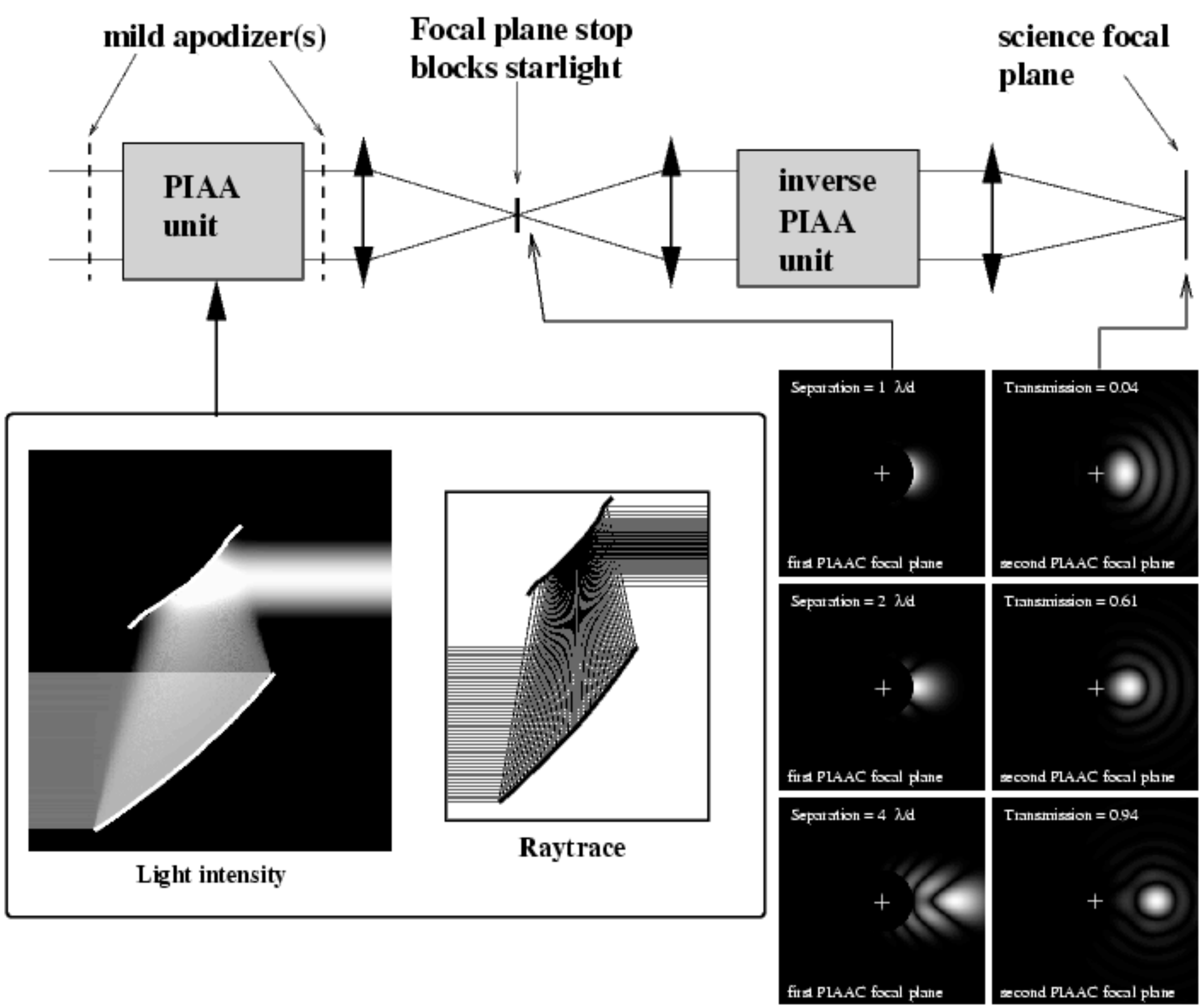

Pupil Mapping for Apodization

Nearly 100% throughput
100% search area
small (<2 lambda/d) Inner Working Angle

Guyon (2003), Vanderbei & Traub (2003, 2005)

Apodizing Phase Plates (Codona, Kenworthy)

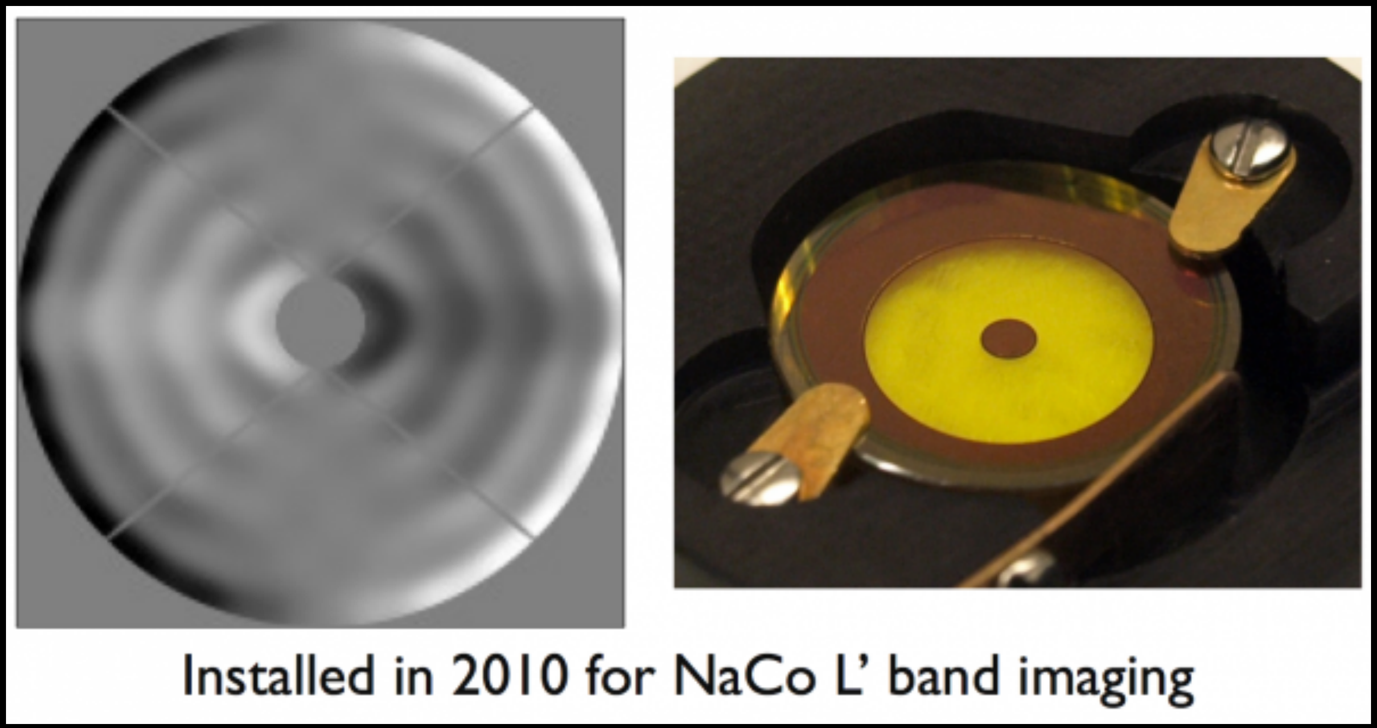

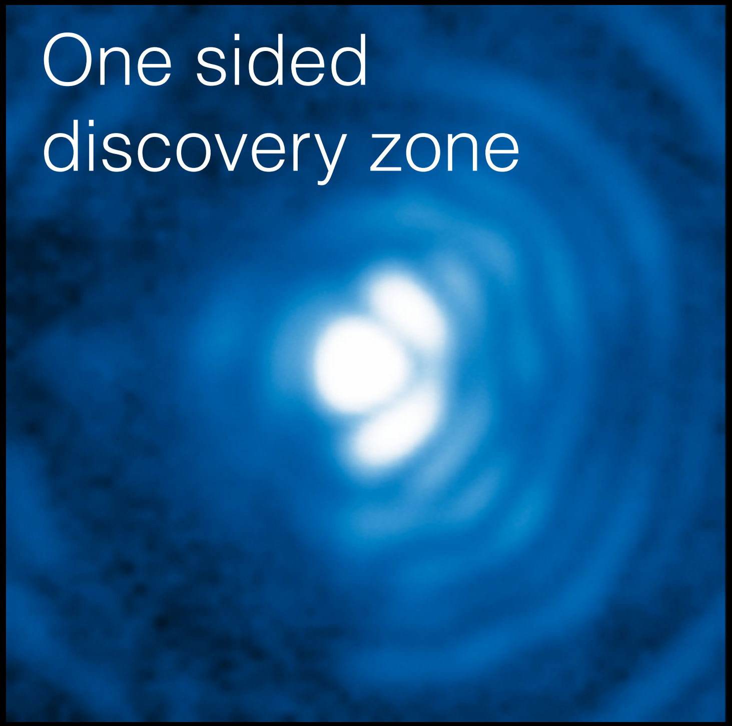

2 sided: with 0/π masks (Carlotti) … or with quarter wave plates & Wollaston prism (Snik)

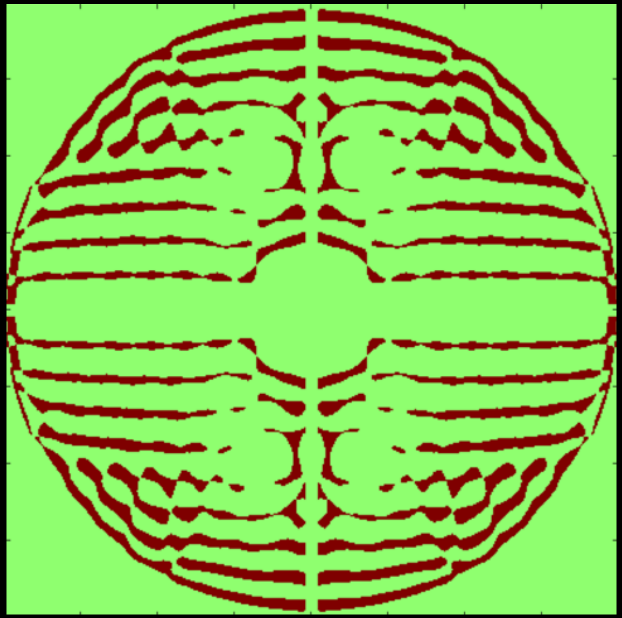

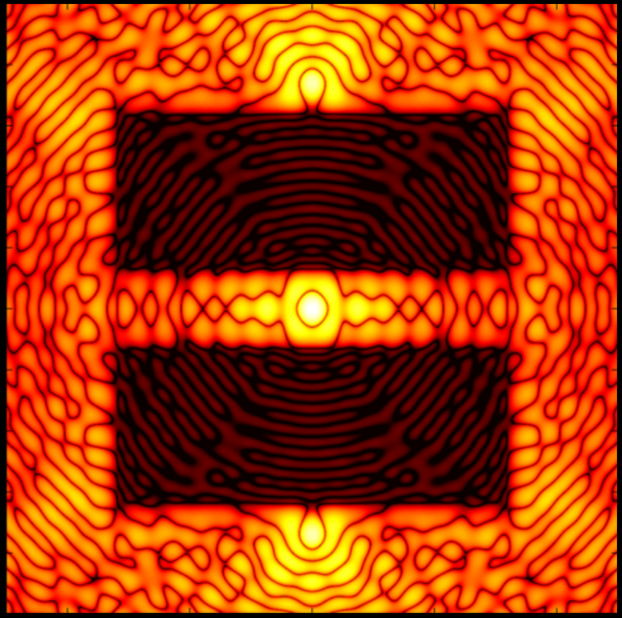

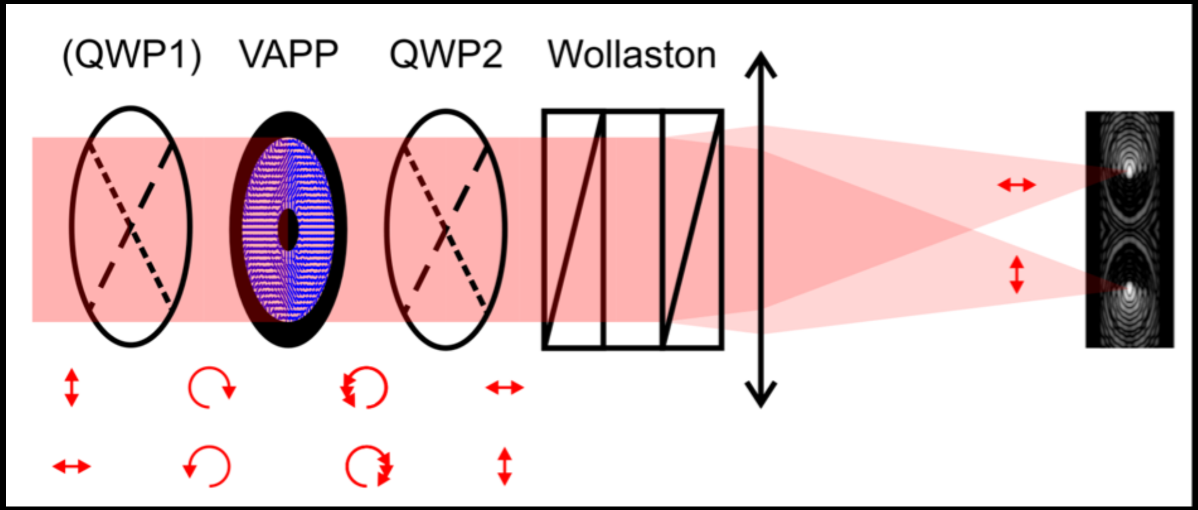

How is Phase used to Change Amplitude?

Coronagraphs That Combine Both

Combine apodized pupil with focal plane mask and Lyot stop: APLC, SPLC, ACAD

Apodized Pupil Lyot Coronagraph

Soummer et al. 2005, 2009, 2011

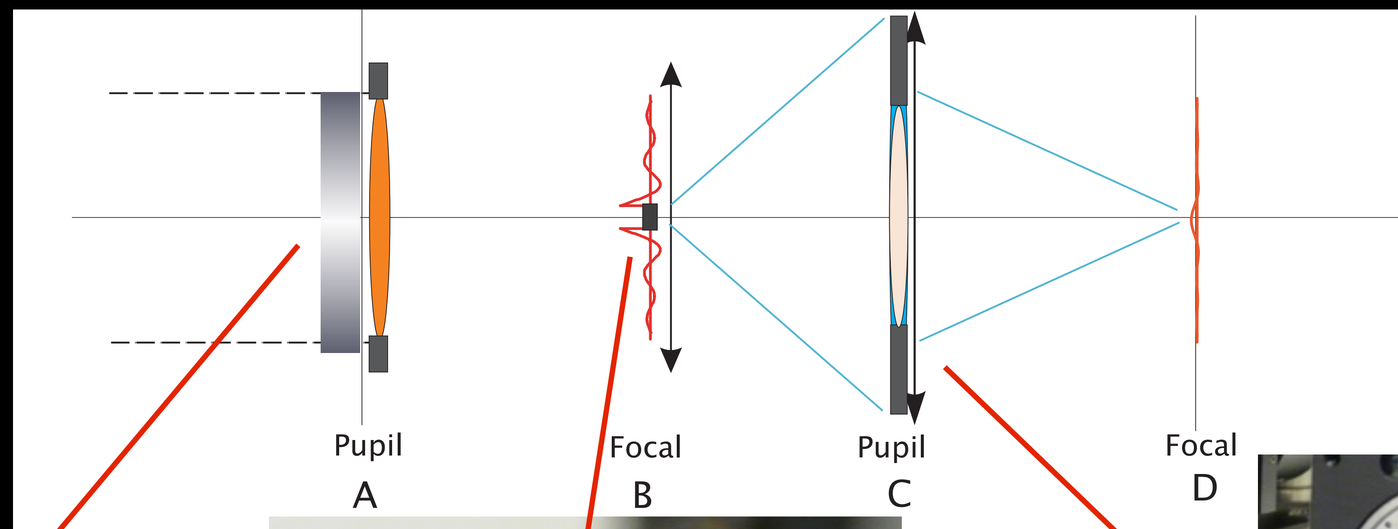

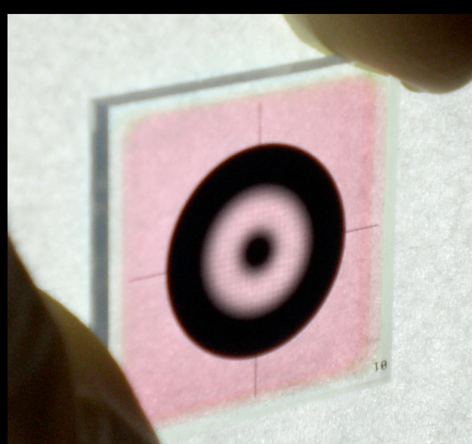

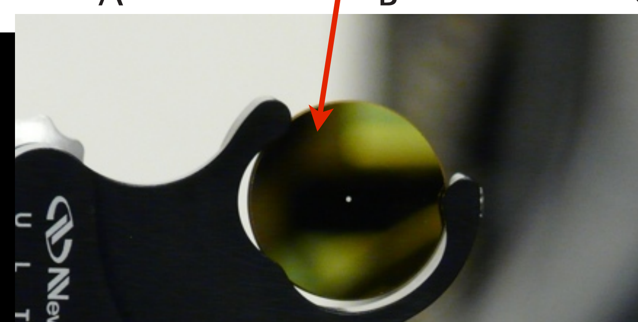

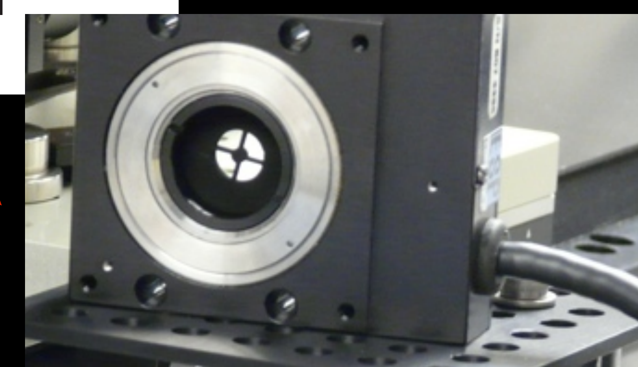

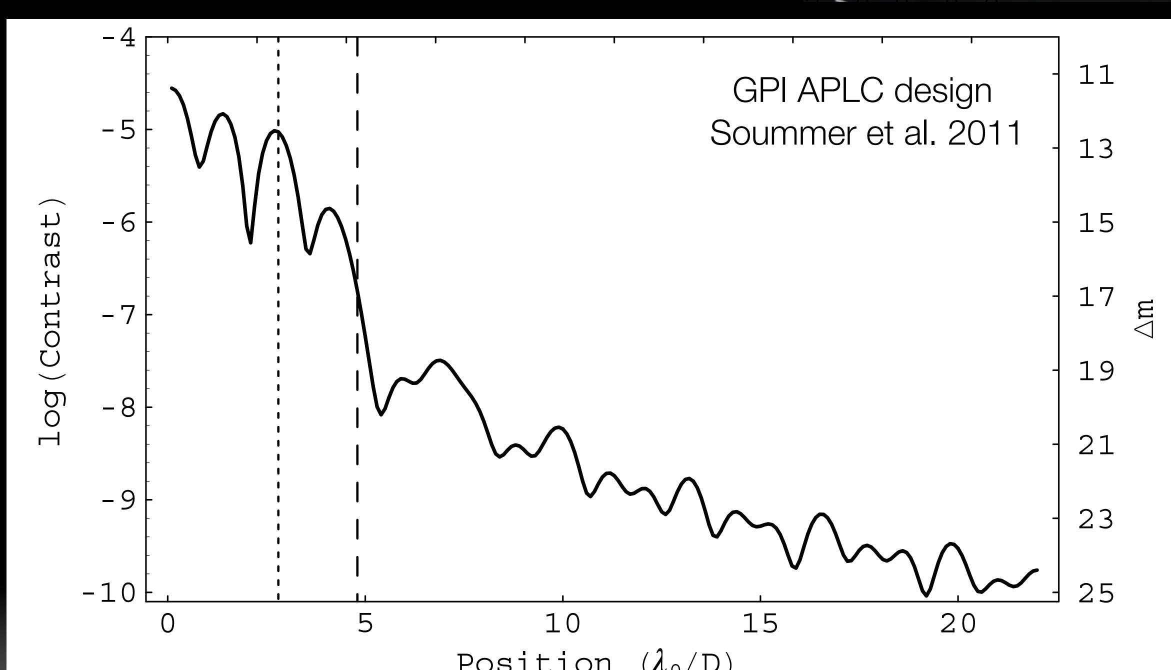

GPI design: contrast > 1e7 at 5 λ/D with central obstruction and 20% bandpass

Apodized Pupil Lyot Coronagraph

- Generalized prolate spheroidal apodizers exist for any aperture geometry and focal mask diameter
- Quasi-Achromatic Solutions exist for large enough mask (e.g. with GPI with 5.6 lambda/D mask *diameter*)

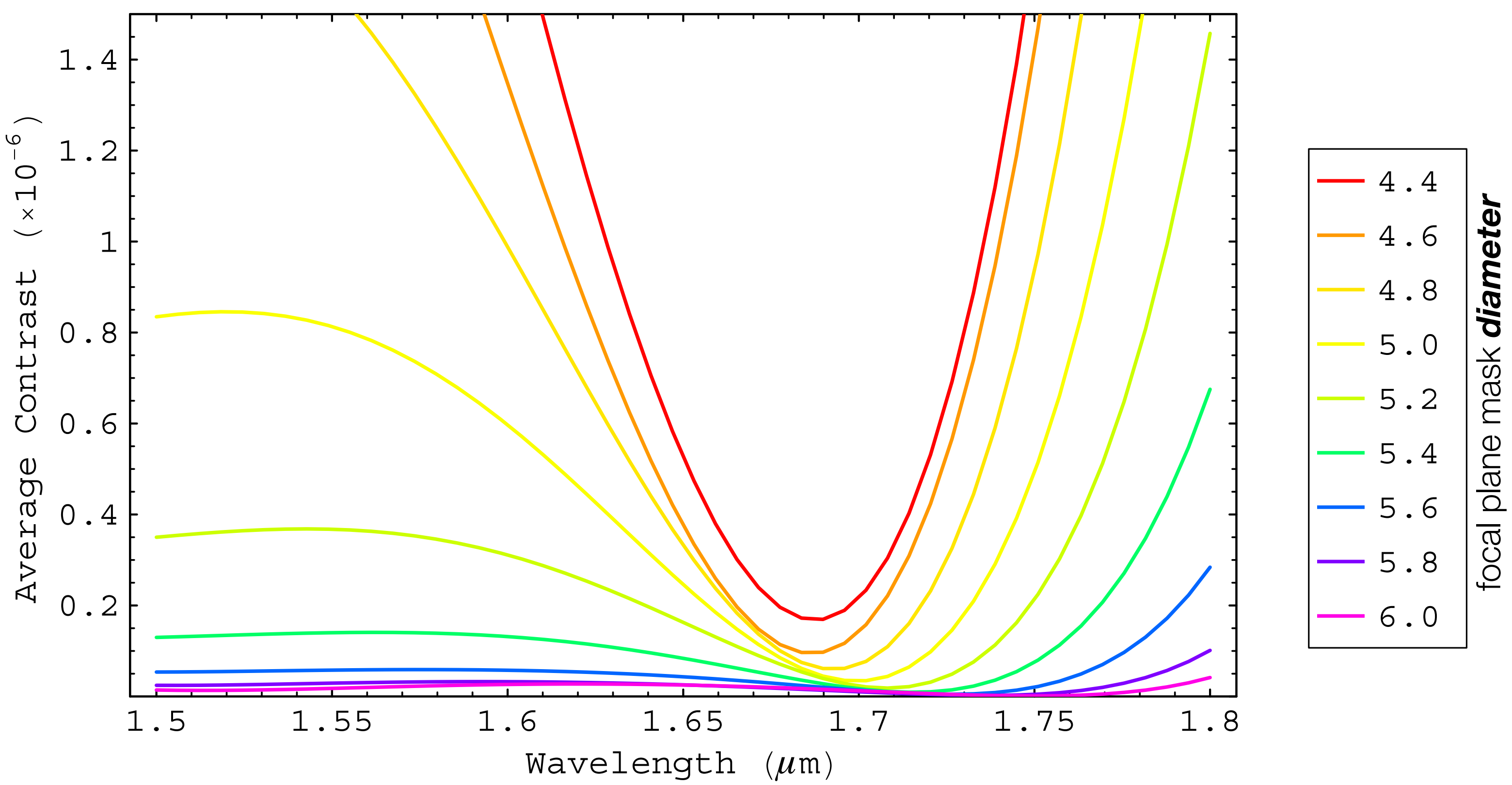

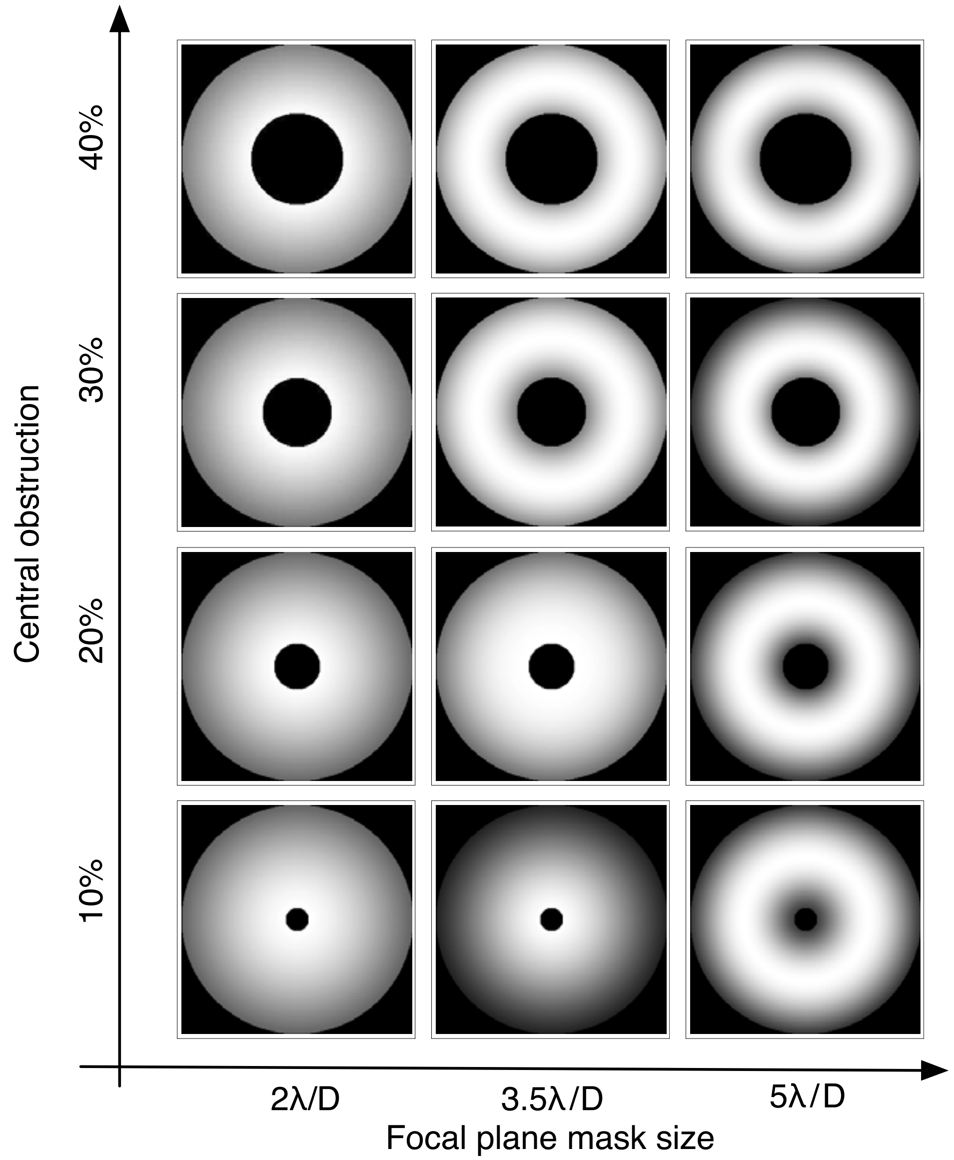

Soummer et al. 2011

2

Shaped Pupil Lyot Coronagraph

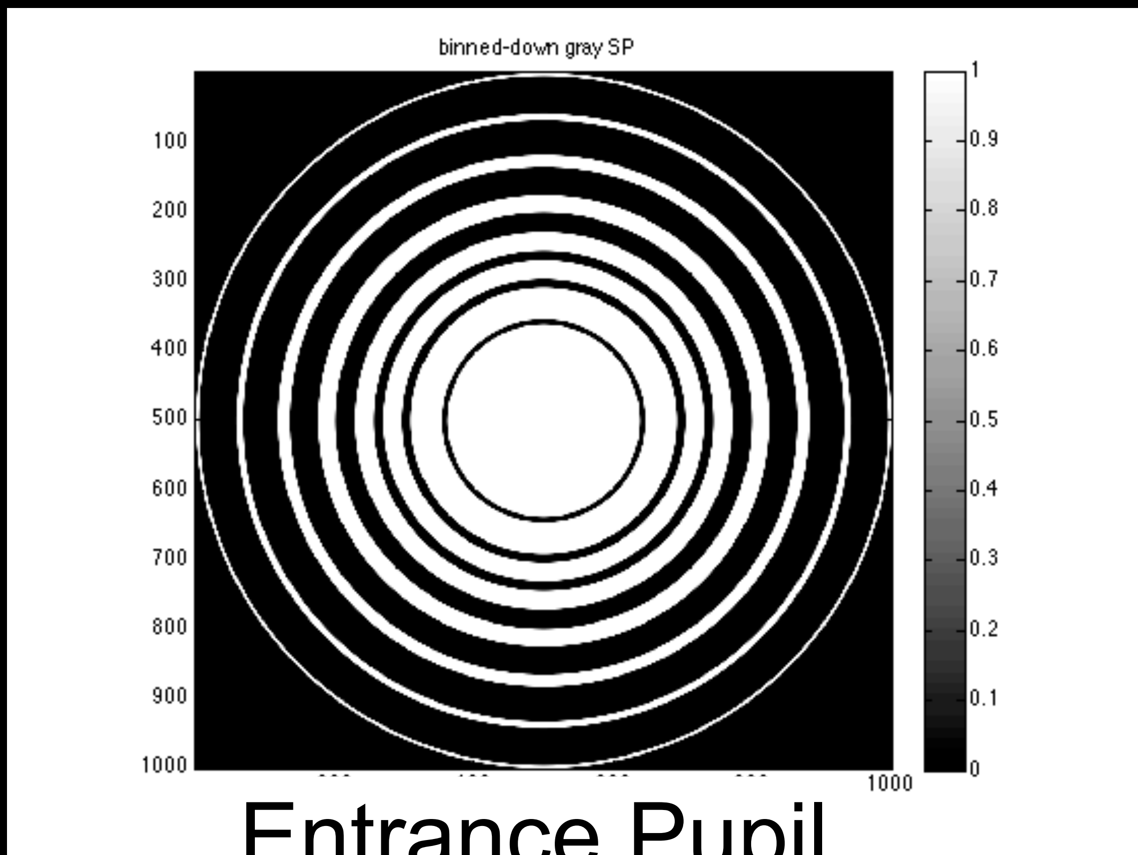

Entrance Pupil

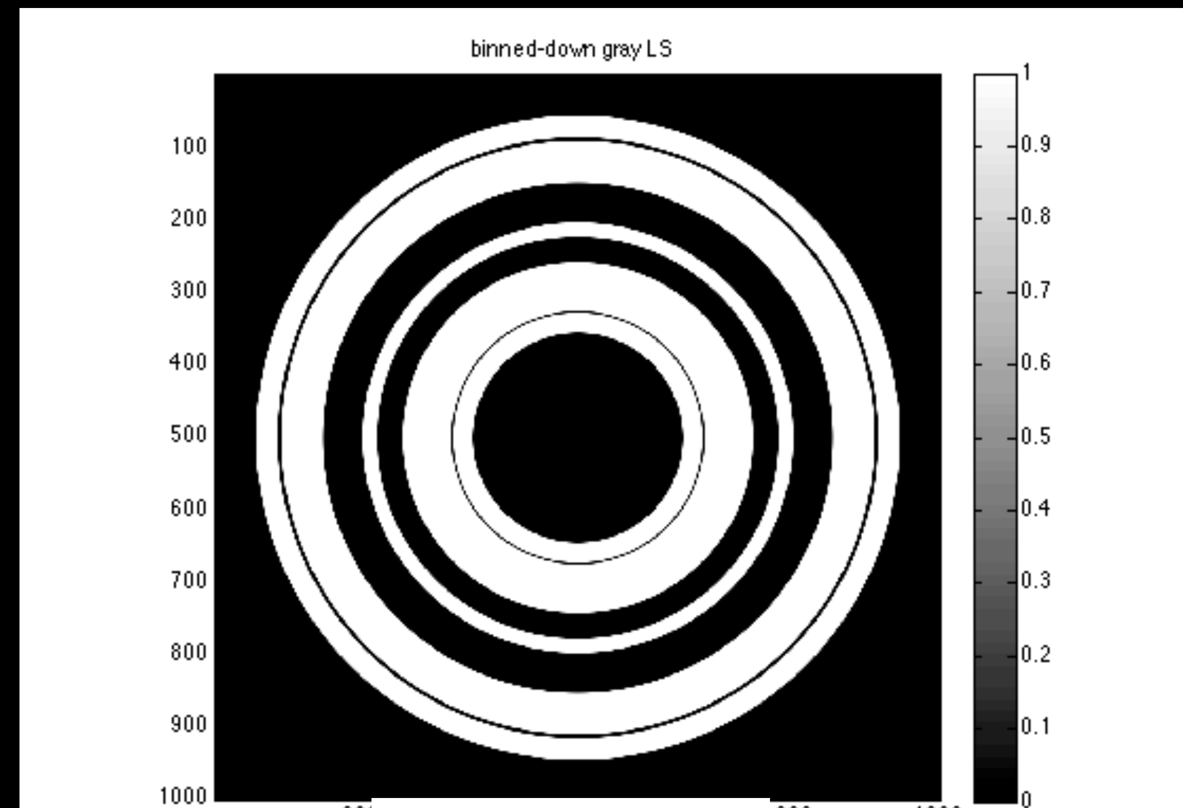

Lyot Stop

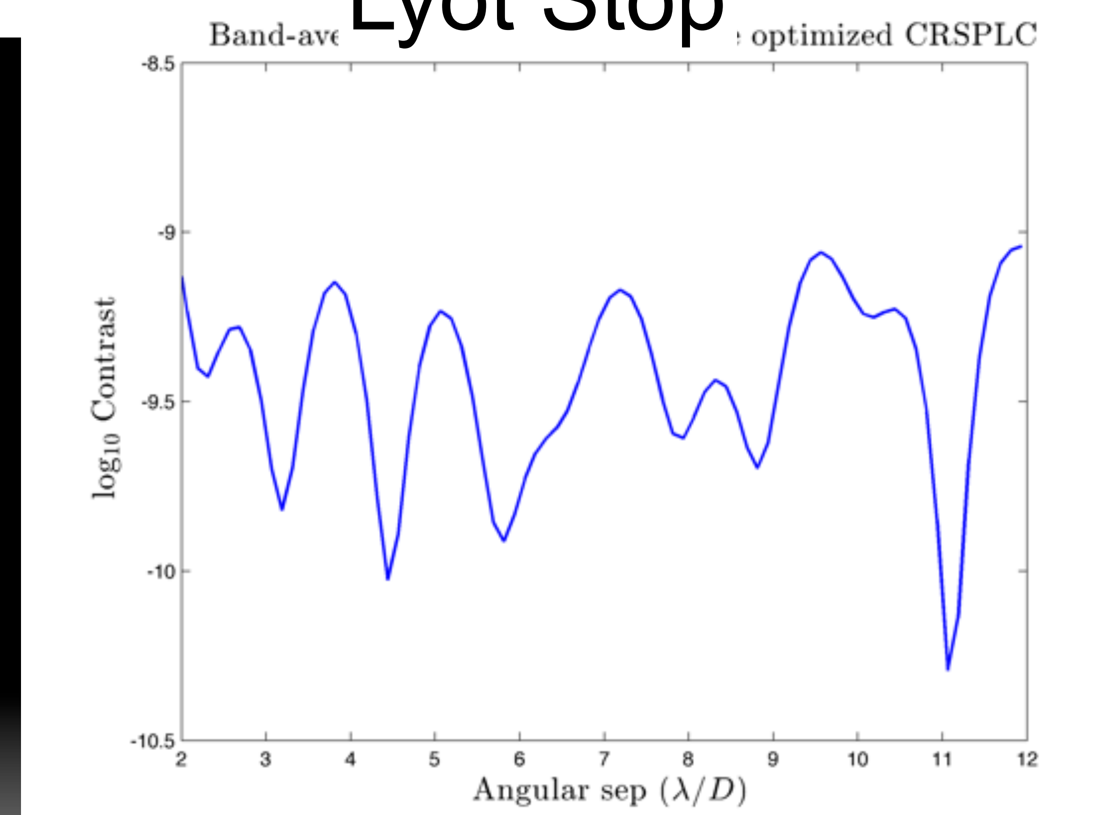

Simultaneously optimize pupil and Lyot plane

Gains smaller iwa and more throughput

from Neil Zimmerman

Phase mask coronagraphs with on-axis telescopes

(Carlotti, Mawet, Pueyo) ; here w/ 4QPM ; ask D.Mawet for Vortex.

obscuration & spiders limit high-contrast ; apodizer can retrieve it

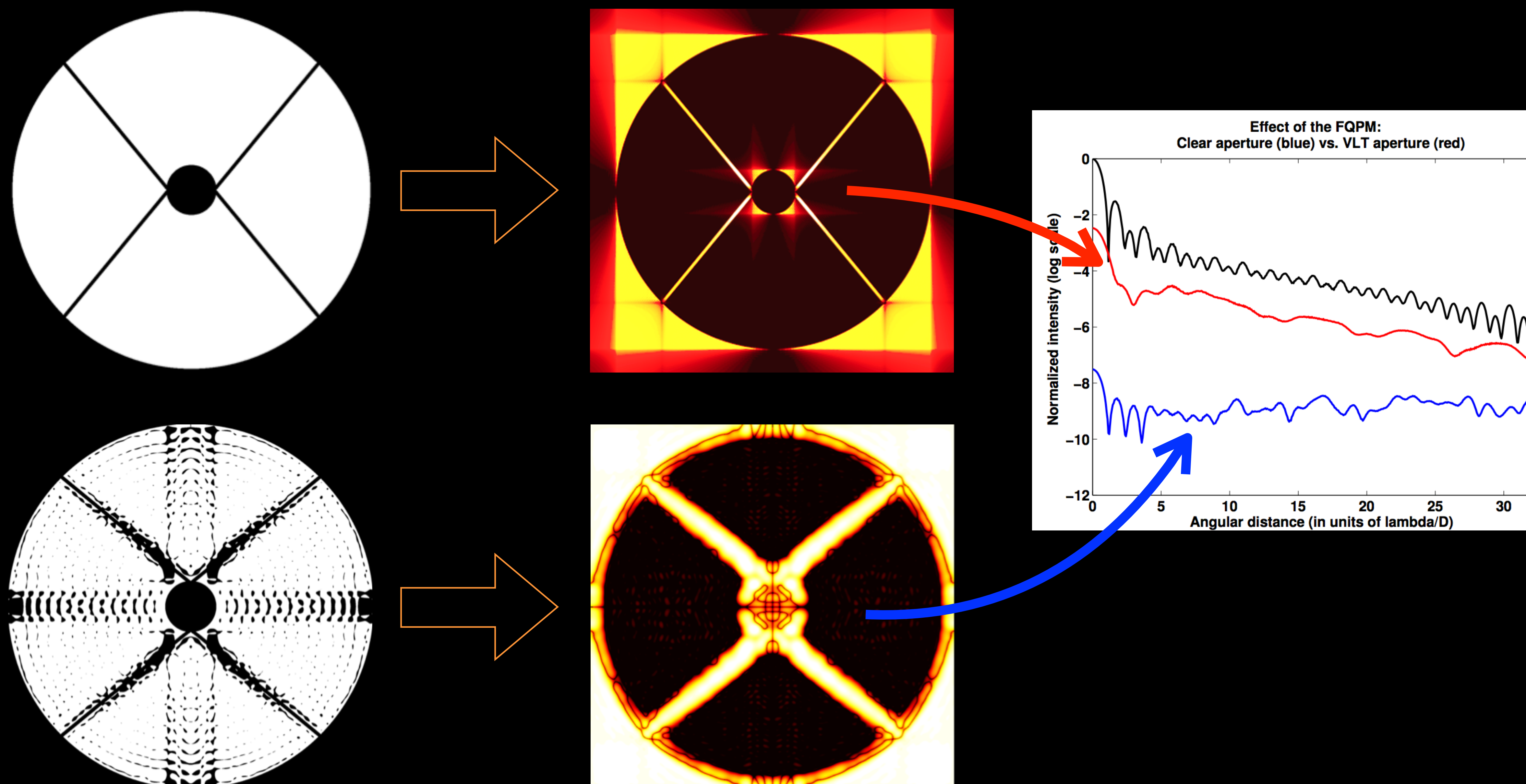

Shaped Pupil Lyot Coronagraph for WFIRST-AFTA

From Neil Zimmerman, Princeton

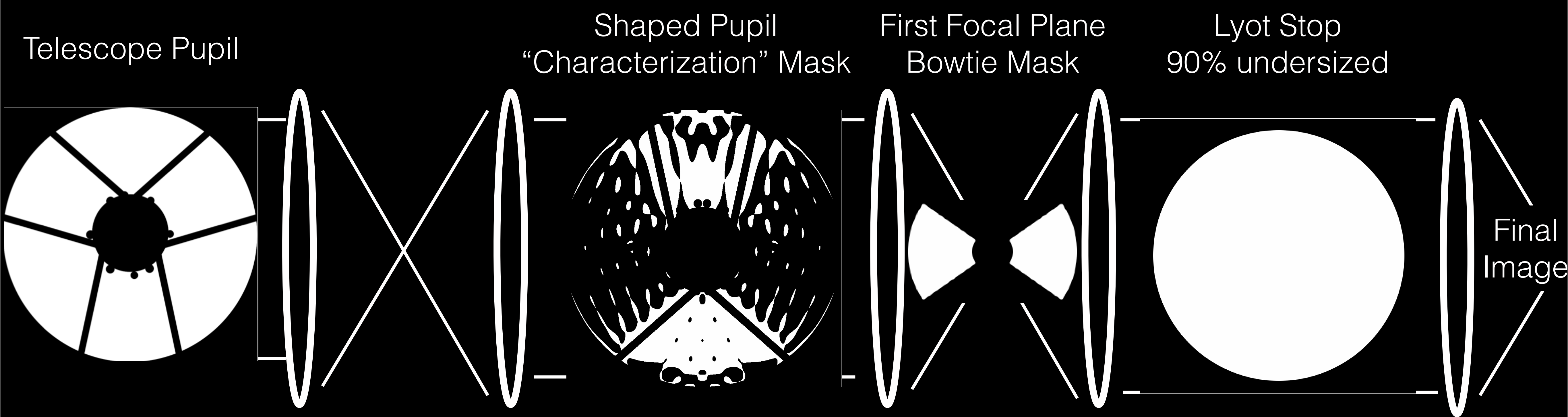

Intensity in First Focal Plane

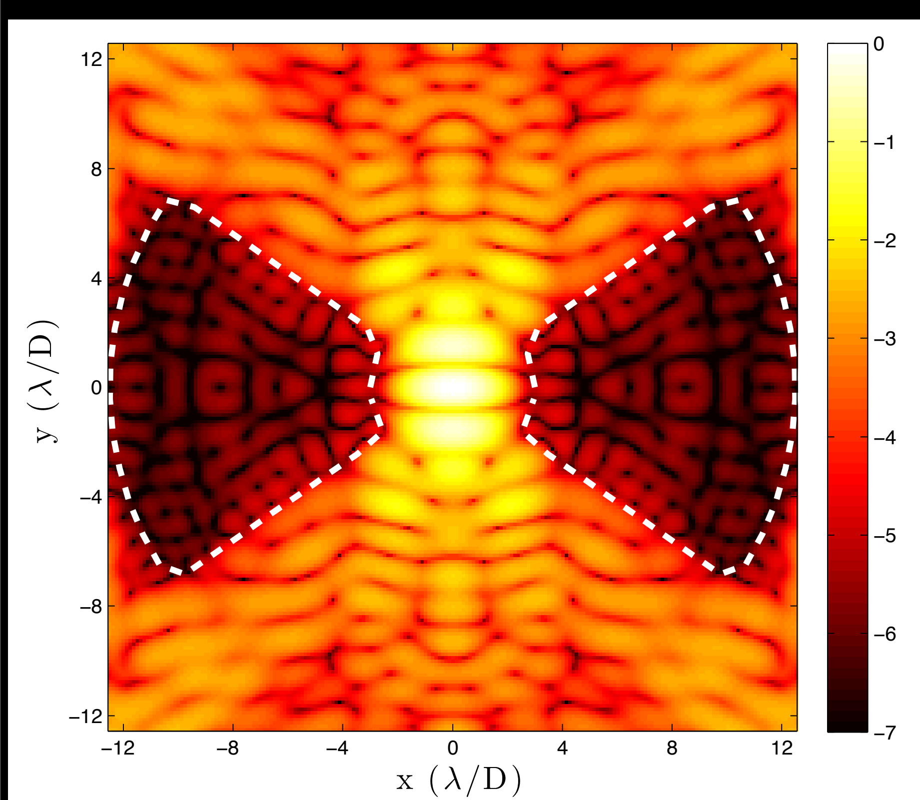

Intensity in Lyot Plane

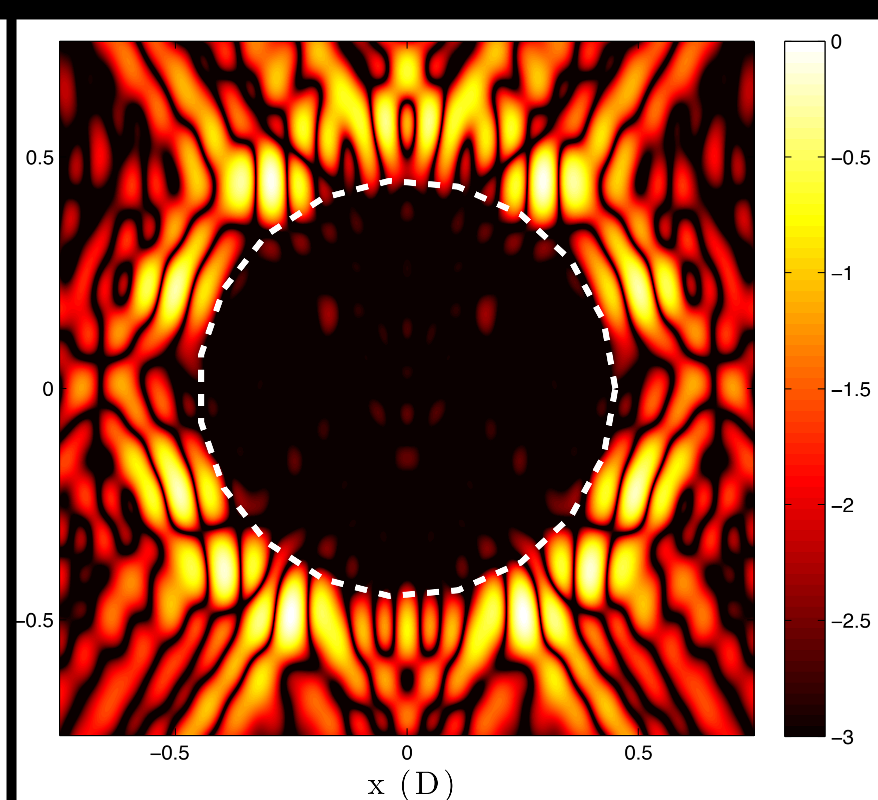

Contrast in Final Image (10^{-8})

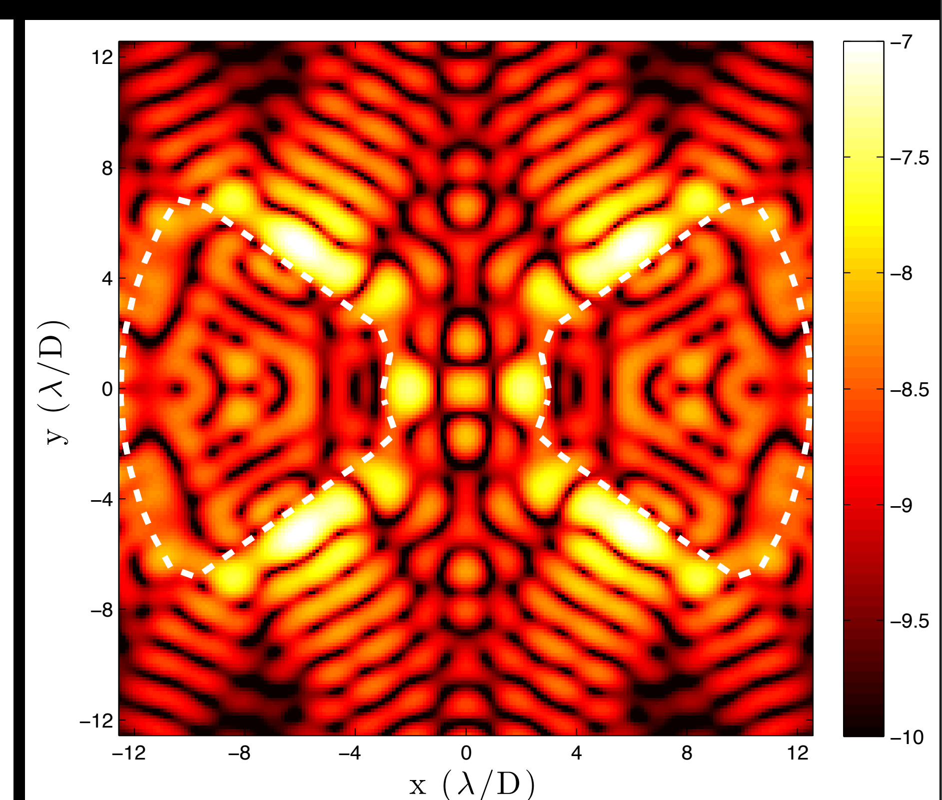

Instrument Performance (off-axis behavior)

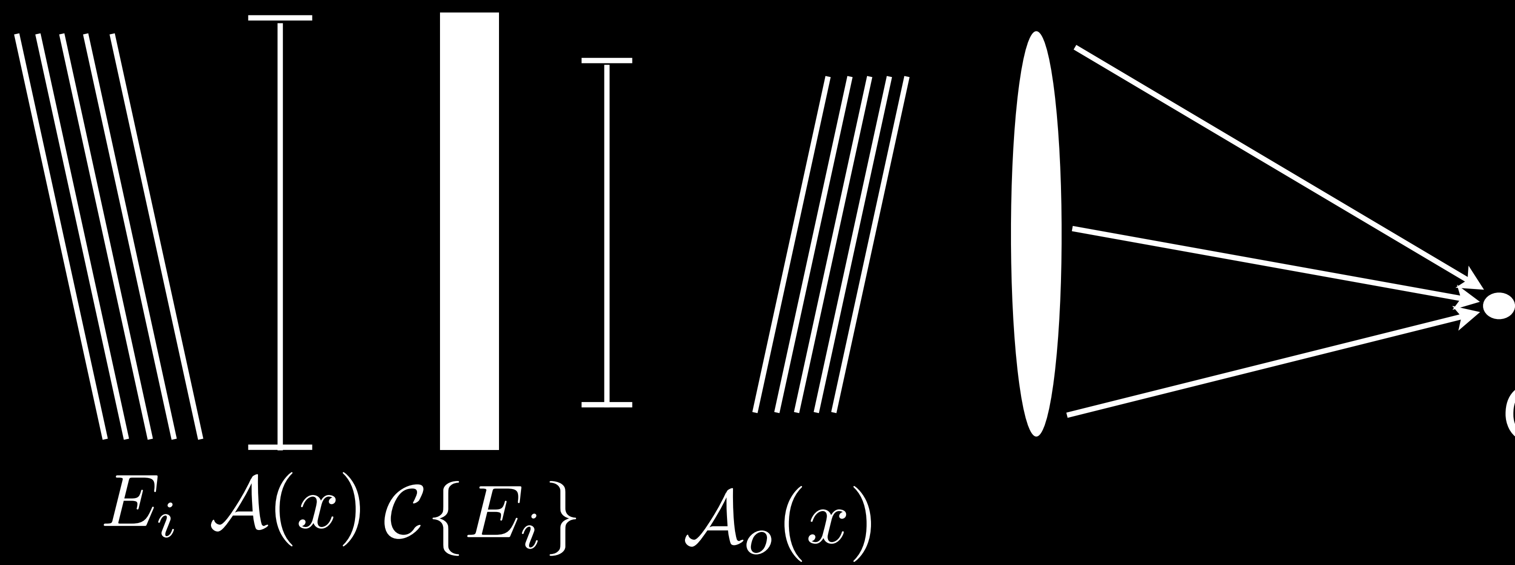

$$P_o(\omega) = \left|\mathcal{F}\left\{\mathcal{A}_o\right\}\right|^2$$

Off-Axis Point Spread Function

Detection Time (Kasdin et al. 2006)

$$t_d = \frac{1}{\beta} \frac{\left(K - \gamma\sqrt{1 + \frac{\tilde{Q}\Xi_{\Delta S}}{\Psi_{\Delta S}}}\right)^2}{T_R \tilde{Q} \Psi_{\Delta S}}$$

$$\beta = \epsilon\eta^2 \Delta\lambda I_p A(T_A)_{airy}$$

<u>Metrics</u>

- Throughput (and iwa)
- Sharpness
- $\tilde{Q} = Q \sum_{\Delta S} \bar{P}_{ij}$

Q is the ratio of the planet flux at the center of the PSF to the background flux there.

$$Q = \frac{C}{C_i + C_{eq}}$$

Instrument Performance (off-axis behavior)

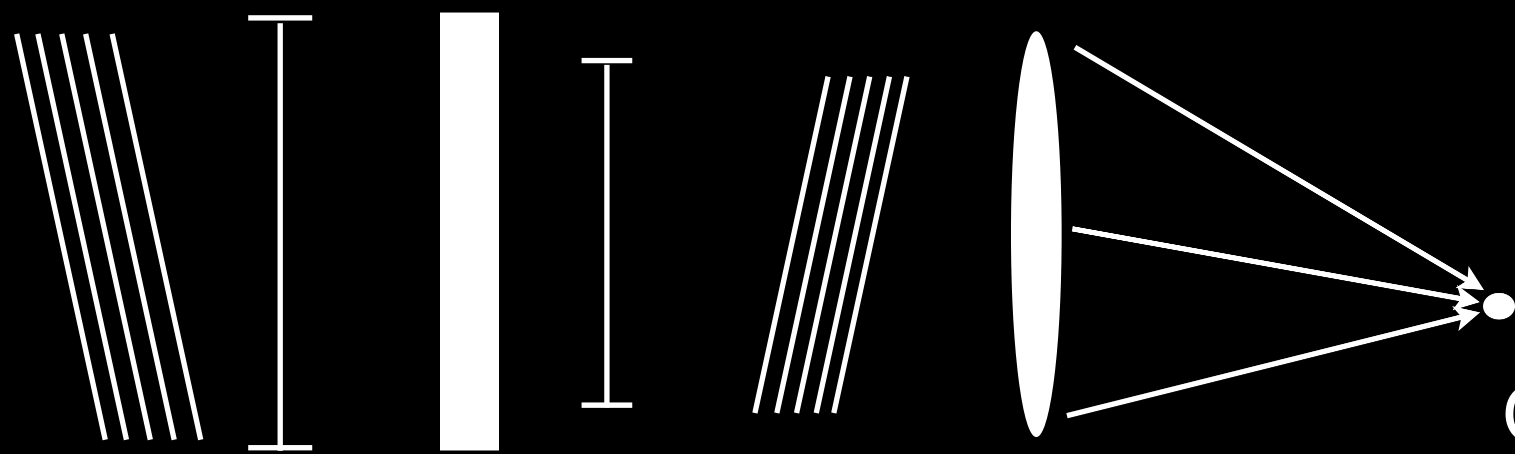

$$P_o(\omega) = \left|\mathcal{F}\left\{\mathcal{A}_o\right\}\right|^2$$

Off-Axis Point Spread Function

Metrics

- Throughput (and iwa)
- Sharpness
- $\tilde{Q} = Q \sum_{\Delta S} \bar{P}_{ij}$

Detection Time (Kasdin et al. 2006)

$$t_s = \frac{(SNR)^2 \left(\Xi \tilde{Q} + \Psi_{\Delta S}\right)}{\beta Q \Psi_{\Delta S}}$$

$$\beta = \epsilon \eta^2 \Delta\lambda I_p A(T_A)_{airy}$$

Q is the ratio of the planet flux at the center of the PSF to the background flux there.

$$Q = \frac{C}{C_i + C_{eq}}$$

Throughput

There are four possible measures of throughput often quoted:

Total Throughput:

$$T = \frac{\int\int_{-\infty}^{\infty} P_o(u,v)dudv}{\int\int_{-\infty}^{\infty} P(u,v)dudv} = \frac{\int\int_{-\infty}^{\infty} |\mathcal{A}_o(x,y)|^2 dxdy}{\int\int_{-\infty}^{\infty} |\mathcal{A}(x,y)|^2 dxdy} = \frac{\tilde{A}_o}{A}$$

For binary pupils $= \frac{A_o}{A}$

Airy Throughput:

$$T_A = T\frac{\int\int_{\Delta S} P_o(u,v)dudv}{\int\int_{-\infty}^{\infty} P_o(u,v)dudv} = \frac{\int\int_{\Delta S} P_o(u,v)dudv}{\int\int_{-\infty}^{\infty} P(u,v)dudv} = \frac{\int\int_{\Delta S} P_o(u,v)dudv}{A}$$

Useful Throughput (Guyon, et al. 2006):

Maximum fraction of planet light that can be separated from starlight.

Effective Throughput:

$$T_R = \frac{\int\int_{\Delta S} P_o(u,v)dudv}{\int\int_{\Delta S} P(u,v)dudv} = \frac{T_A}{(T_A)_{airy}}$$

Note: P_o is a function of angle in image plane.

Inner Working Angle

Where the effective throughput drops by 50%

(Maybe where t_d doubles to allow for sharpness change?)

Perfect Coronagraph

$$T_\Omega \leq 1 - A^2(\theta)$$

A = Airy Function

Guyon, Pluzhnik, Kuchner, Collins & Ridgway 2006, ApJS 167, 81

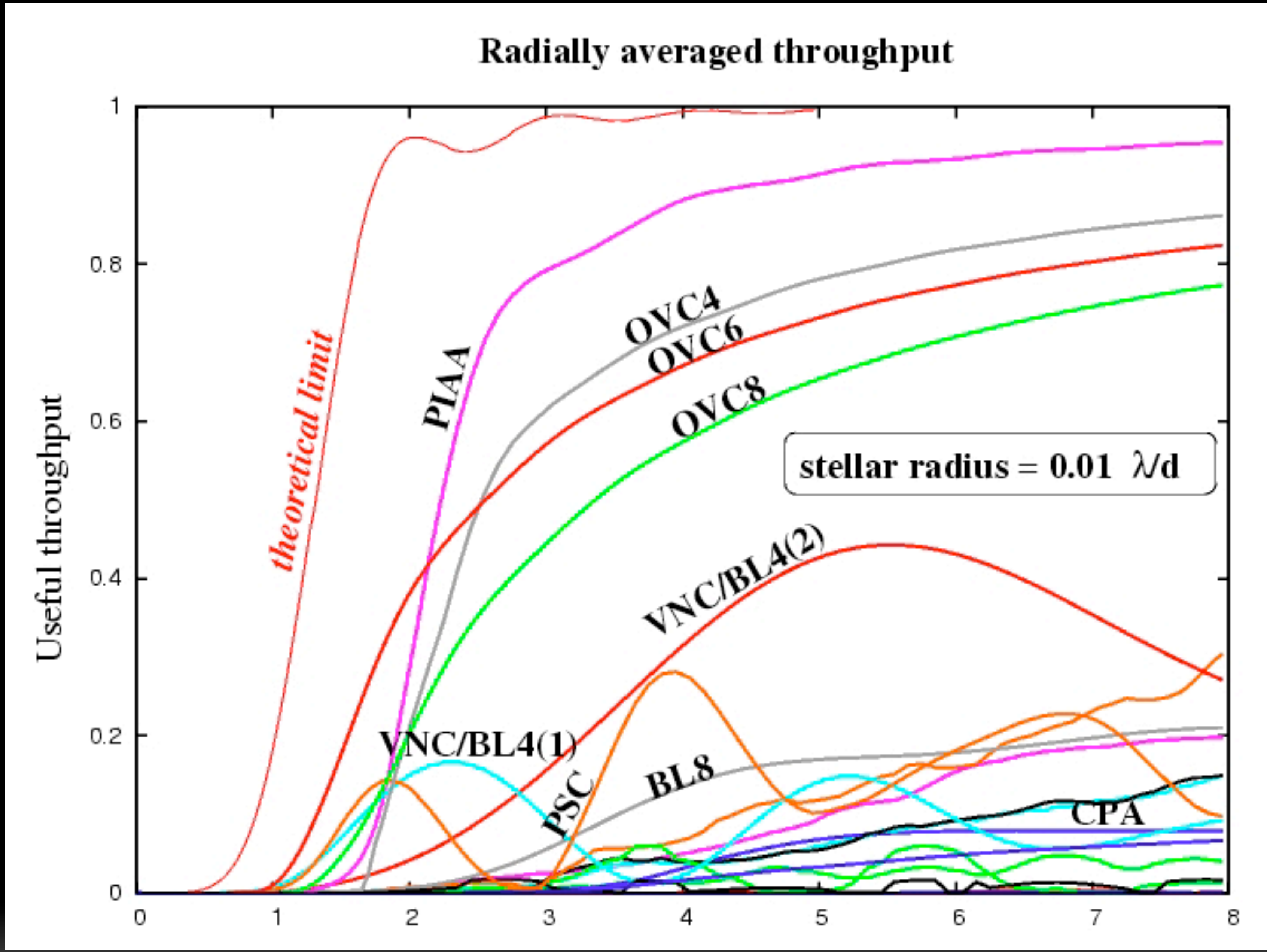

Sharpness

$$\Psi_{\Delta S} = \frac{\sum_{ij} \bar{P}_{ij}^2}{(\sum_{ij} \bar{P}_{ij})^2}$$

Note that sharpness is a strong function of the PSF sampling.

Critically sampled Sharpness

- Airy = 0.12
- Prolate = 0.08
- Lyot = 0.06

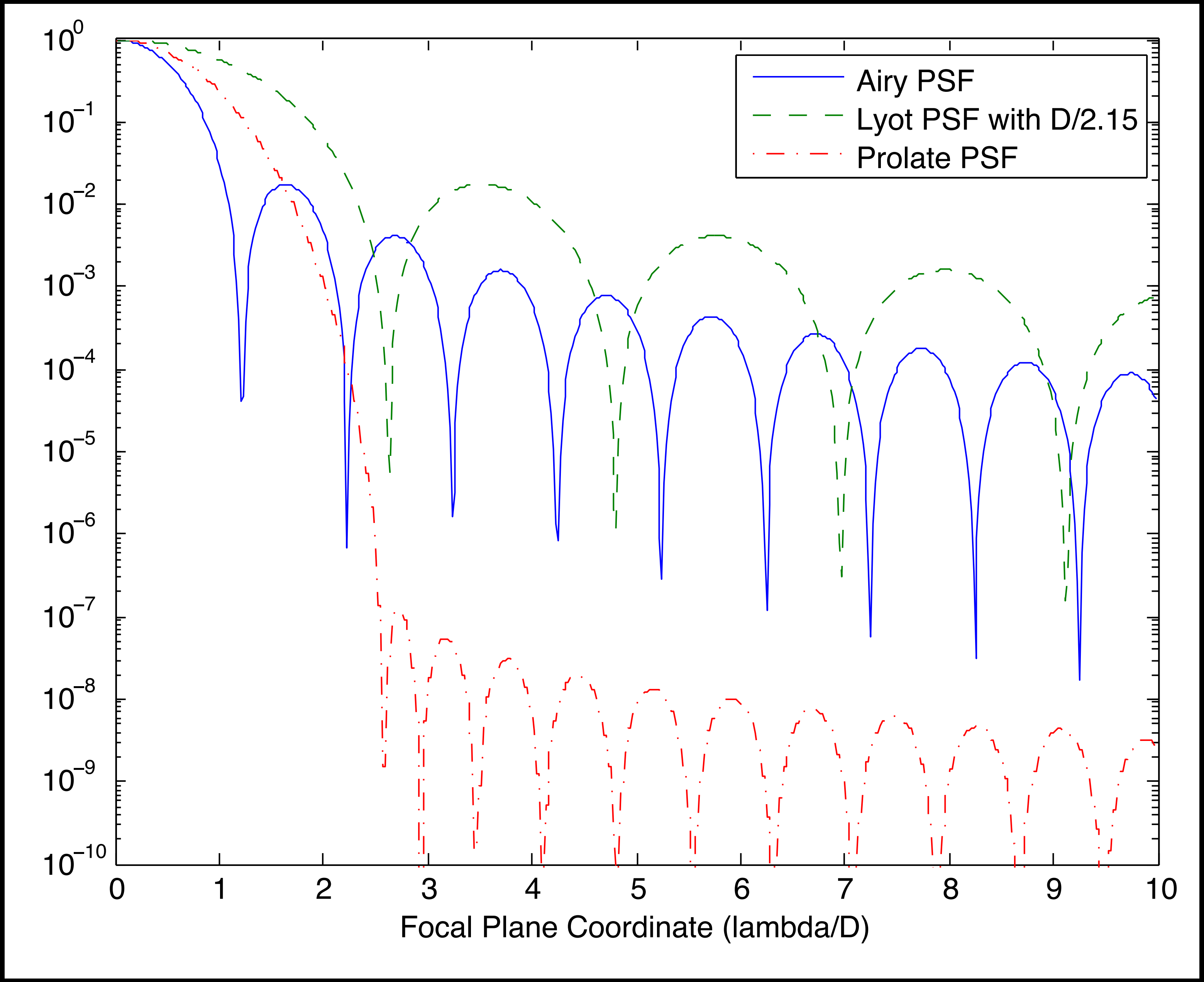

Wavefront Aberrations

Atmospheric distortions and imperfect optics degrade contrast

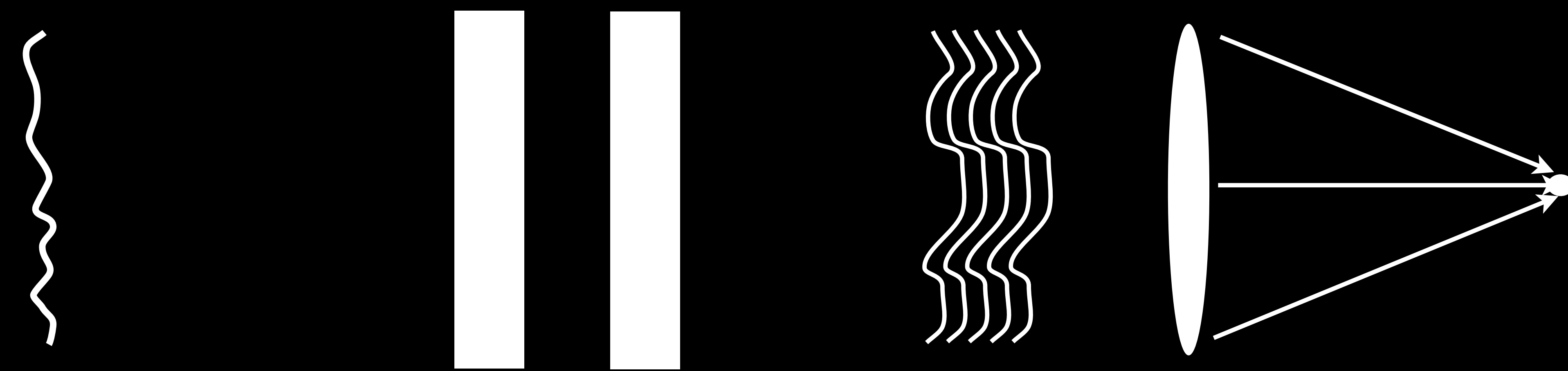

$E_i(1+\epsilon(x))e^{i\phi_a(x)}$ Coronagraph $A_o(x)e^{i\phi(x)}$

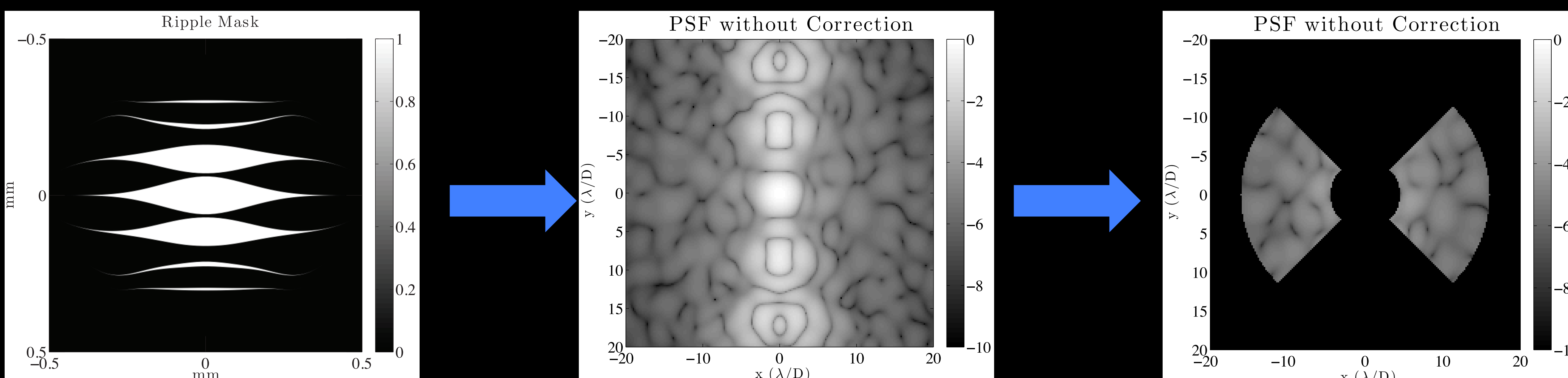

Aberrations significantly degrade contrast: 10^{10} ~10^5

Friday, July 25, 14

Wavefront Aberrations

Atmospheric distortions and imperfect optics degrade contrast

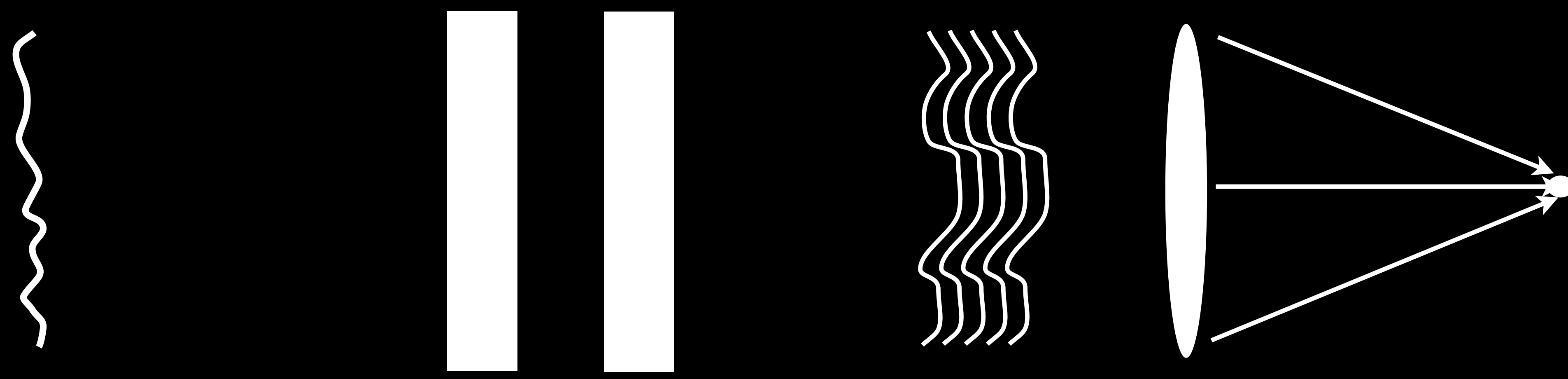

$E_i(1+\epsilon(x))e^{i\phi_a(x)}$ Coronagraph $A_o(x)e^{i\phi(x)}$

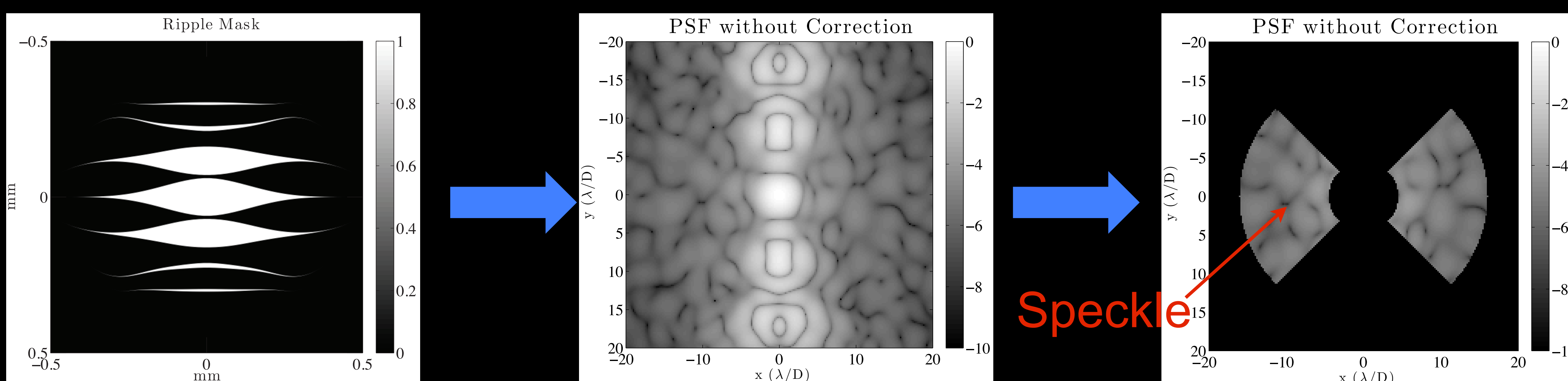

Aberrations significantly degrade contrast: 10^{10} ~10^{5}

Wavefront Aberrations

Atmospheric distortions and imperfect optics degrade contrast

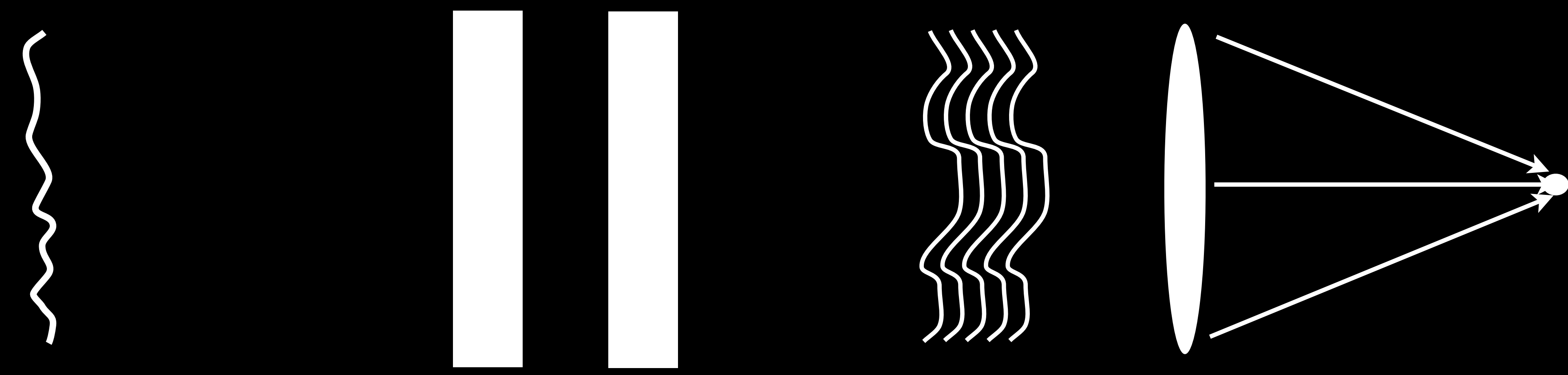

$E_0(1+\epsilon(x))e^{i\phi_a(x)}$ $A_0(x)e^{i\phi(x)}$

Remember: Different coronagraphs have different sensitivities to various orders of aberrations.

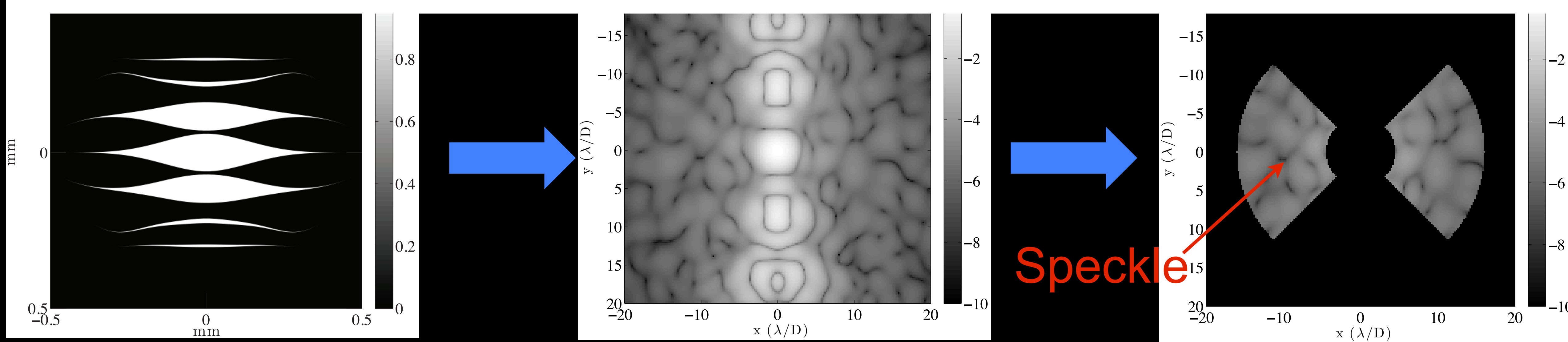

Aberrations significantly degrade contrast: 10^{10} ~10^{5}

Typical Ground Adaptive Optics

Phase Conjugation

Without
Adaptive
Optics

Star Image

With AO

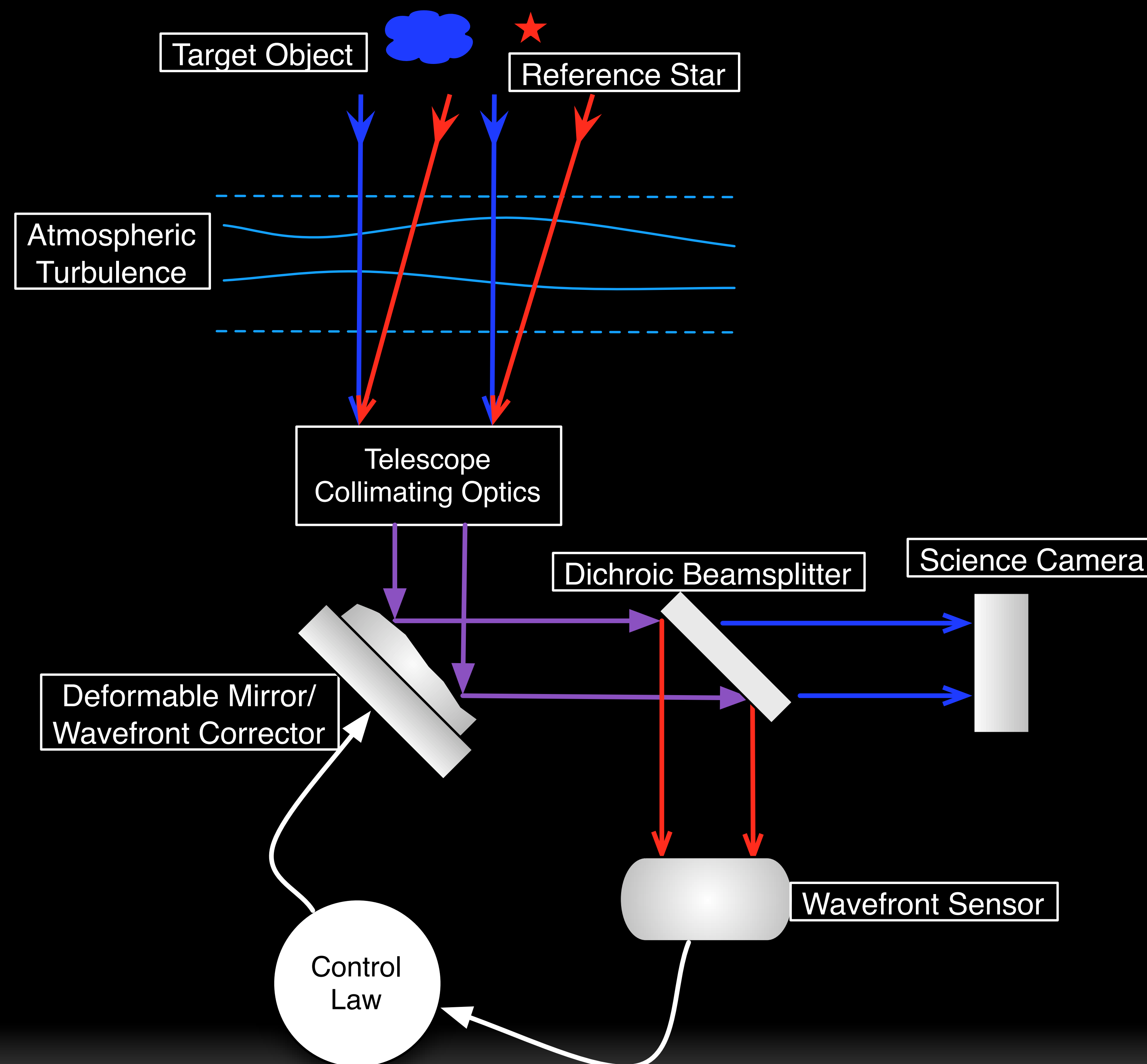

Images and Video from UC Santa Cruz Adaptive Optics course.

Typical Ground Adaptive Optics

Phase Conjugation

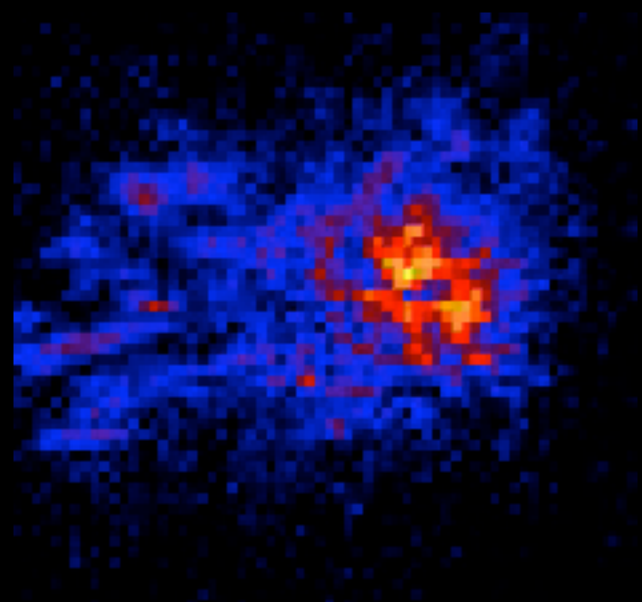

Without Adaptive Optics

Star Image

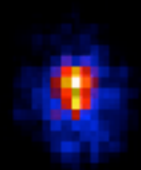

With AO

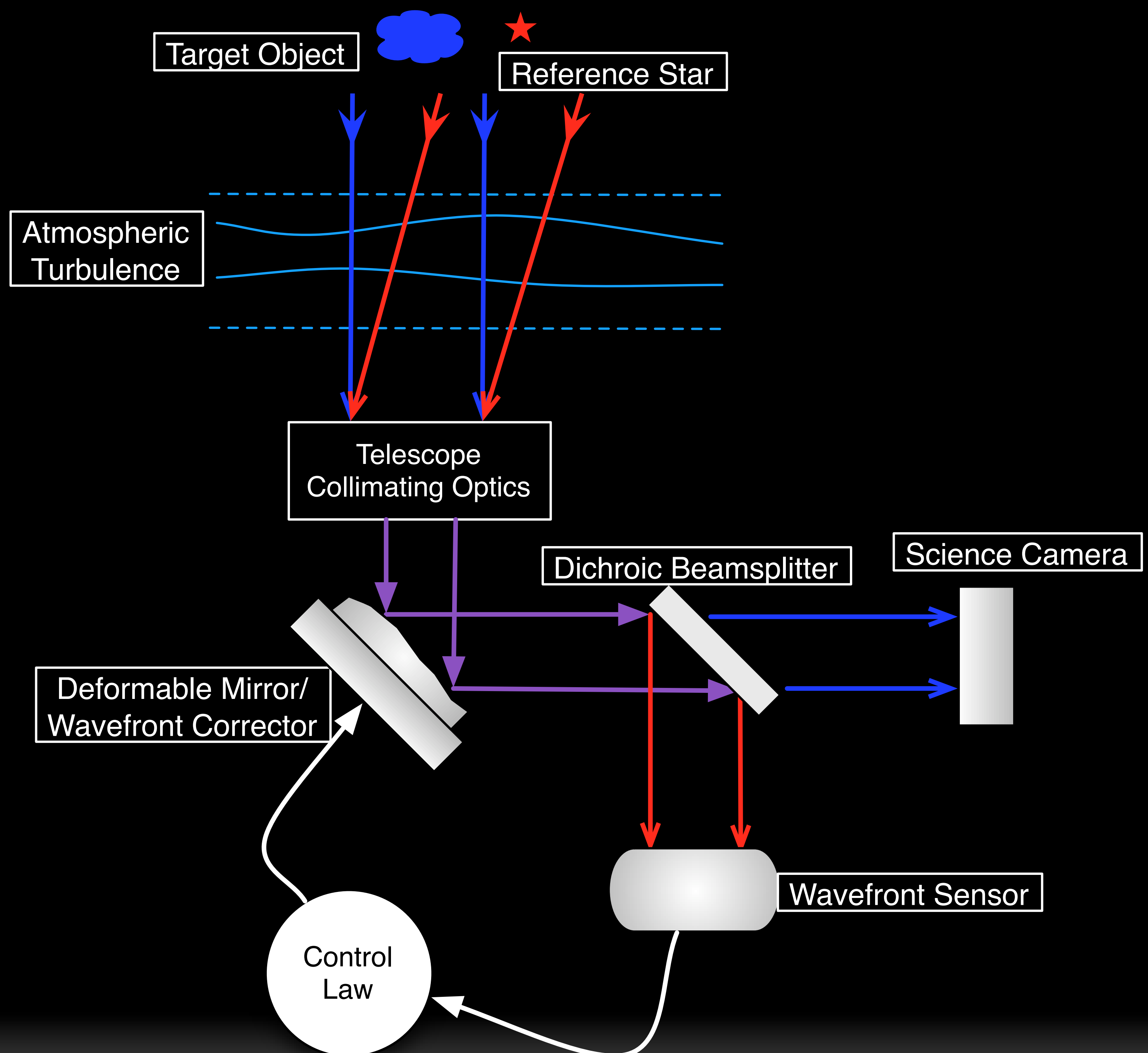

Images and Video from UC Santa Cruz Adaptive Optics course.

Typical Ground Adaptive Optics

Phase Conjugation

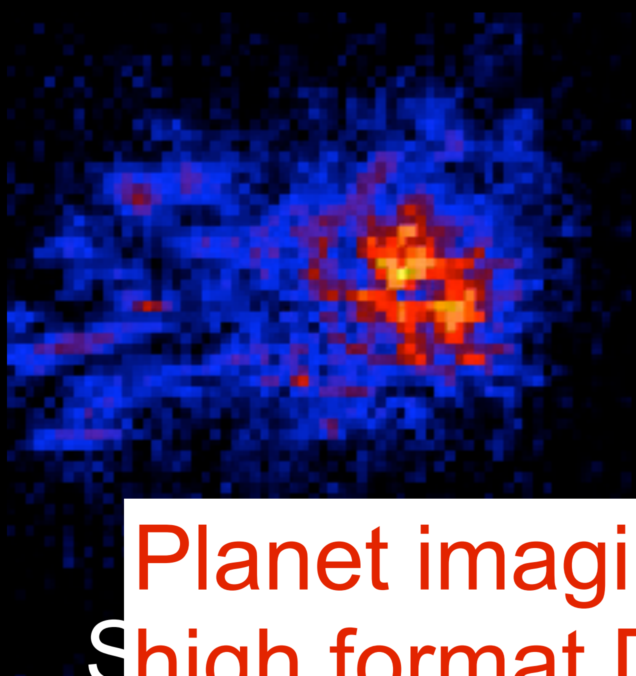

Without Adaptive Optics

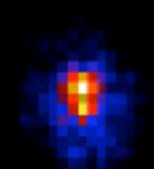

With AO

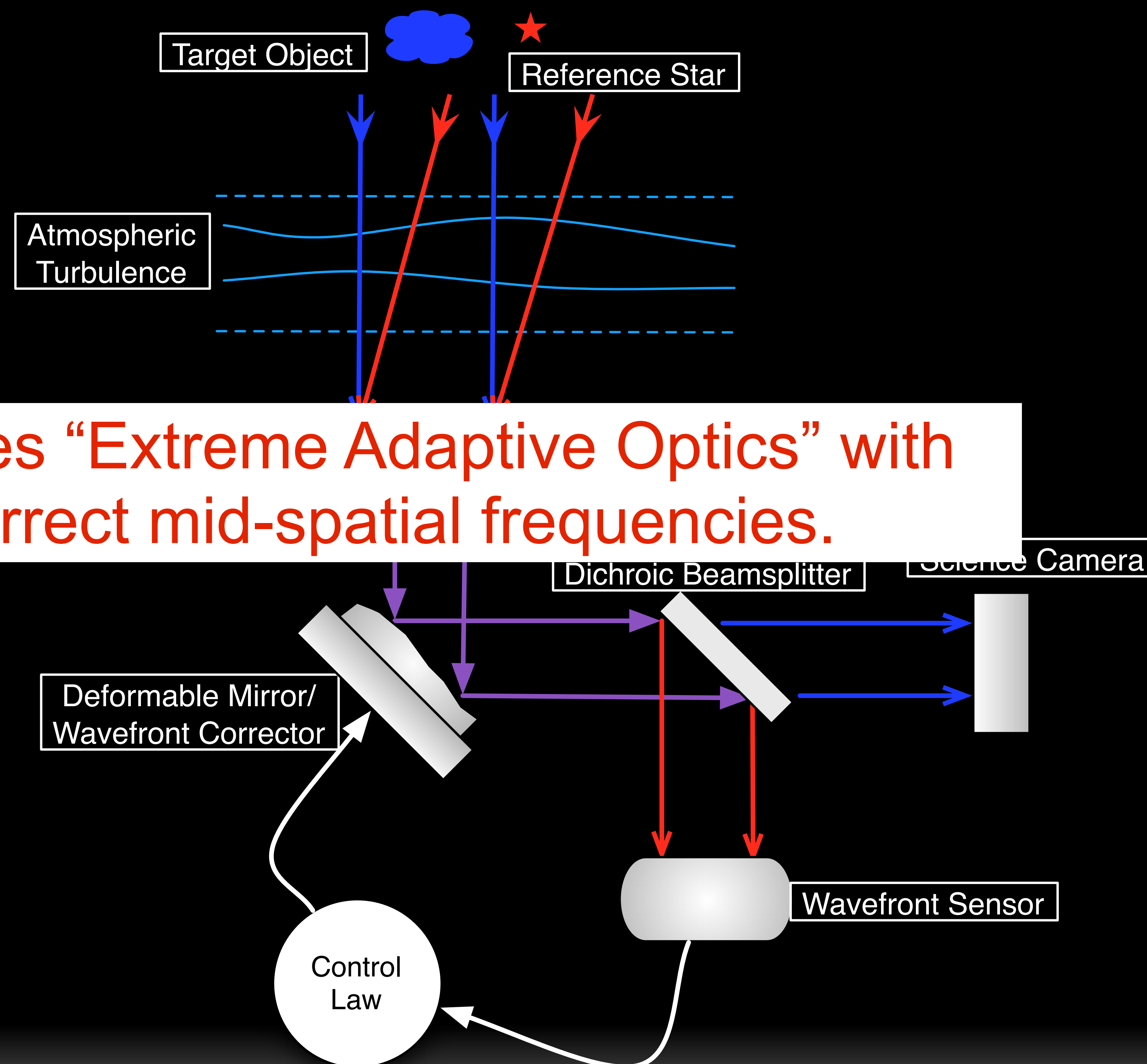

Planet imaging requires "Extreme Adaptive Optics" with high format DMs to correct mid-spatial frequencies.

Images and Video from UC Santa Cruz Adaptive Optics course.

Deformable Mirrors

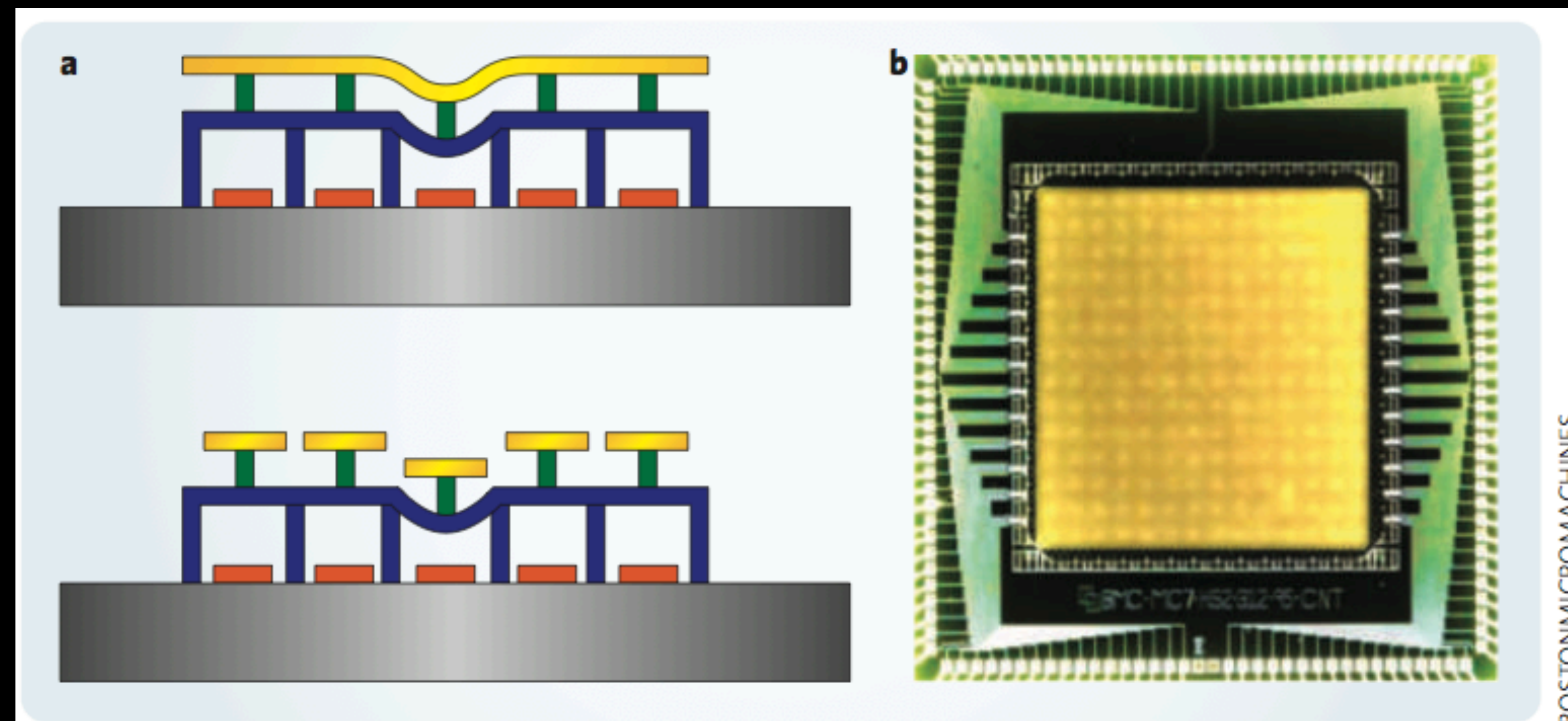

Xinetics Electrorestrictive

MEMS Deformable Mirror (BMC)

- Continuous facesheet
- FOV determined by number of actuators
- Model surface as linear sum of basis functions
- Usually influence function as basis function
  - Measured response from a single poked actuator
  - Approximately Gaussian shape

Direct Images of HR8799 with AO

Marois, Macintosh, et al. (2008)

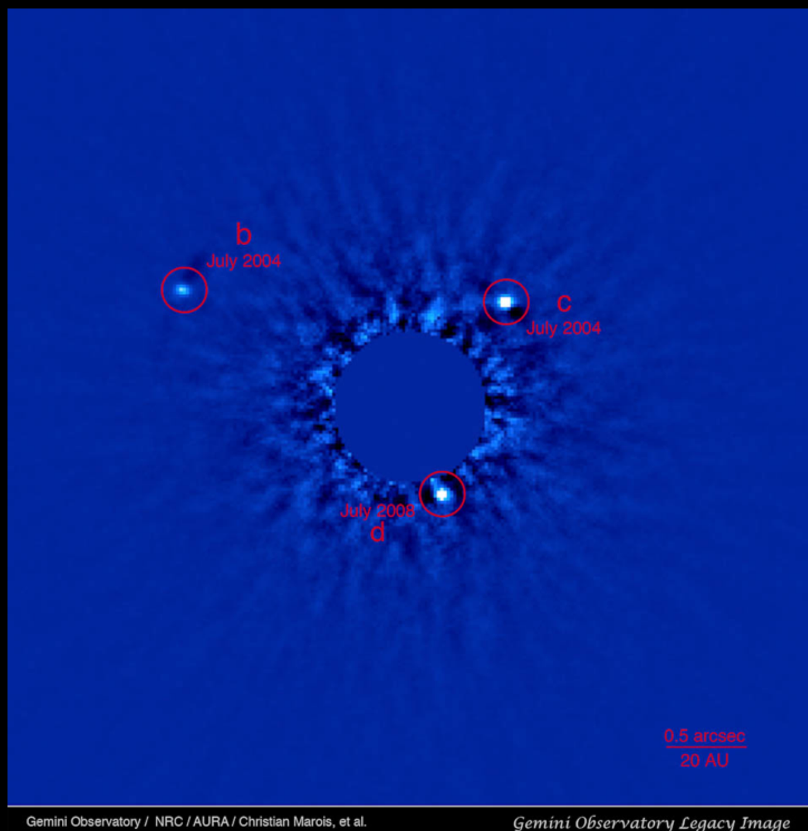

Gemini/NICI (Lyot)

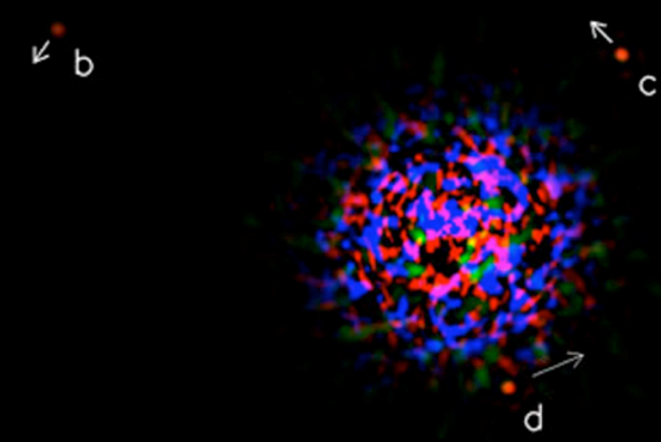

Keck

The planets were later "discovered" in older HST images without AO.

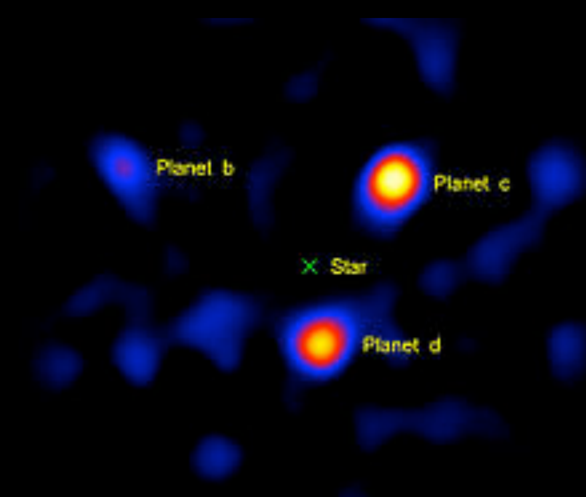

Hale/Palomar (vortex)

Serabyn, et al. (2008)

Next Generation of Extreme AO on ground

GPI, SPHERE, SCExAO+CHARIS

Courtesy Bruce Macintosh

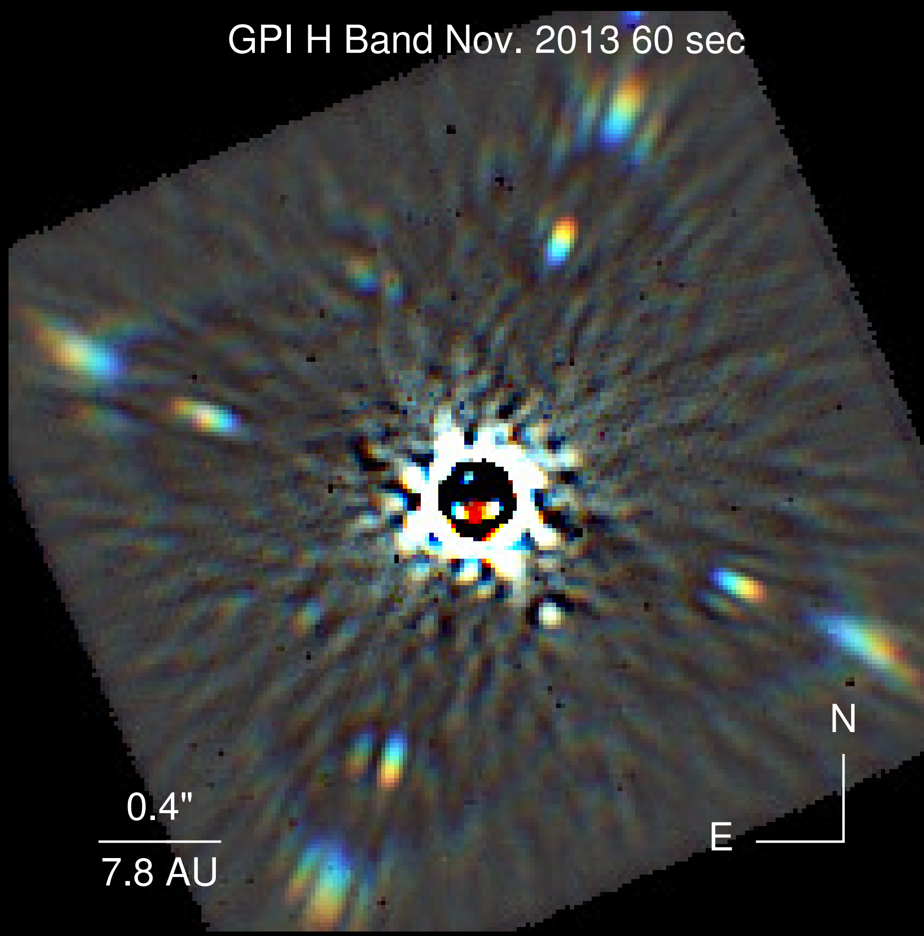

Gemini Planet Imager

APLC coronagraph with 4000 actuator MEMS DM.

Next Generation of Extreme AO on ground

GPI, SPHERE, SCExAO+CHARIS

Courtesy Bruce Macintosh

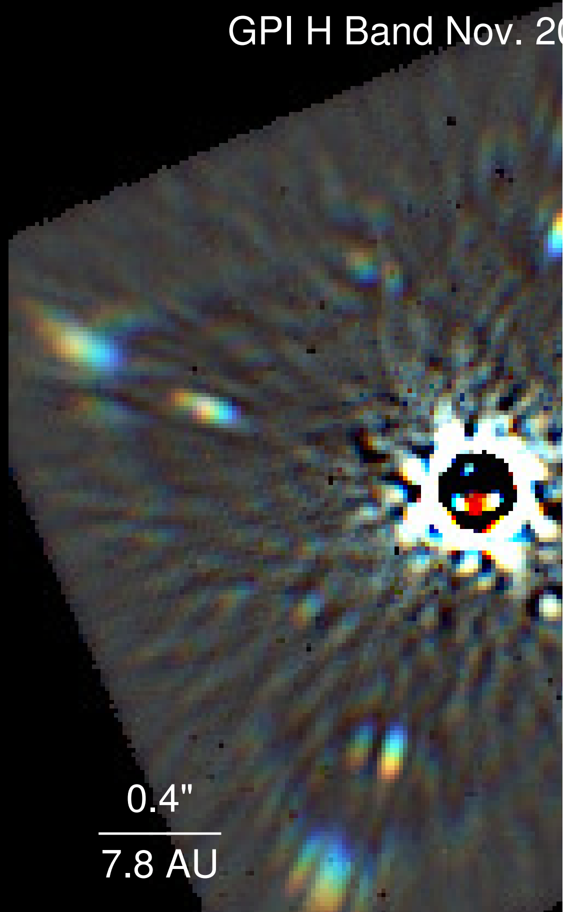

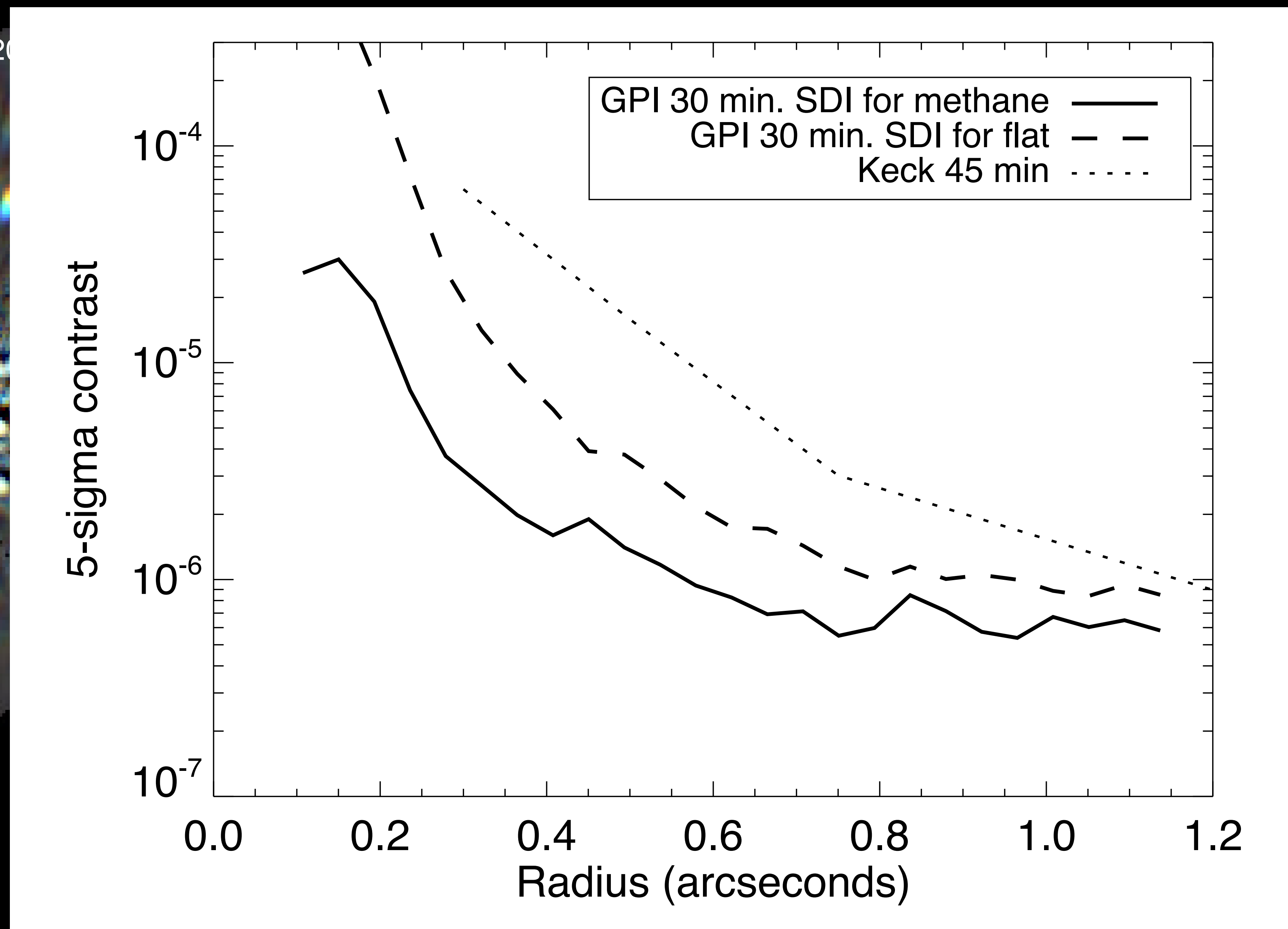

Beyond Extreme AO

On ground, aberrations are predominantly phase.

For very high contrast in space, need to worry about non-common path error and amplitude errors. Limit contrast to 1e-5 to 1e-7.

Solution: Focal Plane Wavefront Sensing and Control with two Deformable Mirrors

Beyond Extreme AO

On ground, aberrations are predominantly phase.

For very high contrast in space, need to worry about non-common path error and amplitude errors. Limit contrast to 1e-5 to 1e-7.

Solution: Focal Plane Wavefront Sensing and Control with two Deformable Mirrors

Today, “coronagraph” refers to both the optical design and the wavefront control system!

Focal Plane Wavefront Sensing & Control

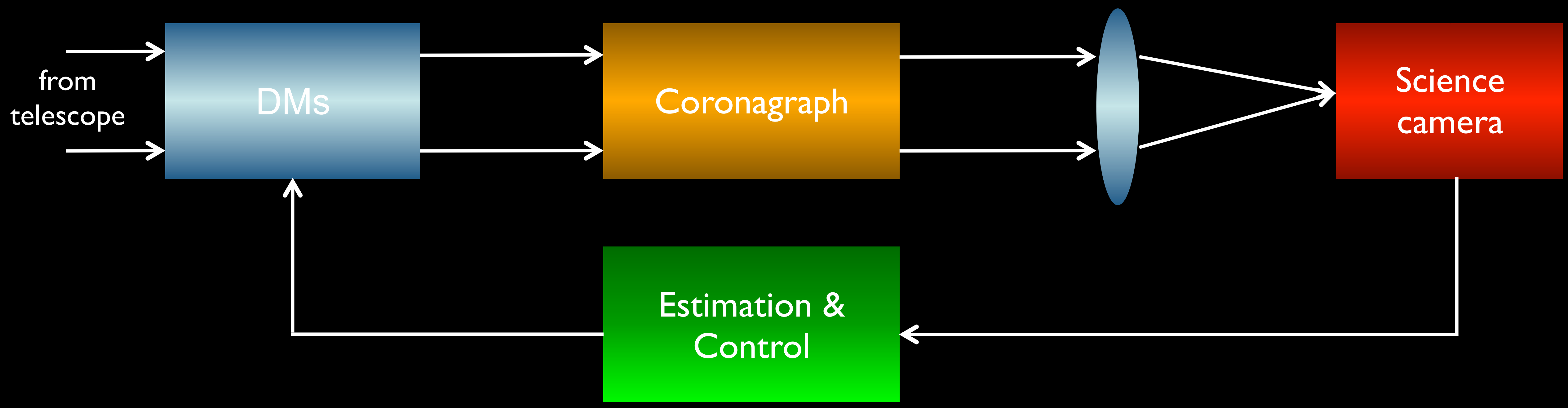

Need to estimate complex field from only intensity

Control Algorithms:
Speckle Nulling (Brown & Burrows)
Energy Minimization (Malbet & Shao)
Electric Field Conjugation (Giveon)
Stroke Minimization (Pueyo)

Estimation Algorithms:
DM Diversity (Borde & Traub, Belikov)
Gerchberg-Saxton (Kay)
Kalman Filtering (Groff)

Single DM Control

Because controlling amplitude, only single-sided dark hole.

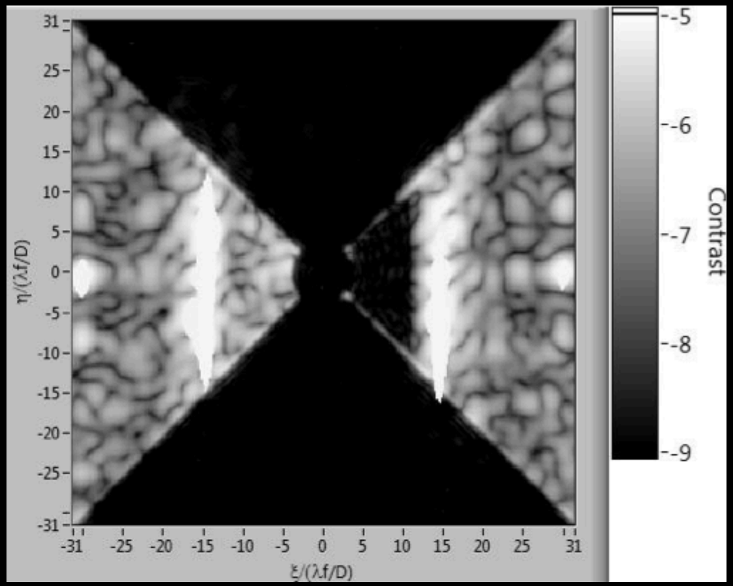

Shaped Pupil
- 4-10 λ/D
- 10% bandpass
- 2.4 x 10^{-9} contrast

[Belikov et al. 2007]

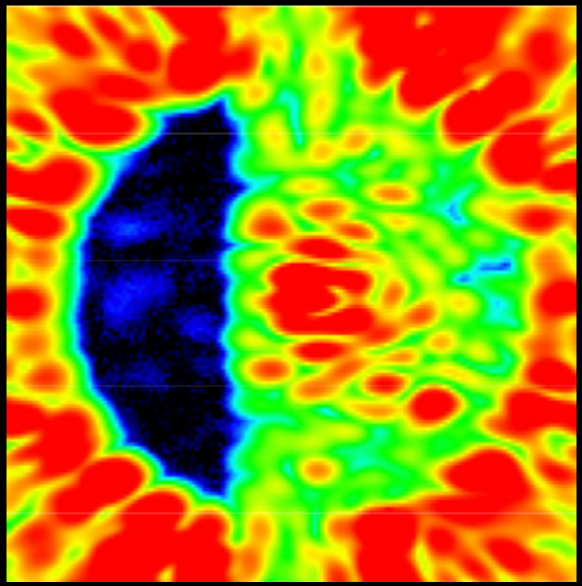

Band-Limited Lyot
- 4-10 λ/D
- 10% bandpass
- 6.4 x 10^{-10} contrast

[Moody et al. 2008]

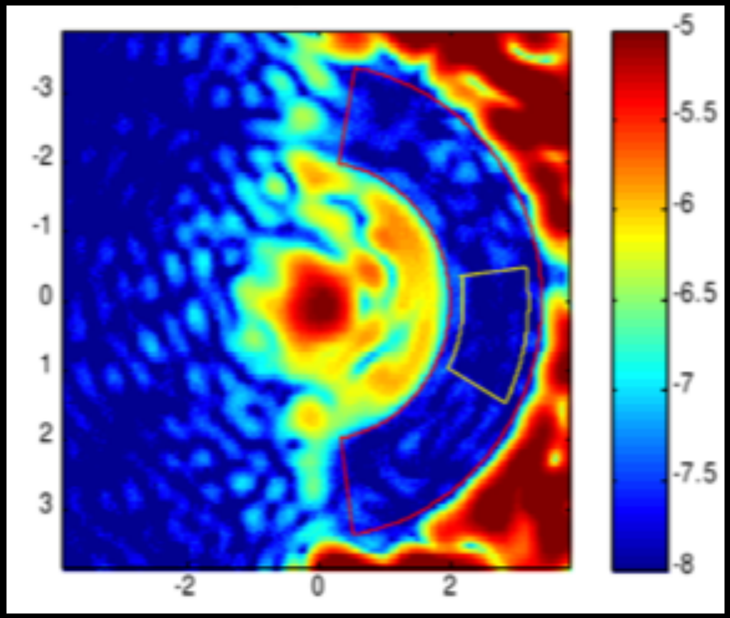

PIAA
- 2-3.4 λ/D
- monochromatic
- 1.9 x 10^{-8} contrast

[Belikov et al. 2011]

Because using phase to amplitude conversion, controller is chromatic and bandwidths limited. OWA determined by # of actuators.

Dual DM Control

First test at JPL HCIT in August, 2013 (monochromatic).

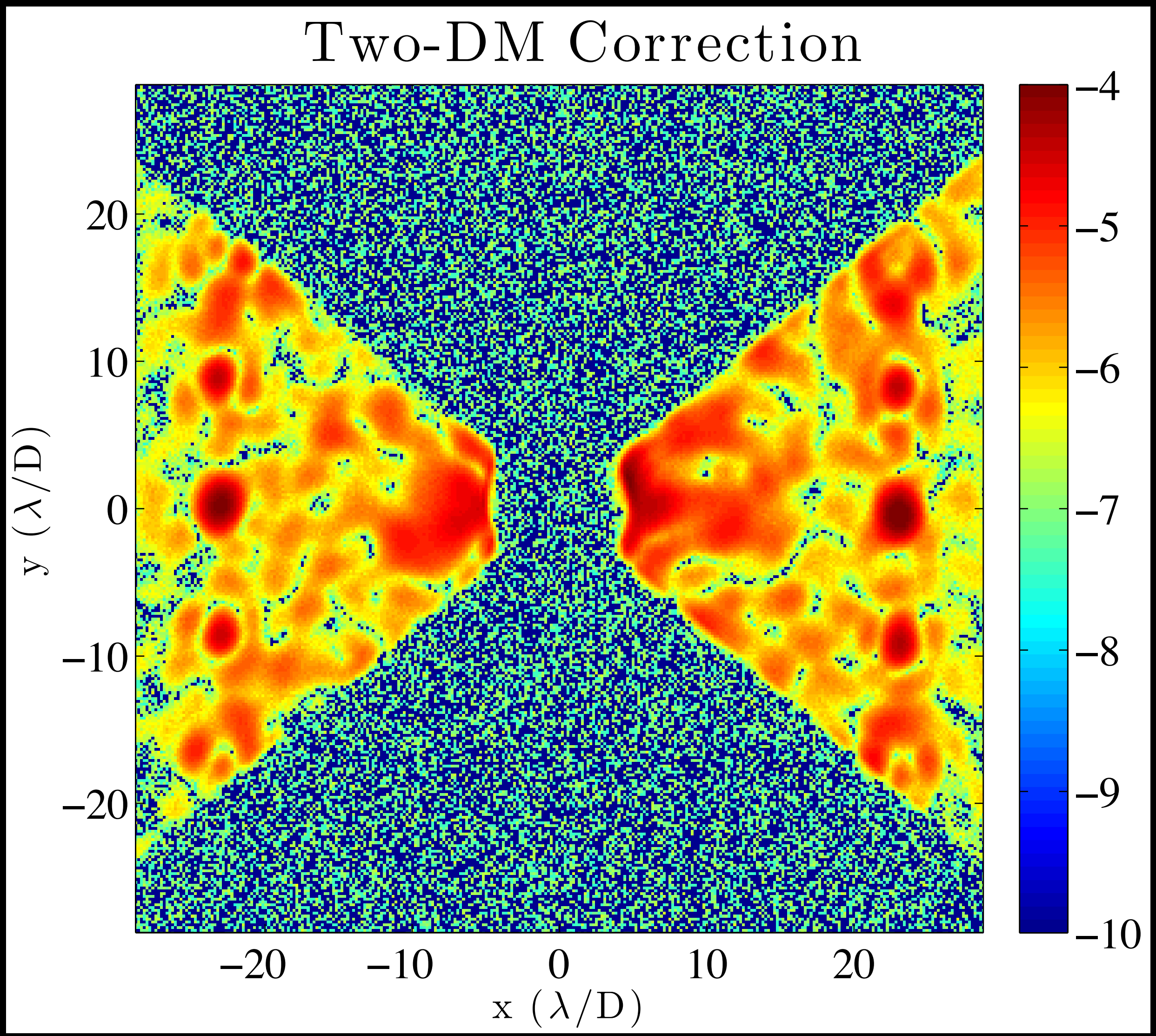

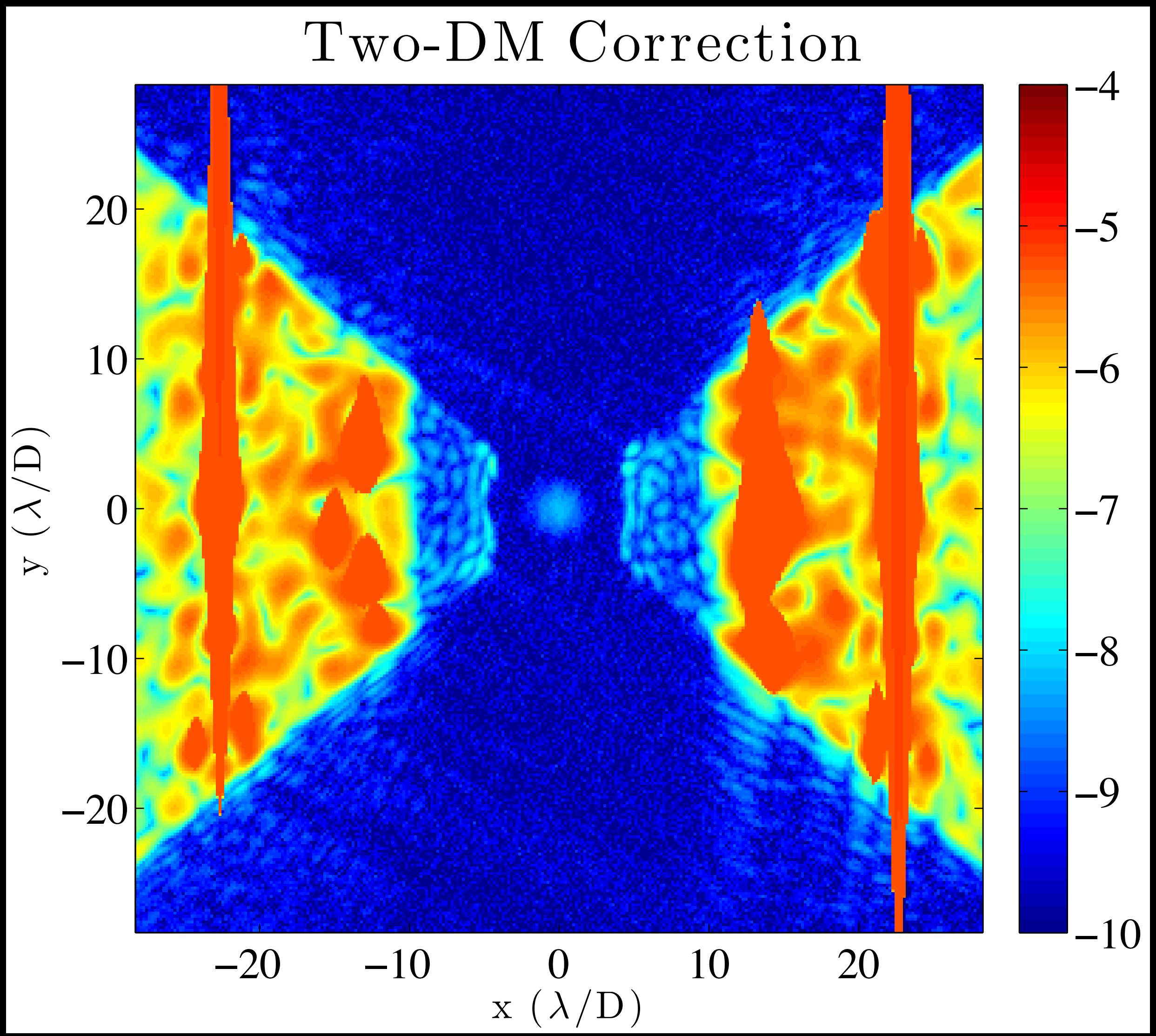

IWA = 5 λ/D
OWA = 9 λ/D
3.6 x 10^{-9} contrast

Riggs, et al. (2013)

Future?

Hybridizing coronagraph with DMs to generate contrast

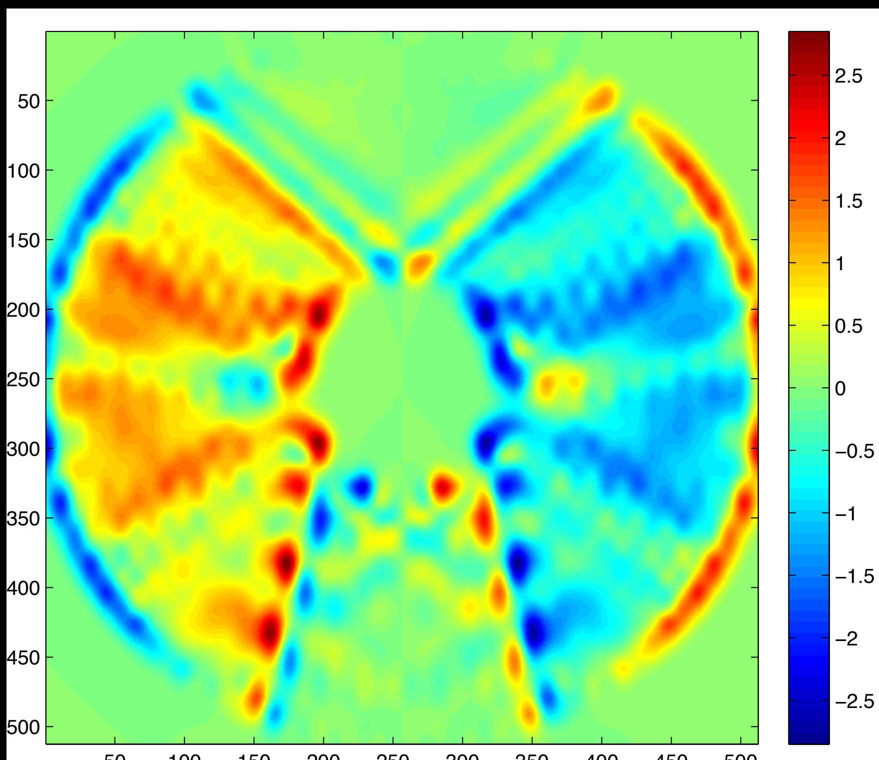

DM Setting

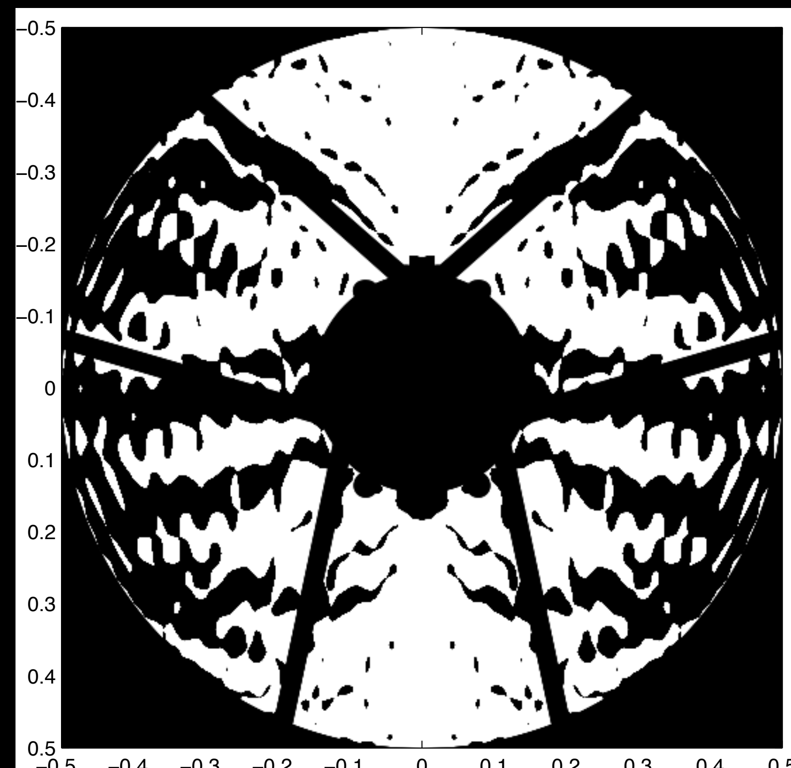

Shaped Pupil

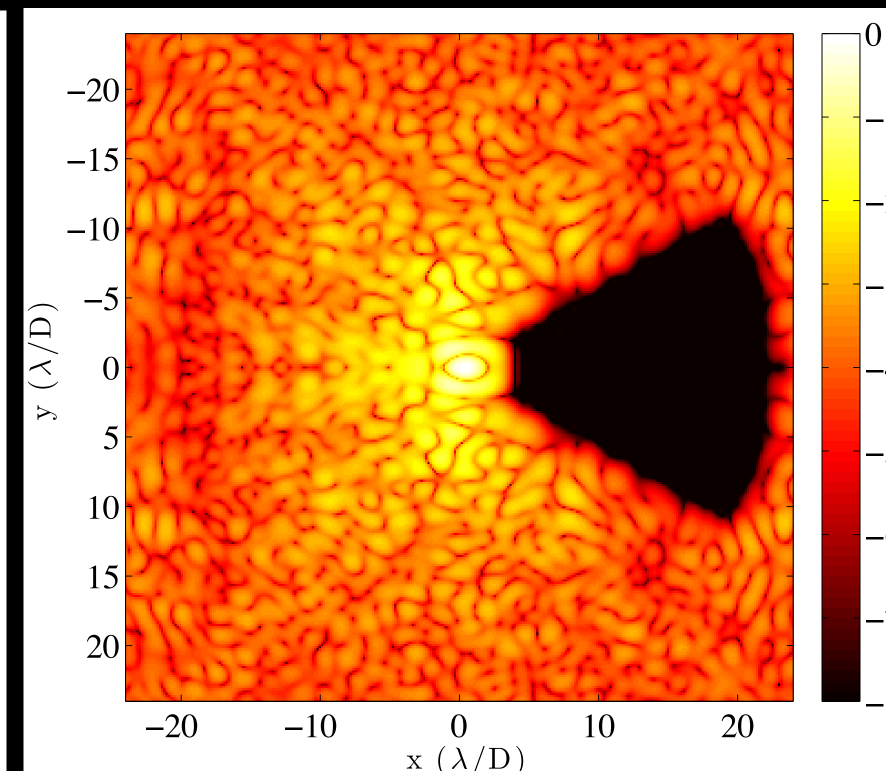

One-Sided Dark Hole

- Contrast: $5x10^{-9}$
- Transmission: 61%
- Stroke: 0.91 \lambda
- IWA: 4 \lambda/D
- OWA: 22 \lambda/D

Riggs, et al. (2014)

Hybrid Lyot Coronagraph

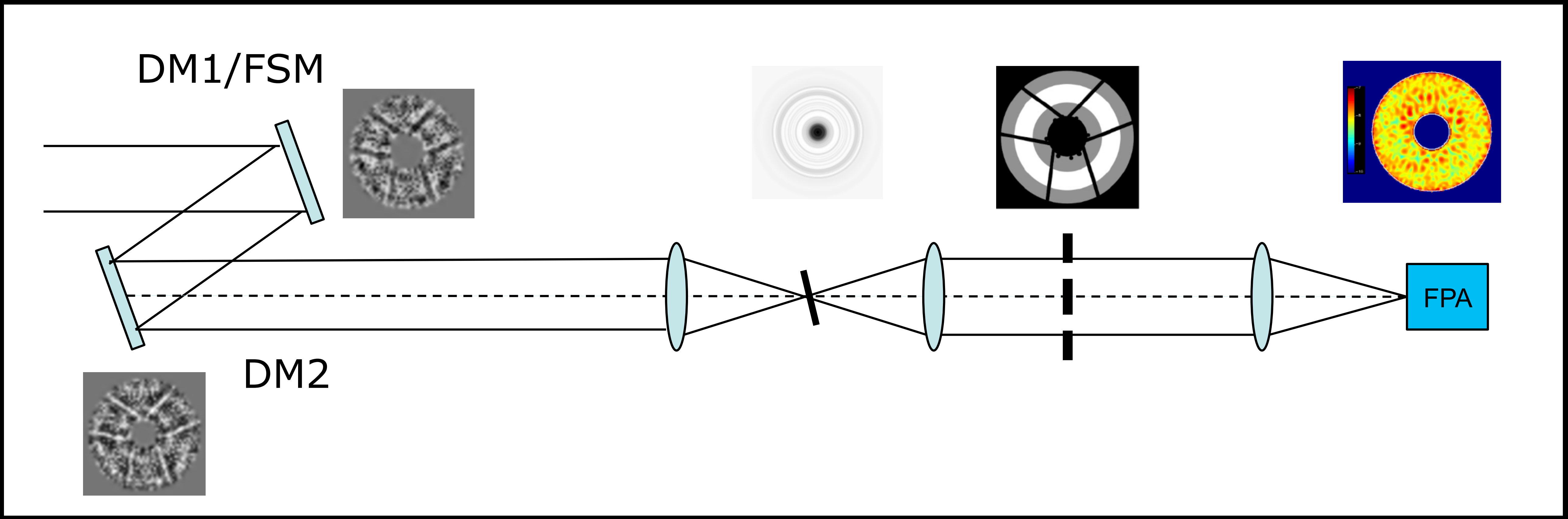

Baseline design for WFIRST/AFTA

From John Trauger, JPL

References

1. Riggs, A.J.E., Zimmerman, N., Carlotti, A., Kasdin, N.J., Vanderbei, R., "Shaped pupil design for future space telescopes," Proc. SPIE, paper 9143-69, (2014).
2. Riggs, A., Groff, T., Carlotti, A., Kasdin, N., Cady, E., Kern, B., and Kuhnert, A., “Demonstration of symmetric dark holes using two deformable mirrors at the high-contrast imaging testbed,” in [Proceedings of SPIE], 8864, 88640T (2013)
3. Traub, W.A., Kaltenegger, L., Jucks, K.W., Turnbull, M.C., "Direct imaging of Earth-like planets from space (TPF-C)", ProcSPIE, id. 626502 (2006)
4. Kuchner, Marc J., Traub, Wesley A., "A Coronagraph with a Band-limited Mask for Finding Terrestrial Planets", ApJ, 570, 900-908 (2002)
5. Rouan, D., Riaud, P., Boccaletti, A., Clénet, Y., and Labeyrie, A., "The four-quadrant phase mask coronagraph. I. Principle", PASP, 112, 1479-1486 (2000)
6. Mawet, D., Riaud, P., Absil, O. and Surdej, J., "Annular groove phase mask coronagraph", ApJ, 633, 1191-1200 (2005)
7. Slepian, D., “Analytic Solution of Two Apodization Problems”, (1965).
8. Vanderbei, R., Kasdin, N.J., Spergel, D., Kuchner, M., "New pupil masks for high-contrast imaging", Proc SPIE, 5170, 49-56 (2003)
9. Carlotti, A., Vanderbei, R., Kasdin, N.J., "Optimal pupil apodizations of arbitrary aperturesfor high-contrast imaging", 19, 26796 (2011)
10. Guyon, O., "Phase-induced amplitude apodization of telescope pupils for extrasolar terrestrial planet imaging", A&A, 404, 379-387 (2003)

References

11. Vanderbei, R., Traub W., "Pupil Mapping in Two Dimensions for High-Contrast Imaging", ApJ, 626, 1079-1090 (2005)
12. Codona, J. et al., "A high-contrast coronagraph for the MMT using phase apodization: design and observations at 5 microns and 2 λ/D radius", ProcSPIE, id. 62691N (2006)
13. Soummer, R., "Apodized Pupil Lyot Coronagraphs for Arbitrary Telescope Apertures", A&A, 618, L161-L164 (2005)
14. Soummer, R., et al., "Apodized Pupil Lyot Coronagraphs for Arbitrary Apertures. II. Theoretical Properties and Application to Extremely Large Telescopes", ApJ, 695 (2009)
15. Soummer, R., et al., "Apodized Pupil Lyot Coronagraphs for Arbitrary Apertures. III. Quasi-achromatic Solutions", ApJ, 729, id. 144 (2011)
16. Carlotti, A., "Apodized phase mask coronagraphs for arbitrary apertures", A&A, 551, id.A10 (2013)
17. Carlotti, A., Mawet, D., Pueyo, L., "Apodized phase mask coronagraphs for arbitrary apertures. II. Comprehensive review of solutions for the vortex coronagraph", A&A, 566, id.A31 (2014)
18. N'Diaye, M., et al., "Apodized Pupil Lyot Coronagraphs (APLC): reduced IWA and increased robustness to low-order aberrations", ProcSPIE (2014)
19. Guyon, O. et al., "Theoretical Limits on Extrasolar Terrestrial Planet Detection with Coronagraphs", ApJS, 167, 81-99 (2006)
20. Marois, C., et al., "Confidence Level and Sensitivity Limits in High-Contrast Imaging", ApJ, 673, 647-656 (2008)

References

21. Serabyn, G., Mawet, D., Burruss, R., "Imaging The Exoplanets In HR8799 With A Vector Vortex Coronagraph On The Palomar 1.5 M Diameter Well-corrected Subaperture", Bul. AAS
#215, 42, 587 (2010)
22. Marois, C., Macintosh, B., Barman, T., Zuckerman, B., Song, I., Patience, J., Lafreniere, D., Doyon, R.,"Direct Imaging of Multiple Planets Orbiting the Star HR 8799", Science, Vol. 322, Iss. 5906, pp. 1348- (2008)
23. Kendrick, R. et al., "Closed-loop wave-front correction using phase diversity", Proc. SPIE, 3356, 844-85 (1998)
24. Malbet, F., Yu, J. W., Shao, M., "High-Dynamic-Range Imaging Using a Deformable Mirror for Space Coronography", PASP, 107, 386 (1995)
25. Pueyo, L., Kasdin, N.J., "Polychromatic Compensation of Propagated Aberrations for High-Contrast Imaging", ApJ, 666, 609-625 (2007)
26. Pueyo, L., Norman, C., "High-contrast Imaging with an Arbitrary Aperture: Active Compensation of Aperture Discontinuities", 769, id. 102 (2013)
27. Give'on, A. et al., "Broadband wavefront correction algorithm for high-contrast imaging systems", Proc. SPIE, 6691, id. 66910A (2007)
28. Groff, T., Kasdin, N.J., "Kalman filtering techniques for focal plane electric field estimation", JOSA, 30, 128 (2013)